ISBN 978-82-326-0522-4 (printed version)
ISBN 978-82-326-0523-1 (electronic version)
ISSN 1503-8181

Doctoral theses at NTNU, 2014:305

Pawan Kumar Shrestha

Stability of tunnels subject to plastic deformation – a contribution based on the cases from the Nepal Himalaya

Doctoral Thesis

Pawan Kumar Shrestha

Doctoral theses at NTNU, 2014:305

NTNU
Norwegian University of Science and Technology
Faculty of Engineering Science and Technology
Department of Geology and
Mineral Resources Engineering

NTNU – Trondheim
Norwegian University of
Science and Technology

NTNU – Trondheim
Norwegian University of
Science and Technology

NTNU

Pawan Kumar Shrestha

Stability of tunnels subject to plastic deformation - a contribution based on the cases from the Nepal Himalaya

Thesis for the degree of Philosophiae Doctor

Trondheim, September 2014

Norwegian University of Science and Technology
Faculty of Engineering Science and Technology
Department of Geology and Mineral Resources Engineering

NTNU – Trondheim
Norwegian University of
Science and Technology

NTNU
Norwegian University of Science and Technology

Thesis for the degree of Philosophiae Doctor

Faculty of Engineering Science and Technology
Department of Geology and Mineral Resources Engineering

ISBN 978-82-326-0522-4 (printed version)
ISBN 978-82-326-0523-1 (electronic version)
ISSN 1503-8181

Doctoral theses at NTNU, 2014:305

Printed by Skipnes Kommunikasjon as

Abstract

The purpose of excavating a tunnel is not fulfilled unless it is stable. One of the major causes of instability in tunnels is induced stresses around it. Tunnels excavated in weak and schistose rock mass below high overburden (rock cover) are prone to instability in the form of tunnel deformation. The deformation in the tunnel takes place to such an extent that it is irreversible and of significant magnitude, which is often known as tunnel squeezing. In order to limit such plastic deformation in tunnels, it is desirable that the response of the rock mass to the induced stresses is known so that requirement of rock support can be estimated. Rock support interaction is an important tool in such endeavor; and the Convergence Confinement Method is the common approach used for this purpose.

Contrary to the assumption of uniform in-situ stresses made in analytical solutions for elasto-plastic analyses, large degree of stress anisotropy condition prevails in most tunnelling conditions. The effect of such anisotropic stress condition leads to varying degrees of deformations around the tunnel contour. Therefore, stress anisotropy is also an important factor that needs to be addressed to ensure a proper support design for tunnels.

This thesis assesses the inter-relationship among rock mass property, in-situ stresses including horizontal to vertical stress ratio, tunnel support pressure and deformation. The work is based on the tunnel cases from the Nepal Himalaya. For this purpose, four completed tunnel projects from that region were selected, where moderate to large tunnel deformations had been recorded. Long term deformation records were analyzed to assess time independent and time dependent deformations. Furthermore, the behavior of average quality rock mass was also evaluated using the records of multiple point borehole extensometer monitored at four tunnel sections. Evaluations were made addressing both the rock mas around the tunnel wall and at depth. In addition, the effect of groundwater on tunnel stability in faulted rock mass was also assessed in a severely squeezed tunnel.

Results of the analyses of the tunnels in weak and schistose rock mass at stress anisotropy states show that a good correlation among tunnel strain, rock mass shear modulus, support pressure, vertical stress and stress ratio of horizontal to vertical stresses exists. Moreover, the study also shows that significant amount of time dependent deformation can occur in such weak rock mass. Such deformation was found to be high in schist and micaceous phyllite, moderate in graphitic phyllite and low in siliceous phyllite. Similarly, analyses incorporating instrumentation data in average

quality rocks show that stress anisotropy cause tensional cracks in tunnel crown and inverts whereas tunnel walls will have compressional failures. Moreover, the study also shows that deformation patterns in tunnels are altered by in-homogeneity in the rock mass. The study on the effect of groundwater in tunnel stability in faulted rock mass shows that groundwater can increase the tunnel strain on average 15% depending on distance from tunnel face and location in the tunnel.

This study suggests relationships that can be used as a basis for an early estimate of instantaneous and final deformations and the corresponding requirement of support pressures in tunnel walls in weak and schistose rock mass. The suggested relationships, however, are for the tunnels in plane strain conditions where face effect is not incorporated. Moreover, the relationships are based on a limited number of tunnel cases. Therefore, further validation is needed using other tunnel cases subjected to plastic deformation.

Acknowledgement

I express my sincere gratitude to the Department of Geology and Mineral Resources Engineering and the Faculty of Engineering Science and Technology of Norwegian University of Science and Technology for the support rendered to me in pursuing this doctoral work.

I take this opportunity to thank my supervisor Associate Professor Krishna Kanta Panthi for the encouragement, motivation, guidance and support towards accomplishment of this PhD study. He has been a constant source of knowledge to me, not only during this period but ever since I came in contact with him. He taught me how to be a researcher and guided me how to organize the research findings. I am indebted to him. I am also thankful for the motivations from Professors Mai Britt Mørk, Bjørn Nilsen, Charlie Li; and Dr. Nghia Trinh for the suggestions in running the numerical models.

I am very much thankful to Gunnar Vistnes and Torkjell Breivik for conducting the rock mechanical laboratory works, Torill Sørløkk and Tijhuis Laurentius for conducting the XRD tests, and Trond Larsen, Simon Hagen, Kjartan Følke and Filip Dahl at Sintef for the laboratory helps. I am also thankful to Wenche Finseth, Aina Myrvold, Knut Olav Solem and other department colleagues for their support during this period. Thanks to all my former and present PhD colleagues. The discussions among the PhD colleagues were refreshing and often fruitful.

Likewise, I am grateful to Nepal Electricity Authority for providing rock samples, data and documents, Himal Hydro and many other friends in Nepal for conducting the field works.

The Nepalese community and friends (Biraj, Chhatra, Kamal, Nabin, Netra, Nicole, Prajwalan, Surya, Umesh, and their families) here in Trondheim have been wonderful. Special thanks to Kritagya, Kriti and Laxmi Panthi, Asish, Sajani and Hari Shankar Shrestha for creating family atmosphere in Trondheim. My family and I will always cherish the time we had during this period. I am indebted to my family back in Nepal for the constant encouragement and support. Specially, I am grateful to my wife Prabina Shrestha for her love, care and support, and sons Ojas and Aarav for filling joy in our lives. Finally, I have no words to express my gratitude to my mother, Ram Kumari. I dedicate this work to her.

Pawan Kumar Shrestha

Trondheim, September 2014

List of papers

Paper I

Analysis of the plastic deformation behavior of schist and schistose mica gneiss at Khimti headrace tunnel, Nepal.

Authors: Pawan Kumar Shrestha and Krishna Kanta Panthi

This paper was published in the Bulletin of Engineering Geology and the Environment, vol. 73(3), pp. 759-773.

Paper II

Assessment of the effect of stress anisotropy on tunnel deformation in the Kaligandaki project in the Nepal Himalaya.

Authors: Pawan Kumar Shrestha and Krishna Kanta Panthi

This paper was published online on 15 July 2014 in the Bulletin of Engineering Geology and the Environment. DOI 10.1007/s10064-014-0641-5.

Paper III

Predicting plastic deformation in tunnels – an analysis based on tunnel cases from the Nepal Himalaya.

Authors: Pawan Kumar Shrestha and Krishna Kanta Panthi

Submitted to Rock Mechanics and Rock Engineering on 16th September 2014. The paper is under review.

Paper IV

Interpretation of deformation characteristics at Kaligandaki Headrace Tunnel using tunnel monitoring records.

Authors: Pawan Kumar Shrestha and Krishna Kanta Panthi

This paper was submitted to the 13th International ISRM Congress 2015, Montreal, Canada.

Paper V

Groundwater effect on faulted rock mass - an evaluation of Modi Khola Pressure Tunnel in the Nepal Himalaya.

Authors: Pawan Kumar Shrestha and Krishna Kanta Panthi

This paper was published in Rock Mechanics and Rock Engineering, vol. 47(3), pp. 1021-1035.

Note on contributions on the papers:

The candidate performed model calibrations, all analyses and wrote the manuscripts. The main supervisor, who is also the co-author of all papers, defined the area of research to be conducted through this PhD study and provided real time instrumented data sets for three case projects excluding Modi Khola Hydroelectric Project, where the candidate himself worked as a design and contracts engineer during the project execution. The main supervisor also reviewed and edited the manuscripts.

Contents

Part I

1. Introduction

1.1 Motivation

Tunnels and underground structures are needed for infrastructure development. However, stress and water induced instabilities are common stability problems in such underground structures. Tunnels obviously are favored to be placed in strong and homogeneous rock mass having low frequency of discontinuities and weakness zones. Strong rock mass have the capacity to withstand high rock stresses. However, it is not always possible to locate underground structures in strong rock mass and avoid weakness and faults zones, and particularly in the Himalayas where young sedimentary rocks in the Siwalik Zone, meta-sedimentary to crystalline metamorphic rocks in the Lesser Himalayan Zone and crystalline metamorphic to igneous rocks in the Higher Himalayan Zone have undergone the effect of tectonic movement resulting in faulting, folding and shearing of the rock mass (Deoja et al., 1991; Upreti, 1999). Thus, the rock mass in this region is highly sheared, schistose and anisotropic (Panthi, 2006).

High stresses in weak rock mass are among the major causes for plastic deformation in tunnels. Excessive deformation in the periphery of a tunnel eventually causes it to collapse. Weak and deformable rocks such as phyllite, schist, schistose gneiss and rock mass in weakness and fault zones are incapable of sustaining high tangential stress thereby resulting in squeezing of the tunnel section (Panthi, 2006). Such phenomena are very common in the tectonically active Himalayan rock mass. Therefore, engineering principles and applications are pre-requisite to ensure safe and economic solutions of the problems.

Plastic deformation in a tunnel is primarily dependent on rock mass property, in-situ stresses and rock support applied. Knowledge of the interaction among these parameters is of great importance for optimum rock support design and successful tunnel construction. Various empirical (Singh et al., 1992; Goel et al., 1995), semi analytical (Hoek and Marinos, 2000) and analytical approaches (Panet, 1995 and 2001; Carranza-Torres and Fairhurst, 2000; Carranza-Torres, 2004) and probabilistic approach of uncertainty analysis (Panthi, 2006; Panthi and Nilsen, 2007) to predict tunnel deformation under stress conditions in underground openings are practiced. However, a

common limitation in most of the solutions is that stress anisotropy in non-circular tunnel has not been incorporated in the analyses.

High degree of stress anisotropy exists in the Himalayan region; and the cause of large plastic deformations in this region may also be related to such high degree of stress anisotropy. Thus, this research is focused on the plastic deformation behavior of the weak and schistose rock mass in tunnels under high degree of stress anisotropy. The analysis focuses in finding inter-relationship among rock mechanical property, applied rock support and in-situ stress conditions in tunnels. The analysis and contribution are based on case studies from the Nepal Himalaya.

1.2 Objective of the study

The objective of this PhD study is to contribute to the understanding related to plastic deformation (large deformation) in tunnels based on case studies from the Nepal Himalaya; where tunnel instabilities subjected to plastic deformation were encountered and posed of considerable challenges in tunnelling. Major objectives of this research are as listed below:

a. Root cause analysis of plastic deformation.
b. Stability analysis of tunnels of the studied cases.
c. Analysis of inter-relation among rock mass property, in-situ stresses, rock support and tunnel deformation.
d. Propose prediction model for plastic deformation in tunnels subjected to stress anisotropy.

1.3 Scope of the study

The scope of this research lies within stability analysis of the tunnels in schistose, weak and deformable rock mass from the Nepal Himalaya. Four completed tunnel projects from that region were used as cases; the locations of which are shown in the geological map of Nepal in Figure 1. Brief descriptions of the projects are presented below.

1.3.1 Khimti 1 Hydropower Project, Nepal

The Khimti 1 Hydropower Project is located in the Lesser Himalayan rock formation. Its headrace tunnel is 7.9 km long and is inverted-D in shape having cross sectional area from 11 m^2 to 14 m^2. Dominant rock types along the tunnel are mainly mica gneiss, banded gneiss and granitic gneiss in intercalation with highly sheared chlorite and talcose mica schist bands. The tunnel was excavated full-face using drill and blast method and supported mostly by steel fiber shotcrete and cement grouted rock bolts. During tunnelling works, deformations in the tunnel were observed and recorded at

some tunnel locations. Measurements of the tunnel deformations made after several days of excavation showed continued deformation of the tunnel walls (CCC, 2002; Shrestha, 2005; Panthi, 2006).

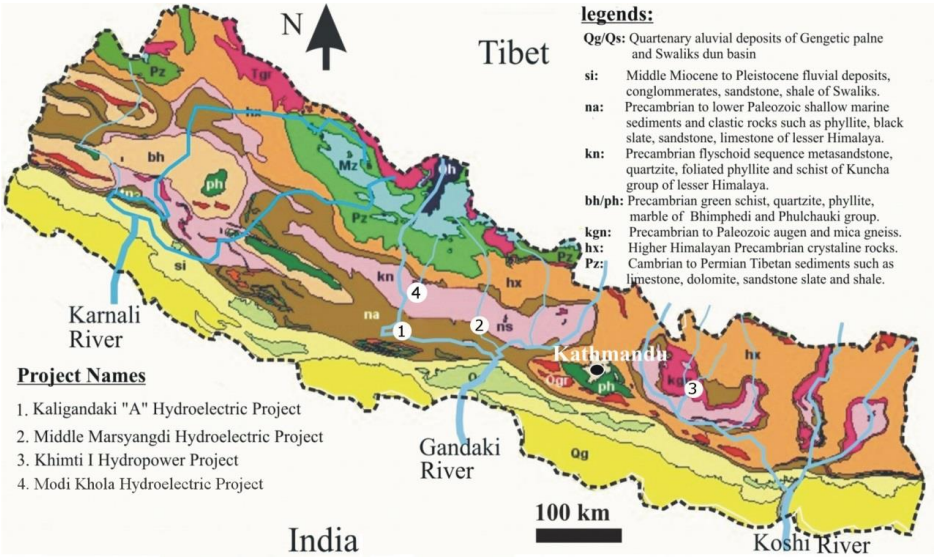

Figure 1: Locations of the studied tunnel projects on the geological map of Nepal (Panthi, 2006)

1.3.2 Kaligandaki 'A' Hydroelectric Project, Nepal

The Kaligandaki 'A' Hydroelectric Project which is also located in the Lesser Himalayan rock formation has 5.9 km long mostly horse-shoe section headrace tunnel with 56 m^2 cross sectional area. The dominant rock type along the headrace tunnel is graphitic and schistose phyllite, which is of poor quality, thinly foliated, jointed and weathered (NEA, 2002; Panthi, 2006). Shear planes and few narrow fault zones were detected along the headrace tunnel. The tunnel was mostly supported by shotcrete, steel ribs and rock bolts. Most of the tunnelling problems were associated with plastic deformation (squeezing), the magnitude of which ranged from a few centimeters to nearly a meter.

1.3.3 Middle Marsyangdi Hydroelectric Project, Nepal

The Middle Marsyangdi Hydroelectric Project area lies in the Midland Zone at the upper part of the Lesser Himalayan rock formation. Its 5.3 km long horse-shoe shaped headrace tunnel with 6.4 m excavation diameter passes basically through fractured quartzite, siliceous and micaceous phyllite in intercalation with meta-sandstone (Panthi,

2006; NEA, 2011). The tunnel was supported by shotcrete, steel ribs and rock bolts. During construction, minor to moderate squeezing was observed along the headrace tunnel.

1.3.4 Modi Khola Hydroelectric Project, Nepal

The Modi Khola Hydroelectric Project is located in Midland Zone of the Lesser Himalayan rock formation. A part of 422 m long pressure tunnel of inverted-D section and of 4 m diameter passes through highly decomposed mica schist, phyllitic schist and crushed quartzite with intercalation of clay minerals. The pressure tunnel encountered a fault of 85 m width composed of fully decomposed soft fault gouge and shattered fault breccia. A series of large over-breaks occurred at locations where the groundwater initiated large deformation leading to immediate collapse of the opening. Later after initial stabilization and advancing further ahead, the same reach started squeezing heavily up to 1.5 m and even buckling closely spaced steel ribs (Paudel et al., 1998; HH, 2001).

1.4 Structure of the thesis

This thesis is presented in two parts. In *Part I*, along with the motivation, objective and scope of the study (Chapter 1); the following chapters are presented:

Chapter 2: Plastic deformation and tunnel stability

Chapter 3: Methodology

Chapter 4: Results and discussions

Chapter 5: Conclusion and recommendations

References

Part II encloses complete set of articles as selected original papers. All together five articles have been presented, of which three are published in international journals, one is submitted to an international journal and is under review and one has been submitted to an international conference.

In addition, other publications by the candidate during the PhD study are also listed in Appendix A. And, representative FLAC^{3D} numerical codes used in the analyses are presented in Appendix B.

2. Plastic deformation and tunnel stability

2.1 Plastic deformation

Displacement of rock mass around a tunnel opening is basically an interaction of rock mass property, induced stresses and applied support (Hoek and Brown, 1980; Brady and Brown, 2006). Deformation of tunnel is a response of rock mass to induced stresses around the tunnel opening whereas application of tunnel support offers resistance to further displacement of the rock mass. Importantly, such phenomenon is well noticeable in rock mass of weak and schistose character having low to medium strength, deformable or particulate in nature. In such rock mass, the deformation of tunnel takes place to such an extent that it is irreversible and of significant magnitude. Such deformation in tunnels is defined as plastic deformation.

Irrespective of its magnitude, deformation in tunnel can be categorically distinguished as an instantaneous deformation and a long term deformation. Generally, the first observation in tunnel will be the instantaneous response of the rock mass upon opening of the tunnel. Such an effect is assumed to reach at its maximum state when the effect of tunnel face as a fictitious support is ceased (Panet, 1995; Carranza-Torres and Fairhurst, 2000). Rock support interaction that includes such instantaneous response of the rock mass at this early stage of tunnel excavation to induced stresses is the basic approach adopted in tunnel support design. It is also noticed that tunnels in weak and schistose rocks continue to deform as time advances. Total deformations in tunnels at long term are thus inclusive of instantaneous and time dependent deformations.

A simple illustration of tunnel longitudinal deformation profiles at various stages is shown in Figure 2. As a tunnel is excavated, it will have displacement of value U_e at the tunnel face. By the time applied rock support comes in effect, an additional displacement U_s will occur exhibiting longitudinal deformation profile similar to curve ABC. If the tunnel is unsupported, it will have displacement of U_f represented by curve ABD. In weak and schistose rock mass, additional time dependent deformation will take place. In such case the tunnel contour without support will have deformation profile similar to curve ABE with additional displacement of U_t. But when the tunnel is supported, the time dependent behavior will be additional displacement of U'_t only represented by curve ABE'.

The work in this thesis focuses on these deformation behaviors of tunnels, hence the relevant basic principles and studies practiced are briefly discussed herein.

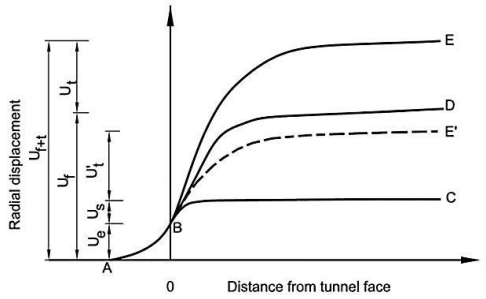

Figure 2: Idealized tunnel longitudinal deformation profiles

2.2 Instantaneous deformation

Upon excavation of a tunnel, the state of in-situ stresses in rock mass is disrupted and re-distributed around the opening periphery. These induced stresses, which depend on the magnitude and direction of principal stresses and geometry of the opening, are set up around the tunnel periphery in the form of tangential and radial stresses. Once these stresses exceed the strength of the rock mass, integrity of the rock mass is disturbed resulting to displacement which is observed in the tunnel contour.

Assessment of tunnel displacement and stresses around it can be readily evaluated by using close form solutions. In a circular tunnel in a plane strain condition in a homogeneous and elastic rock mass at isostatic stress environment, Lamé (1852) and Kirsch (1898) suggested elastic solutions for estimation of radial and tangential stresses and radial displacement around the tunnel contour. In reality, the rock mass is not a perfectly elastic material, which upon a certain degree of loading behaves as a plastic material (Goodman, 1989). Various analytical solutions of elasto-plastic behavior of rock mass in tunnel are available (Salençon, 1969; Hoek and Brown, 1980; Brown et al., 1983; Detournay and Fairhurst, 1987; Carranza-Torres and Fairhurst, 1999; Carranza-Torres, 2004; Sharan, 2003 and 2005; Alejano et al., 2009) and an appropriate one should be chosen according to stress-strain behavior of the rock mass.

The stress-strain behavior of rock mass varies according to the rock mass quality (Hoek and Brown, 1997). There are several methods to quantify quality of rock mass like *Q*-system (Barton et al., 1974), Rock Mass Rating (*RMR*) system (Bieniawski, 1973 and 1989), Rock Mass Index (*RMi*) system (Palmström, 1996); but Geological Strength Index (*GSI*) (Marinos and Hoek, 2000) which is incorporated in the Hoek and Brown failure criterion (Hoek et al., 2002) has been linked in this research. Accordingly, poor

to very poor rock masses having *GSI* value less than 30 are assumed to exhibit elastic perfectly plastic (EPP) behavior whereas good and very good rock mass having *GSI* value more than 70 will have elastic brittle (EB) failure after reaching the peak load. And, average quality rock mass (30>*GSI*>75) will have strain softening (SS) behavior that lies between the EPP and EB behaviors (Hoek and Brown, 1997; Crowder and Bawden, 2004).

On assumptions that the rock mass is homogenous, isotropic and in-situ stresses are at isostatic condition, Carranza-Torres (2003 and 2004) presented elasto-plastic solutions for a circular tunnel in a linear Mohr-Coulomb material and in material that satisfies the non-linear Hoek and Brown failure criterion, respectively. Basic principle in these solutions is that, when internal pressure (p_i) at the tunnel contour is less than the initial in-situ stress value σ_0, the tunnel wall converges. If the internal pressure (p_i) falls below critical support pressure (p_i^{cr}), then failure of the rock mass surrounding the tunnel occur thereby forming a plastic region of radius R_{pl} around it (Figure 3). Extent of such plastic region varies according to the stress-strain behavior of the rock mass. For rock mass having same peak strength, the plastic radius will be the least in EPP material and will be the largest in EB material. SS rock mass will have plastic radius in-between the two radii of EPP and EB materials.

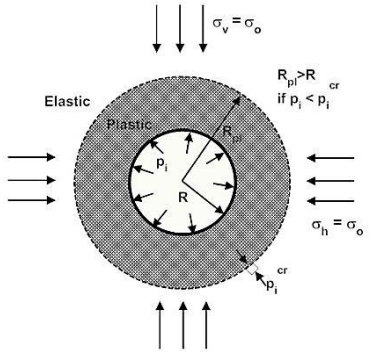

Figure 3: Elasto-plastic regions around a circular tunnel (after Carranza-Torres, 2004)

Unlike assumption of linearity made in the Mohr-Coulomb failure criterion, most rock masses behave non-linear characteristics (Hoek et al., 2002). The non-linear Hoek and Brown failure criterion is now widely accepted in rock engineering community. This failure criterion was originally proposed (Hoek and Brown, 1980) for hard intact rock having coefficient $a = 0.5$ but later was generalized (Hoek and Brown, 1997; Hoek et al., 2002) so that it can also be used in weak rock mass. Following this failure criterion, the elasto-plastic solution presented by Carranza-Torres (2004) is a useful tool in estimation of radial and tangential stresses and displacement at and around tunnel contour. Key aspect of this solution is that two failure envelopes, namely peak strength

and residual strength of the rock mass have been dealt such that the EB material model is represented. Once the residual strength of the rock mass is kept equivalent to the peak strength, the solution can be used for the EPP materials.

Between these two limiting cases (EB and EPP) of post failure behaviors of rock mass, average quality rock mass exhibiting strain softening behavior can still carry some post peak load and display strain. Unlike the peak and residual parameters in the EB and EPP behaviors, it is not easy to obtain representative values of parameters to simulate the SS behavior (Alejano et al., 2010). Peak and residual parameters like cohesion (c) and friction (ϕ) for the Mohr-Coulomb failure criterion or uniaxial compressive strength of intact rock (σ_{ci}), m_b, s and a parameters of the Hoek and Brown failure criterion have to be estimated properly to represent the SS behavior. In an attempt to estimate the residual parameters, Cai et al. (2007) and Alejano et al. (2009) made suggestions to reduce GSI value so that residual parameters m_b^r, s^r and a^r of the Hoek and Brown failure criterion can be estimated. Crowder and Bawden (2004) state that estimate of GSI value can be made by reducing m_b and s values to half and nil, respectively. Once these parameters are known, the residual friction (ϕ^r) and cohesion (c^r) of the Mohr-Coulomb failure criterion can be estimated using the relations suggested by Hoek et al. (2002). However, the transition from the peak and residual values of these parameters play an important role in the SS behavior. Alejano et al. (2010) proposed drop modulus (M) to be used to represent the strain softening process. Alternately, this post peak behavior can be represented by introducing segmental linear drops so that a step wise elasto-brittle-plastic process can be modelled instead of strain softening behavior (Wang et al., 2010). Typical tangential stresses (σ_θ), radial stresses (σ_r), radial displacements (u_r) and plastic radii (R_{pl}) in a tunnel of radius (R) in rock mass having same peak strength but different post failure behavior modes (EB, EPP and SS) are presented in Figure 4.

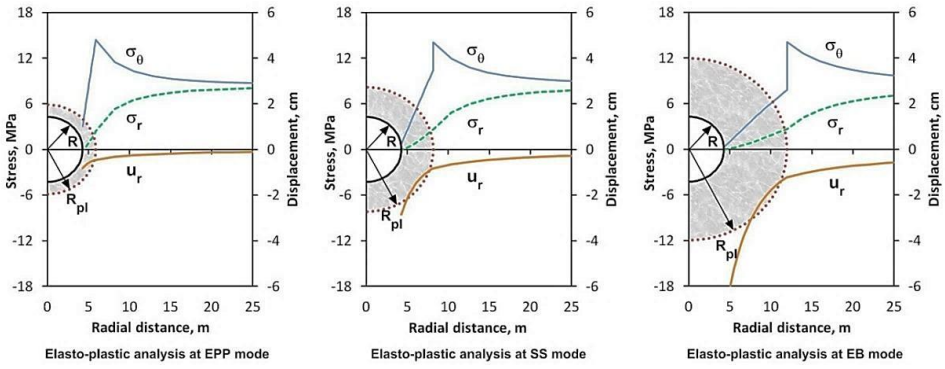

Figure 4: Stress and displacements around a circular tunnel in elastic perfectly plastic, strain softening and elastic brittle modes

Ground reaction curves

Stresses and displacement in the rock mass surrounding a tunnel opening not only depends on the rock mass properties and the in-situ stresses but also on the properties of applied support and timing of support installation. Ground reaction curve (GRC), also termed as Characteristic Curve (Brown et al., 1983), is such an inverse inter-relationship of displacement of rock mass around tunnel opening and support pressure in which the radial displacement in the tunnel decreases as the internal support pressure on the tunnel contour is increased. One of the principal utilization of elasto-plastic analysis is to determine GRC of the rock mass such that possible deformation of tunnel contour can be estimated at specified support pressure and its time of application, which is measured in terms of distance from the tunnel face.

GRCs vary according to the rock mass quality. As the rock mass quality is linked to GSI value; therefore lower the GSI value, like in weak and schistose rock, high will be the deformation. As shown in Figure 5, tunnel deformation (or strain) is significantly high in weak rock mass; whereas in rock mass having same peak strength but different post failure behavior modes like EB, EPP and SS, highest and lowest deformation will be on EB and EPP materials, respectively (Alejano et al., 2010).

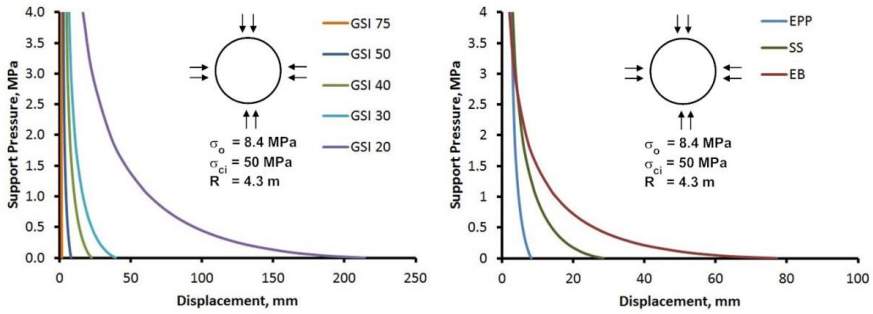

Figure 5: Ground reaction curves of different quality rock mass and post failure modes

Main application of GRC together with support characteristic curve (SCC) and longitudinal deformation profile (LDP) is in Convergence Confinement Method (CCM). The CCM method has been known since 1930s and the term has been widely used in underground excavation works (Brown et al, 1983; Panet, 1995 and 2001; Carranza-Torres and Fairhurst, 2000; Oreste, 2009). Combining the GRS, SCC and LDP; it gives a simplified approach in estimating support pressure to limit the tunnel deformation at desired level, the process which is also termed as 'rock support interaction'. The CCM method is also based on the same assumptions as made in the elasto-plastic analyses performed for constructing GRCs, except that the tunnel is at the state of plane strain condition. The CCM method is also designed such that the effect of tunnel face is

addressed. In this sense, the CCM method is a 3-dimensional problem addressed in 2-dimensional approach.

Longitudinal deformation profiles

Tunnel face has an important role in the tunnel stability. Tunnel deformation tends to get its maximum magnitude when the tunnel section in consideration is far away from the tunnel face. It is significantly less in magnitude when the tunnel section is close to the tunnel face. An instantaneous deformation as estimated using the elasto-plastic solutions therefore may not be applicable unless the effect of the tunnel face is considered. Therefore, an insight of development of longitudinal deformation profile (LDP) along the tunnel axis is pre-requisite in the tunnel design. There have been numerous works on LDP of tunnels at different rock mass conditions. Based on elastic model, Panet (1995) suggested relationship for deformation profile behind tunnel face in which the radial deformation at the tunnel face would be at least 25% of the maximum deformation. Similarly, Chern et al. (1998) and Hoek (1999) (in Carranza-Torres and Fairhurst, 2000) suggested best fit curves for the relationship between tunnel radial displacement and distance to the face using recorded data. Best fit curve suggested by Hoek (1999) seems more realistic and flatter compared to the elastic curve suggested by Panet (1995). Lately, based on 2-dimensional models on EPP materials, Vlachopoulos and Diederichs (2009) suggested Equations (1) and (2) to estimate tunnel radial deformation (u_r) in rock mass and on tunnel wall.

$$u^* = \frac{u_r}{u_{max}} = u_0{}^*.\ e^{X^*} \text{ for } X^* < 0 \quad (1)$$

$$u^* = 1 - (1 - u_0{}^*).\ e^{\frac{-3X^*}{2R^*}} \text{ for } X^* \geq 0 \quad (2)$$

where, $u_0{}^* = \frac{1}{3} e^{-0.15R^*}$

And, u_{max} is the maximum radius displacement in tunnel at distant from the face, $R^*$is the normalized plastic radius or the ratio between the plastic radius R_{pl} and tunnel radius R; X^* is the distance to the tunnel face normalized with the tunnel radius R.

Similar to GRC, LDP is also an inherent characteristic of rock mass at certain loading condition. The radial deformation changes considerably according to the distance from the tunnel face. In strong rock mass conditions, rate of development of deformation is high and reaches its maximum state at relatively short distance from the tunnel face compared to the rock mass having weaker strength. In weak rock mass the increase in deformation takes longer time and continues to develop even after the face effect has diminished (Figure 6). Similarly, such rate of displacement is high in EPP post failure mode compared to post failure modes of SS and EB materials.

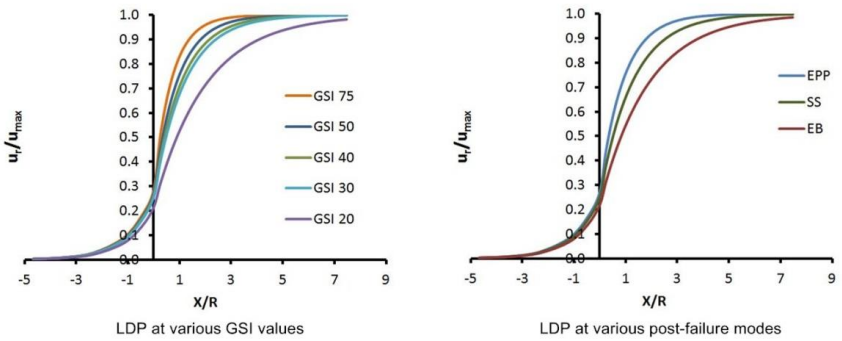

Figure 6: Longitudinal deformation profiles of different quality rock mass and post failure modes

Close form solutions are simplified and also consider assumptions. The deformation computation procedures discussed above have two important assumptions that can vary in real tunnelling cases. First, the in-situ stresses are assumed uniform all around the tunnel with a single value of σ_o; and the second is that the tunnel is circular in shape. In reality, both of these assumptions may or may not be the case.

Stress anisotropy

In-situ stresses around tunnels located at depth vary according to overburden and tectonic contribution in the stress. Stress measurements show that vertical stress (σ_v) in MPa is approximately 0.027 times the overburden depth measured in meter (Hoek and Brown, 1980; Martin et al., 2003), which is the specific weight of common rock material. In contrary, estimation of horizontal stress is a fairly complex procedure. The horizontal stress is composed of gravity-led horizontal stress (σ_h) and component of tectonic stress (σ_t), as presented in Equation (3) (Panthi, 2012). The gravity-led horizontal stress is attributed to the effect of Poisson's ratio (ν) together with the vertical stress. When the Poisson's ratio (ν) of rock is low, e.g. 0.10 in schistose and thinly foliated rocks (Panthi, 2006), the gravity-led horizontal stress becomes merely close to 10% of the vertical stress. On the other hand, estimation of the tectonic stress is a difficult task unless it is back calculated or directly measured.

$$\sigma_h = \frac{\nu}{1-\nu}\sigma_v + \sigma_{tec} \tag{3}$$

Tectonic stresses vary according to the extent of tectonic movement, its movement direction and degree of schistosity and shearing. Based on the measured horizontal stresses in the Nepal Himalaya (Nepal, 1999), tectonic stress magnitude varies between 3 and 4 MPa if rock mass is schistose and sheared. According to Panthi (2012), the

orientation of the tectonic stress in the central part of the Himalaya is very close to North-South. Thus, tunnels oriented North-South will have least effect of the tectonic stress across its section. Under such circumstance, the total in-plane horizontal stress in a tunnel at high depth can be well low, resulting to high degree of stress anisotropy.

Under stress anisotropy around a tunnel opening, magnitude and uniformity of displacements estimated by elasto-plastic analyses will vary greatly. There have been limited solutions to address stress anisotropy in tunnel. Kirsch (1898) presented elastic solution with biaxial loading condition where vertical and horizontal stresses could be varied in a circular tunnel at plane strain condition (Goodman, 1989). Despite the fact that the Kirsch Solution can be a useful tool in the state of stress anisotropy, its validity in elastic medium only may result to lower degree of displacement in the tunnels.

Detournay and Fairhurst (1987) presented semi-analytical elasto-plastic solution for deep circular tunnels in non-uniform far field stresses and showed that, when the vertical stress is higher than the horizontal stresses, elliptical inelastic region is formed around the tunnel where mean radius of such region is equal to the average of major and minor semi-axes of the ellipse. Major extension of such elliptical plastic zone is normal to the direction of maximum far field stresses, and the point of maximum displacement is located initially on the tunnel wall along the axis parallel to the maximum stress but gradually changes to the wall normal to the maximum stress direction as the mean plastic radius increases (Fairhurst and Carranza-Torres, 2002). The solution however is limited to certain degree of deviatoric stresses. Later, Detournay and John (1988) presenting design charts for deep circular tunnels under non-uniform loading condition (Figure 7) stated that as deviatoric stress increase the failure region around an unsupported tunnel will be like a butterfly shape. Pan and Chen (1990) and Carranza-Torres and Fairhurst (2000) also made similar conclusion for tunnels at high degree of stress anisotropy. Carranza-Torres and Fairhurst (2000) further stressed that elasto-plastic numerical analyses should be carried out at high stress anisotropy case when the stress ratio (k) is less than 0.6. In overall, the effect of high degree of stress anisotropy will create tensile failure at crown and compressive/shear failure at walls (Nilsen and Thidemann, 1993; Brady and Brown, 2006).

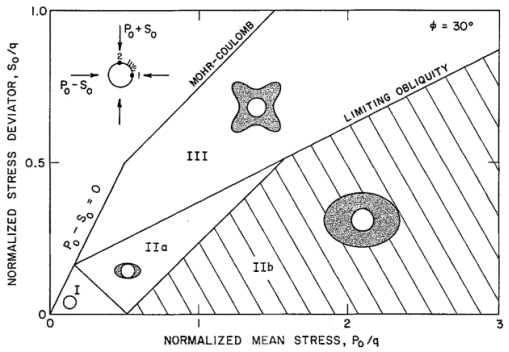

Figure 7: Effect of non-uniform stress in tunnel failure region (Detournay and John, 1988)

Tunnel shape

Another important aspect in the tunnel design is shape of the opening. Not all tunnels are excavated in circular shape; particularly drill and blast tunnels are excavated in horseshoe or inverted-D in shape. Unlike circular tunnel, tunnels in these shapes will have relative stress concentration and distressing around the tunnel periphery. Hoek and Brown (1980) presented stress diagrams for tunnels in elastic medium in different shapes and stress ratios (Figure 8). Accordingly, Hoek and Brown (1980) suggested coefficients for the ratio of tangential stress to vertical stress with respect to stress ratio for different shapes of tunnel, each at the roof and the side walls. These show that, at high degree of stress anisotropy, the tangential stresses will be lesser at the wall but higher at the crown of inverted-D shaped tunnel compared to circular tunnels. When tangential stresses exceed strength of the rock mass, rock bursting or spalling will result in competent rocks; whereas in weak and schistose rocks squeezing will be observed (Nilsen and Palmström, 2000).

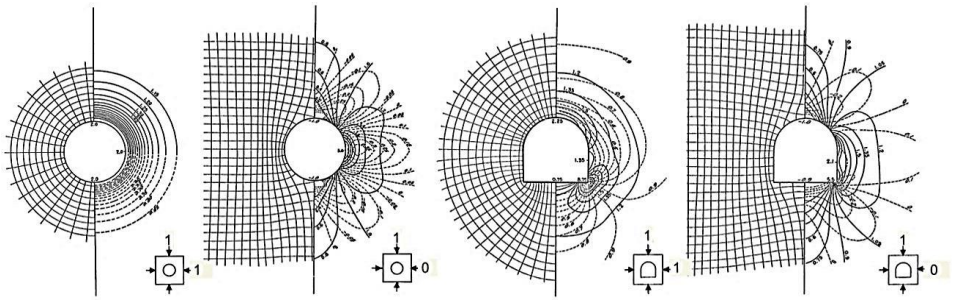

Figure 8: Stress diagrams in elastic medium at uniform and non-uniform strsses in circular and inverted-D shaped tunnels (Hoek and Brown, 1980)

2.3 Long term deformation

Whereas the instantaneous deformation in tunnel is a result of yielding of rock mass due to tunnel excavation progress and stress redistribution around it, long term deformation in tunnel is further enhanced by the creep effect. Creep has a significant effect in time dependent deformation of rock mass which may occur under long term exposure to a constant load subjected to the rock mass. It is essentially a time dependent behavior of rock mass where strain increases without increment of stress on the rock mass. Creep in rock mass is characterized by three stages, namely primary creep, secondary creep and tertiary creep (Goodman, 1989). During the primary creep event, the strain increment at the initial stage is rapid but decreases with time. The secondary creep takes place at higher deviatoric stresses where the strain rate increment is virtually constant, and the tertiary creep occurs when the load is near the peak strength of the rock material showing increment in strain rate with time that eventually results to failure as shown in Figure 9 (Goodman, 1989).

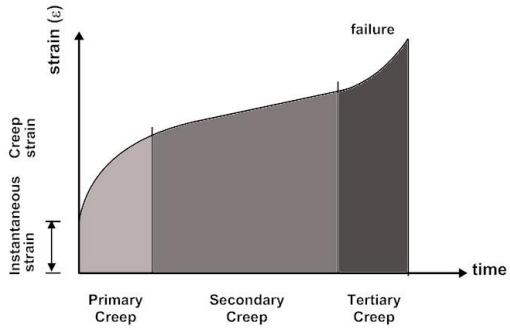

Figure 9: Idealized creep curve (based on Goodman, 1989)

Time dependent deformation

Time dependent behaviors can be modelled either by simulating creep characteristics of the rock mass in rheological models or by empirical methods. If laboratory data of the creep characteristics are available, tunnel creep curves can be fitted. Various rheological visco-elastic and visco-plastic models (Goodman, 1989; Pan and Dong, 1991a, b; Gioda and Cividini, 1996; Sterpi and Gioda, 2009, Debernardi and Barla, 2009) have been presented for this purpose, where a number of mechanical elements, such as spring, dashpot, slider that account for material stiffness, viscosity and strength of the rock mass are composed. Goodman (1989) presented five different creep visco-elastic models; namely Maxwell body, Kelvin or Voigt body, generalized Maxwell body, generalized Kelvin body and Burgers body that may fit creep behavior of the rock mass. The Maxwell model assumes that the creep behavior is linear whereas Kelvin model has

exponentially decreasing strain rate. The generalized Maxwell body initially has an exponential strain rate and becomes constant later. The generalized Kelvin model includes the instantaneous strain that is followed by strain at an exponentially decreasing rate, whereas the Burgers model is a combination of Maxwell and Kelvin models in a series that includes instantaneous strain followed by strain at an exponentially decreasing rate and finally becomes constant.

Most of the rock mass behaves plastically once stress exceeds strength of the rock mass. Visco-plastic time dependent models are believed to represent the tunnel response associated with severely squeezing condition. With advent of powerful computers, numerical modelling is now very common in addressing complex creep visco-plastic models. Few of visco-plastic constitutive models practiced today are Burgers-creep visco-plastic model combining Burgers creep model with Mohr-Coulomb model (CVISC) (Itasca, 2009) and Stress hardening elasto-visco-plastic model (SHELVIP) (Debernardi and Barla, 2009). Empirical models such as power law (Obert, 1965), exponential law (Singh and Mitchel, 1968) and hyperbolic law (Mesri et al., 1981; Phienwej et al., 2007) are also practiced. Benefit of empirical models is that these are directly derived from the observed relationships of time, stress, and strain or strain rate of creep test results (Phienwej et al, 2007).

Despite the fact that these simple to advanced creep models are simulated in numerical modeling, representation of rock mass creep properties is always an important issue. Whereas in-situ creep tests are rarely conducted, creep properties of rock mass as input parameters in simplified analytical or in numerical modelling are often based on limited laboratory data. Therefore, reliability in estimation of time dependent deformation in tunnels depends on the accuracy of creep input parameters.

The Convergence Law

Panet (1979) proposed elastic solutions for convergence of tunnel walls as a function of distance to the tunnel face. Sulem et al. (1987b) proposed analytical solution for the determination of wall displacements and ground pressure acting on the tunnel support for the case of time dependent stress, strain and failure behavior around a circular tunnel in a creeping rock mass with plastic yielding; the results of which allow time effects to be included in the convergence confinement method. This solution was in coherent with the convergence law presented by Sulem et al. (1987a) which states that closure in tunnels must be expressed as a function of distance to the tunnel face and time of excavation. Earlier, Sulem et al. (1987a) presented a curve fitting technique in order to determine total tunnel displacement based on such information. Accordingly, convergence ($C_{(x,t)}$) at distance (x) in meter from the tunnel face and t days from the time of tunnel excavation can be estimated using Equation (4).

$$C_{(x,t)} = C_{\infty x}\left[1 - \left(\frac{X}{x+X}\right)^2\right]\left[1 + m\left\{1 - \left(\frac{T}{t+T}\right)^n\right\}\right] \quad (4)$$

Here, X is a length related to the distance of influence of the tunnel face, T is a characteristic parameter of the time dependent properties of the ground, $C_{\infty x}$ is an instantaneous closure as obtained in the case of an infinite rate of face advance, m represents increment of instantaneous deformation due to effect of rheology, and n is a constant normally taken as 0.3. A typical example of tunnel deformation according to time advance and corresponding face distance is shown in Figure 10.

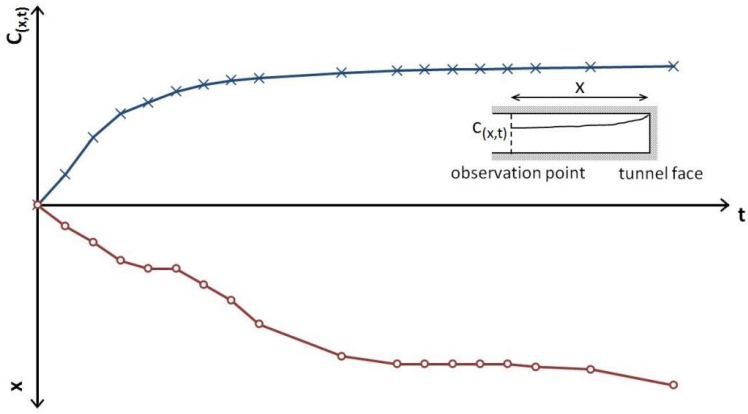

Figure 10: Typical convergence and tunnel face distance against time

The Equation (4) can be divided into two components, i.e., time independent ($C_{(x)}$) and time dependent ($C_{(t)}$) closures represented by Equations (5) and (6), respectively.

$$C_{(x)} = C_{\infty x}\left[1 - \left(\frac{X}{x+X}\right)^2\right] \quad (5)$$

$$C_{(t)} = C_{\infty x} m\left[1 - \left(\frac{X}{x+X}\right)^2\right]\left[1 - \left(\frac{T}{t+T}\right)^n\right] \quad (6)$$

These equations are very much practiced in predicting tunnel deformation, back calculating lost displacement (Panet, 1996; Schubert et al., 2003; Barla et al., 2008; Vu et al., 2013;) and in estimation of time independent and dependent tunnel displacements (Kontogianni et al., 2006; Asadollahpour et al., 2014). The significance of the above equations lies in the fact that the time dependent deformation and the final closure in

tunnel can be estimated based on convergences actually measured with respect to distance to tunnel face and time of excavation. This procedure can ensure reliable prediction than the simplified analytical solution which is based on limited laboratory data of creep characteristics of rock mass.

2.4 Tunnel squeezing

International Society for Rock Mechanics (ISRM) (in Barla, 2001) defines squeezing as *the time dependent large deformation which occurs around the tunnel and is essentially associated with creep casued by exceeding a limiting shear stress.*

Early definition of squeezing is cited to Terzaghi (1946) and later various authors (Jethwa et al., 1984; Adyan et al., 1993; Kovari, 1998; Barla, 1995; Hoek and Marinos, 2000) have documented and described squeezing phenomenon in various tunnels. Barla (2001) summarizes that squeezing is synonymous of overstressing of rock mass around tunnel and does not include deformations due to loosening of jointed rock mass in tunnel, such as rock bursting, spalling, etc.; and that magnitude of tunnel convergence associated with squeezing, the rate of deformation, and the extent of yielding zone around the tunnel depend on the geological conditions, the in-situ stresses relative to the rock mass strength, the ground water flow, pore pressure and the rock mass properties. Thus squeezing, predominantly in weak rock and particulate rock mass, is cumulative of the deformation at the early stage during excavation termed as 'instantaneous deformation' and the deformation resulted due to creep as time elapses.

Potentiality and degree of tunnel squeezing

Potentiality and estimation of large tunnel deformation (squeezing) in weak rocks can be done using empirical and semi-analytical methods. At an early stage of tunnel design when there is little information available, squeezing can be estimated using empirical relations. Two empirical relations are worth mentioning in this regard. Singh et al. (1992) proposed a demarcation line above which possibility of tunnel squeezing can be expected. The suggestion was based on overburden and Q-values of rock mass of tunnels from the Himalayan region. Since the rock mass Q-value has already accounted for rock stress effect, this criteria has double effect of stress (Panthi, 2006). In order to avoid contradiction of the double effect of stress in the relationship proposed by Singh et al. (1992); Goel et al. (1995) proposed squeezing and non-squeezing criteria using rock mass number which is the Q-value without the stress reduction factor (SRF) and width or diameter of the underground opening.

The limitation of the above suggestions is that the magnitude of potential tunnel deformation cannot be estimated. Kovari (1998) suggested relation that estimates radial displacement in a circular tunnel based on vertical stress, stress on lining, modulus of

elasticity, Poisson's ratio, cohesion and friction angle of rock mass and a coefficient 'k' which varies according to the ratio of plastic radius and tunnel radius. Though this method does not tell exact value of 'k' but identifies that deformation in tunnel is affected with change in modulus of elasticity of the rock mass (Shrestha, 2005). Hoek and Marinos (2000) showed that tunnel strain can be related to ratio of rock mass strength and vertical stress. Based on the closed form analytical solutions for circular tunnels in isostatic stress field performed by Duncan-Fama (1993) and Carranza-Torres and Fairhurst (1999), Hoek and Marinos (2000) found that there was good correlation between tunnel strain with ratio of rock mass strength and vertical stress, the trend line of which is presented as Equation (7). Furthermore, the effect of tunnel support in the tunnel strain was also presented as Equation (8).

$$\frac{\delta_i}{d_0} = 0.2 \times \left(\frac{\sigma_{cm}}{\sigma_v}\right)^{-2} \tag{7}$$

$$\frac{\delta_i}{d_0} = \left(0.2 - 0.25 \times \frac{p_i}{\sigma_v}\right) \times \left(\frac{\sigma_{cm}}{\sigma_v}\right)^{\left(2.4\frac{p_i}{\sigma_v} - 2\right)} \tag{8}$$

Where, δ_i is tunnel side wall deformation in meters, d_0 is original tunnel diameter in meters, p_i is internal support pressure in MPa, σ_v is vertical stress in MPa, and σ_{cm} is rock mass strength in MPa. Equation (7) is used to compute tunnel strain when support pressure is applied, and Equation (8) is used when there is no or negligible support pressure in the tunnel.

Advantage of this Hoek and Marinos approach is that, the relationship can be used to first-estimate potentiality of squeezing in weak rocks at depth. The relationship is relatively simple, requiring only the rock mass strength and support pressure as input and the vertical stress can be computed using rock cover and specific weight of the overlying rock mass.

2.5 Tunnel stability subject to plastic deformation

The Q and RMR rock mass classification systems are probably the most used tool in tunnelling and underground works. Application of these two systems is not only limited to classify rock mass but also in estimating support requirement in an empirical approach. During subsequent tunnelling, respective rock mass parameters required to compute the overall rock mass quality are recorded following any of the classification system, and required support are readily chosen from standard charts or tables (Barton et al., 1974; Grimstad and Barton, 1993; Bieniawski, 1973 and 1989). However, these systems do not quantify deformation in tunnel or be used in optimization of support such as in the CCM method. Whereas, Hoek and Marinos (2010) states that the GSI classification system is to be used as an input in the Hoek and Brown failure criterion

(Hoek et al., 2002) in estimating rock mass strength, which can eventually be used in the semi-analytical and analytical solutions.

Tunnels subjected to plastic deformation can be handled with appropriate support measures. Support offers resistance to convergence of tunnel walls. Such resistance pressure is defined as support pressure experienced by the applied support. As the inward movement of ground depends on rock mass quality and in-situ stresses, correspondingly resistance pressure varies according to its stiffness and maximum capacity (Panet, 2001). Support pressure p_i in a circular tunnel (in MPa) can be defined (Carranza-Torres and Fairhurst, 2000) by Equation (9).

$$p_i = K_s u_r \tag{9}$$

Where, K_s is elastic stiffness of the applied support (in MPa/m) and u_r is the corresponding radial displacement (in meters). K_s basically depends on material properties and dimension of the applied support and is responsible for the instant load bearing capacity of the support. If a compound support is applied and is assumed to behave linearly elastic, stiffness of such compound support will be the sum of the stiffness of each of the support elements (Oreste, 2003b). Various types of supports, their stiffness and maximum capacities (p_{max}) as closed rings in various diameters have been discussed and derived by Hoek and Brown (1980), Hoek (1998), Brady and Brown (2006), Carranza-Torres and Fairhurst (2000), Panet (2001) and Oreste (2003a, b).

The Convergence Confinement Method

The response of support and resulting closure in a tunnel can be represented by Support Characteristic Curve (SCC). For the purpose of rock support interaction in tunnels, SCC together with GRC and LDP can be incorporated in the CCM method. A typical simplified example is shown in Figure 11. Support can be applied at x^A distance from face when the ground would already have u_r^A displacement. The support will come in effect gradually as characterized by the elastic stiffness K_s. It eventually reaches an equilibrium point A where the characteristic lines of the ground and support intersect; resulting in further displacement of tunnel wall (u_r^{AA}-u_r^A) at which the effective support pressure will be p_i^A. Otherwise, the support can be applied at x^B distance from the face that will result in a new equilibrium point B and corresponding displacement in the tunnel wall by u_r^B. Though the displacement is high at this stage, the required support pressure will be p_i^B. At this lowered support pressure requirement, support with lower capacity (p'_{max}) can be applied instead of stronger or heavier support required in the previous case.

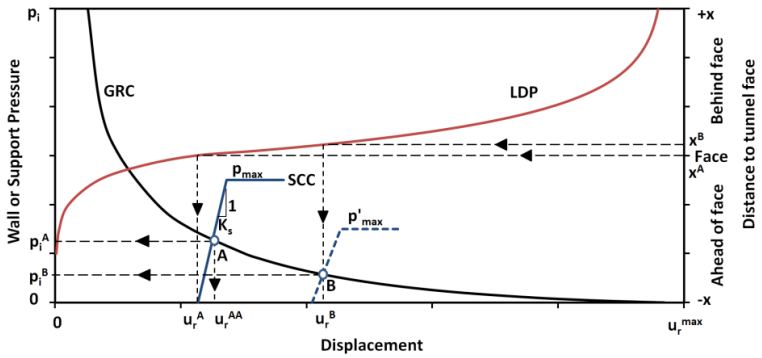

Figure 11: Typical representation of ground reaction curve, support characteristic curve and longitudinal deformation profile of a circular tunnel

Rock support interaction and the determination of the support requirement using the above method should consider two further important issues; namely time dependent deformation due to rheological properties of the rock mass and time dependent strength development of the applied rock support (Pan and Dong, 1991a and 1991b)). In weak and schistose rock mass when the time dependent effect takes place, the characteristic curve will be such that exhibits additional deformation of (u_r^t-u_r^{AA}) as shown in Figure 12, thereby imposing additional pressure on rock support by (p_i^B-p_i^A). Often, ground improvement will be necessary ahead of the tunnel face. The advantage of ground improvement is that the tunnel will be subjected to less deformation (u_r^C) and thus will require less support pressure (p_i^C).

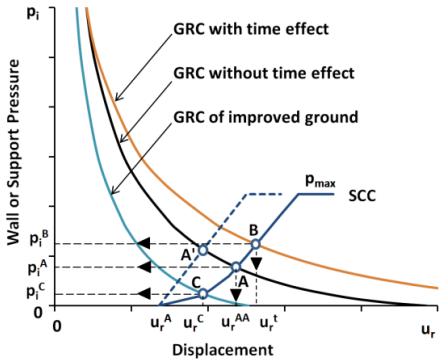

Figure 12: Schematic rock support interaction with and without time effect and of improved ground

Support like, for example shotcrete has time dependent behavior in attaining its peak strength and elastic modulus (Chang and Stille, 1993; Oreste, 2003b). As elastic stiffness and maximum support capacity of shotcrete are dependent on its elastic modulus and compressive strength, respectively; SCC of shotcrete will be non-linear as shown in the Figure 12. Oreste (2003b) presented a procedure for the determination of SCC of shotcrete lining as a circular ring that accounts for its time dependent behavior. Such non-linear behavior of support results in increased tunnel deformation as the peak elastic stiffness is attained, whereas a linear SCC would achieve an equilibrium point with GRC at *A'* resulting in a lower degree of deformation but higher support pressure would be required.

Threshold of tunnel strain to instability

Sakurai (1983) stated that tunnel strain level in excess of approximately 1% is associated with onset of tunnel instability. Later, Chern et al. (1998) also presented similar data. Hoek and Marinos (2000) presented potentiality of squeezing in tunnels which is categorized into five classes according to the magnitude of tunnel strain, as shown in Figure 13. According to this categorization, difficulty in tunnelling builds up once rock mass strength falls below 40% of the in-situ stress level, and it escalates substantially once the ratio of the rock mass strength to in-situ stress falls below 20%.

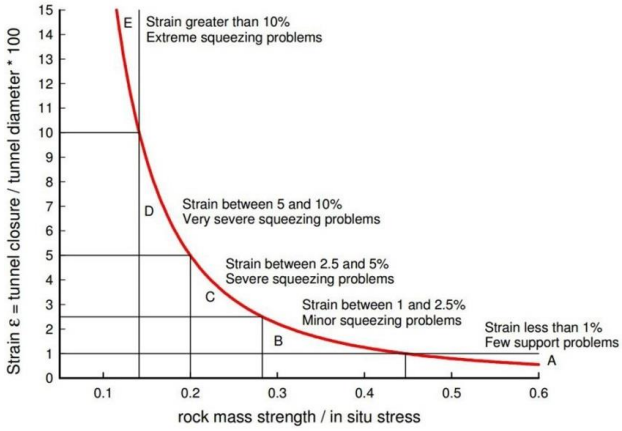

Figure 13: Approximate tunnel strain with degree of difficulty associated with tunnel squeezing at no support (Hoek and Marinos, 2000)

Tunnel convergence may terminate or continue to deform depending upon whether the tunnel is allowed to deform at an early stage or not. If the tunnel is restrained to deform, then stress accumulates on the tunnel support. Application of heavy support is not always the optimum solution. Excavating a tunnel at a larger geometry to

accommodate possible tunnel deformation has to be such that it does not trigger further instability of the tunnel. An optimum process known as 'rock support interaction' using the CCM method is always desirable in weak and schistose rock mass. In the context of excavating tunnel at fairly large size to allow tunnel deformation or excavating in stages so that squeezing potentials are manageable, conventional tunnelling methods like using drill and blast or road heading offer flexibility. Barla (2001) therefore, states that in deep tunnels whenever severely squeezing conditions are anticipated; conventional tunnelling is preferred over mechanized tunnelling. Nevertheless, there always remains uncertainty of rock mass characterization resulting in inaccuracies in estimation of tunnel strain and corresponding support requirement. In this aspect, uncertainty analysis (Panthi, 2006; Panthi and Nilsen, 2007) is an alternative option in ascertaining possible risks in tunnel excavation.

3. Methodology

3.1 General methodology

The works in this PhD study are mainly based on actually instrumented field data and laboratory assessments. Actual tunnel deformation records are the primary data based on which back analyses have been conducted in most of the tasks accomplished in the study. The general methodology adopted in this thesis work is presented in Figure 14; however, case specific changes in the methodology have been made accordingly.

Important input parameters such as rock mass parameters and applied rock support were obtained during subsequent tunnel excavations. Rock mass qualities at the studied locations were based on tunnel mapping logs, whereas mechanical properties such as uniaxial compressive strength of intact rock were obtained from laboratory tests done during constructions. Since the case studied projects were completed few years back, only limited rock samples from tunnel core log were available for further laboratory tests by the candidate himself at the NTNU rock mechanical laboratory. In addition, Panthi (2006) conducted laboratory tests on rock samples from the studied tunnel projects, and the resulted data have been used in this thesis. Few other input parameters, such as in-situ rock stresses have been estimated based on field measured rock stresses (Nepal, 1999) at the project areas or at nearby locations. In addition, few additional laboratory tests such as x-ray diffractions (XRD) tests on rock samples from the tunnel cores have also been performed at the NTNU laboratory.

Analytical and numerical approaches are the principal methods used for analyzing the deformation behavior of selected tunnel sections. The results by each of the methods are compared with actual deformations. Adopted analytical methods used in the analysis are those mostly practiced in the rock mechanics and rock engineering field; whereas the FLAC^{3D} code (Itasca, 2009) has been used as a numerical method. Finally the results are synthesized such that relationships among rock mass property, in-situ stresses and support pressures are established.

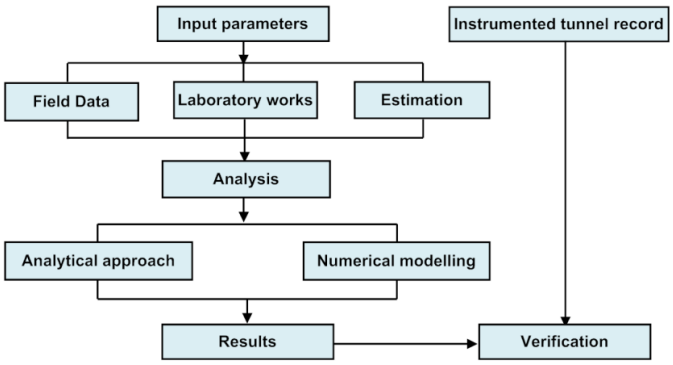

Figure 14: General methodology used in the PhD study

3.2 Paper specific approach of analysis

3.2.1 Paper I

Approach of the analysis in Paper I was to estimate omitted tunnel deformations and verification of such deformations by using analytical and numerical methods. The recorded measurements were the prime input data, whereas the rock mass properties were estimated based on the laboratory results and on-site evaluated rock mass qualities. Moreover, the in-situ stresses were estimated based on in-situ stress measurement records in areas surrounding the tunnel project location. The Convergence Law proposed by Sulem et al. (1987a, b) was used to compute tunnel displacements and these were compared with actually measured displacements. Displacement variables were chosen based on the best fit curves, and early tunnel displacements were estimated accordingly. Elasto-plastic analyses were conducted for each of the tunnel sections and early displacements were computed using the Convergence Confinement Method. Further, FLAC^{3D} numerical modelling was done for each tunnel section. The resulted early displacements by these three methods were compared and discussed. Schematic diagram of the approach adopted in the paper is presented in Figure 15.

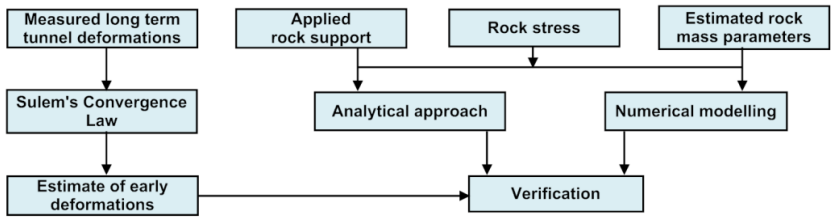

Figure 15: Approach of analysis used of the Paper I

3.2.2 Paper II

First, the rock mass parameters were back calculated using the Hoek and Marinos (2000) approach. Actual deformation measurements, tunnel logs and laboratory tested uniaxial compressive strength data were used as input. All together 77 different tunnel sections were selected where tunnel strain exceeded 2%. Elasto-plastic analyses were conducted for each of the tunnel sections, primarily considering a uniform stress equivalent to the vertical stress and the tunnel was assumed circular of equivalent area of the actual tunnel sections. In order to evaluate rock mass response in the tunnel, tunnel deformations in each tunnel section were computed for support pressures ranging from 0 to 2.4 MPa. Trendlines were established between tunnel strain (ε) and ratio of shear modulus (G) and vertical stress (σ_v) for each support pressure value. Next, numerical modelling was done in twelve representative tunnel sections. The ratio (k) of horizontal (σ_h) to vertical stresses (σ_v) varied in the selected tunnel sections from 0.22 to 0.38. The modelled tunnel section was inverted-D in shape representing actual tunnelling condition. Similar to the analytical approach, tunnel wall displacements were computed numerically in each tunnel section for support pressure ranging from 0 to 2.4 MPa; and trendlines were established between resulted tunnel strain (ε) at spring level and ratio of shear modulus (G) and vertical stress (σ_v) and stress ratio (k). The approach adopted in this paper is shown in Figure 16.

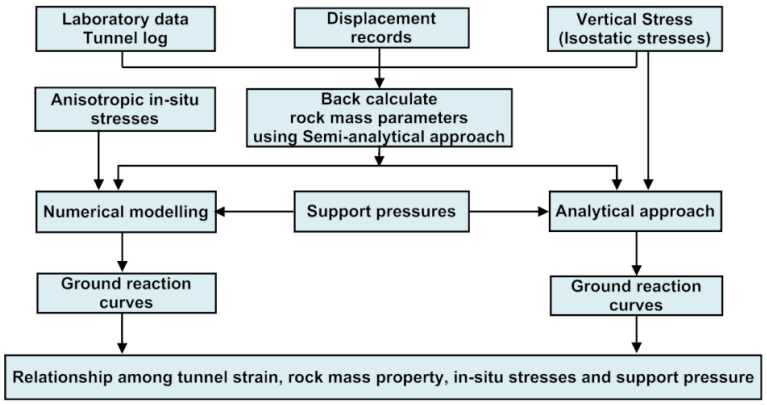

Figure 16: Approach of analysis of the Paper II

3.2.3 Paper III

Long term deformation records of 24 tunnel section from three tunnel projects were analyzed individually using the curve fitting technique by Sulem et al. (1987a, b) such that instantaneous (time independent) and time dependent deformations were categorically identified for the each tunnel case. Finally co-relationship between rock

mass shear modulus (G), vertical stress (σ_v), ratio (k) of horizontal stress (σ_h) to vertical stress (σ_v), support pressure (p_i) and tunnel strain (ε) were established. The approach of analysis adopted in this paper is presented in Figure 17.

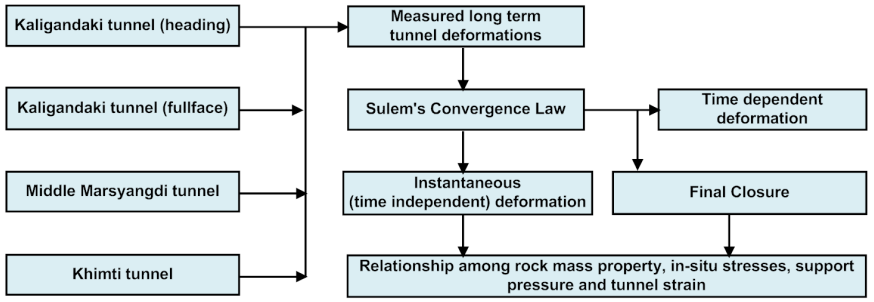

Figure 17: Approach of analysis of the Paper III

3.2.4 Paper IV

Instrumentation records of deformation of tunnel walls and surrounding rock mass and measured support pressures were used to evaluate rock mass parameters in this paper. Based on the semi-analytically determined rock mass parameters, analytical analysis and numerical modelling for each of the cases were performed. Finally, the resulted tunnel deformations around the tunnel walls and surrounding rock mass were compared and discussed. Figure 18 presents the approach of analysis used in this paper.

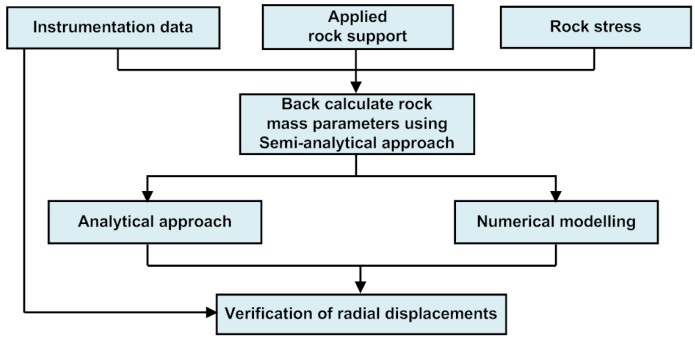

Figure 18: Approach of analysis of the Paper IV

3.2.5 Paper V

In this paper, a semi analytical approach was used to back calculate rock mass parameters and numerical modelling was done incorporating groundwater effect in the tunnel that was subjected to plastic deformation. The resulting tunnel deformation was verified with the actually recorded deformations in the squeezed tunnel in faulted rock mass. Numerical simulation was done to evaluate the effect of groundwater in tunnel deformation. The approach adopted in this paper is presented in Figure 19.

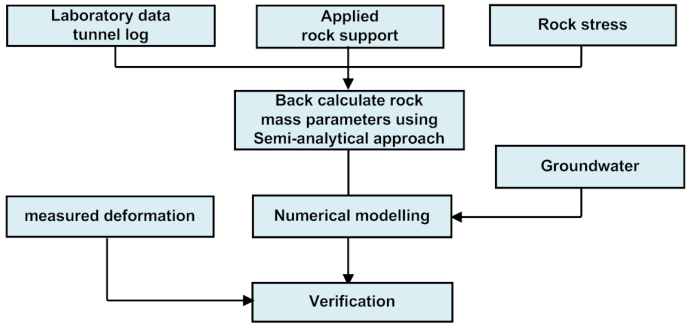

Figure 19: Approach of analysis of the Paper V

4. Results and discussions

4.1 Paper composition

Immediate tunnel stability is a prime matter of concern during excavation where rock mass quality, rock stress and rock support are key parameters that influence the stability of tunnels. As the tunnel advances and when the face effect ceases, stability of the tunnel reaches a critical stage. In addition, time dependent rheological behavior of the rock mass imposes further stress on applied support or leads to further deformation of the tunnel. This PhD study has been focused on these issues with tunnel cases from the Nepal Himalaya. Five papers have been selected for this thesis those cover various aspects of tunnel stability subjected to plastic deformation. Paper I evaluates stability of tunnels in schist and schistose mica gneiss rock mass. Paper II analyses 77 tunnel cases where high degree of stress anisotropy exist. The effect of stress anisotropy together with rock mass quality and support pressure in tunnel deformation are analyzed. Paper III distinguishes time independent and time dependent deformations in long term tunnel deformation; whereas Paper IV addresses the behavior of radial displacement of rock mass surrounding tunnel openings in stress anisotropic condition which is based on instrumentation records. Finally, Paper V presents tunnel instability at relatively shallow depth in faulted rock mass where groundwater aggravated the tunnel instability leading to squeezing conditions. Composition of the papers in the PhD study is presented in Figure 20.

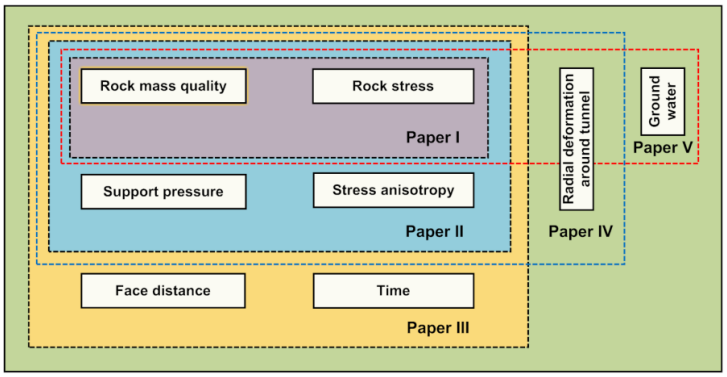

Figure 20: Composition of the papers used in the PhD study

4.2 Results and discussions

4.2.1 Paper I

Shrestha, P.K. and Panthi, K.K. (2014). Analysis of the plastic deformation behavior of schist and schistose mica gneiss at Khimti headrace tunnel, Nepal. Bulletin of Engineering Geology and the Environment, vol. 73(3). pp. 759-773.

Tunnel deformation records are often omitted at the early stage of excavation. The tunnelling crew may often overlook possibility of time dependent deformation of rock mass around the tunnel. During excavation of Khimti headrace tunnel, deformations were recorded only after several days of excavation and when the tunnel face had advanced well ahead. This paper analyses the plastic deformation behavior of four typical sections of the headrace tunnel excavated in schist and schistose mica gneiss. The analysis has been conducted in consideration of time of excavation, distance from tunnel face, in-situ stress, rock mass quality and applied rock support.

The analysis using the Sulem's approach shows that the computed and measured displacements match very well. Results of the analyses also show that there can be several combinations of deformation parameters in the Sulem's approach that can yield low value of errors. The final closures, which are the results of combination of deformation parameters m and $C_{\infty x}$, are close to actual values. However, a large variation in values of $C_{\infty x}$ can exist that can be governed by the value of m. An alternative approach of finding the value of $C_{\infty x}$ is using analytical or numerical methods. Accordingly, the resulted displacements using analytical and numerical methods were found to be comparable to the instantaneous deformations estimated by the Sulem's approach. This led to establish a basis to adopt this approach in the analysis of long term displacement records in the other tunnel projects, such as those presented in Paper III.

Analytical and numerical solutions of the failed tunnel cases of Khimti headrace tunnel shows that, the tunnels would have lesser degree of deformation at early stages, whereas as the time progresses, considerable displacement occurred. Such increments in deformations are noticeable particularly in two of the selected tunnel sections in schist and schistose mica gneiss. Moreover, high displacements were noticed particularly at the unsupported invert and at the walls of the tunnel sections.

Further, numerical analyses showed that, when horizontal to vertical stress ratio (k) was close to unity or where the deviatoric stress (σ_v - σ_h) was less, the failure zones around the tunnels were elliptical shape as shown in Figure 21 (a), (b) and (d). Similarly, the tunnel section having the lowest stress ratio (k) had higher deformation in the walls. At such high anisotropic stress situation, plastic region around the tunnel becomes a butterfly-like shape as shown in Figure 21 (c). These results are similar to

those presented by Detournay and John (1988) as in the Figure 7 and as discussed by Carranza-Torres and Fairhurst (2000). The instantaneous deformation computed by the Sulem's approach for this typical case of high degree of stress anisotropy deviated significantly from that computed by the Convergence Confinement Method. This indicates that the CCM method considering average of horizontal and vertical stress estimates lower amount of deformation in the tunnel walls subjected to high degree of stress anisotropy.

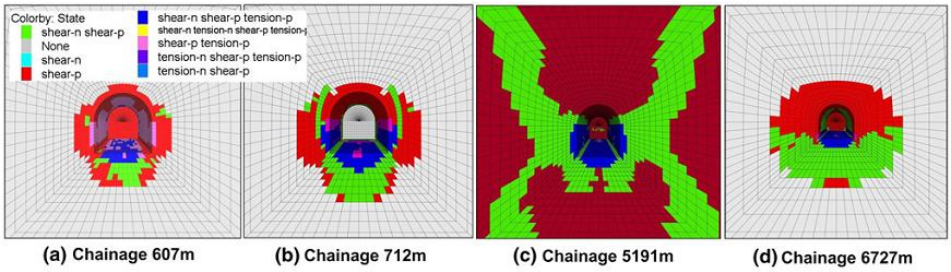

Figure 21: Plastic regions around the Khimti tunnels

4.2.2 Paper II

Shrestha, P.K. and Panthi, K.K. (2014). Assessment of the effect of stress anisotropy on tunnel deformation in the Kaligandaki project in the Nepal Himalaya. Bulletin of Engineering Geology and Environment. Published online 15 July 2014. DOI 10.1007/s10064-014-0641-5.

This paper has been prepared on this basis that deformation pattern in the tunnel will be altered by the effect of change in the assumptions made in the analytical solutions. This paper thus assesses response of ground with respect to in-situ stresses and support pressure by analytical and numerical approaches; where numerical modelling is done for inverted-D shaped tunnels in actual stress anisotropy condition.

One of the important rock mass properties that exhibit rock mass deformation is the deformation modulus (E_{rm}). When rock mass around a tunnel opening is subjected to induced stresses, behavior of the rock mass that undergoes deformation is a matter of interest towards support design. Therefore, rigidity modulus (or shear modulus, G) of the rock mass has been adopted in the assessment of deformation behavior of the rock mass in relation to support pressure and in-situ stresses.

The outcome of the analysis shows that there is a good correlation between these parameters, and a relationship can be established that estimates tunnel strain at plane strain condition at any given value of the other parameters. First, this relationship was formulated from the results of elasto-plastic analyses of 77 tunnel sections that had

more than 2% tunnel strain. A power function was established between tunnel strain (ε) and the ratio of shear modulus (G) and in-situ vertical stress (σ_v) in which the constants of the function could be estimated for any value of support pressure (p_i). On this basis, it was envisaged that a similar relationship could also be established in an anisotropic stress environment. Numerical analyses on selected 12 tunnel sections at stress ratios ranging from 0.22 to 0.38 revealed that tunnels in such non-uniform stress environment would have lesser degree of deformation compared to that in isostatic vertical stress conditions. It was also observed that the tunnel crown would have rather closer deformation to those considering average of vertical and horizontal stress condition; on the other hand, the tunnel walls would have deformation values in-between the average in-situ stress and isostatic vertical stress conditions. The relationship formulated for the analytical solution can thus be updated with the effect of stress anisotropy represented by stress ratio (k) and is presented as Equation (10). The constants of the power function can be computed for any support pressure value (p_i). Relationship of support pressure and the power function constants at tunnel spring level are presented in Equations (11) and (12).

$$\varepsilon_{spl} = a_{spl} \left(\frac{2G}{\sigma_v(1+k)/2} \right)^{b_{spl}} \tag{10}$$

$$a_{spl} = 742.23\, {p_i}^2 - 1870.6\, p_i + 1654.7 \tag{11}$$

$$b_{spl} = -0.1541\, {p_i}^2 + 0.2022 p_i - 2.0003 \tag{12}$$

4.2.3 Paper III

Shrestha, P.K. and Panthi, K.K. (2014). Predicting plastic deformation in tunnels – an analysis based on tunnel cases from the Nepal Himalaya. Under review in Rock Mechanics and Rock Engineering. Submitted on 16 September, 2014.

Basis for the works in this paper are Paper I and II. Whereas Paper I showed that long term deformation in tunnel can be a good reference for assessment of instantaneous deformation in tunnel, Paper II formulated a relationship to predict tunnel deformation. Paper III evaluates long term deformations of 24 tunnel sections in four different rock mass conditions from three tunnel projects in order to assess time independent and dependent components in total deformation in the tunnels.

At the time of tunnel excavation, the prime concern will obviously be the immediate stability of the tunnel, but as the tunnel progresses, weak and schistose rock continue to deform generating extra pressure on applied support. Therefore, tunnel support should be designed in such a way that future possible tunnel deformation is also addressed. If longitudinal tunnel deformation records are available, it may be possible to

estimate such future tunnel deformation. The curve fitting procedure based on the Convergence Law proposed by Sulem et al. (1987a, b) is a useful tool in this endeavor. Accordingly, Paper III computes instantaneous and final closures determining time independent and dependent variables; and correlates such deformations with respect to rock mass shear modulus (G), support pressure (p_i), vertical stress (σ_v), and horizontal to vertical stress ratio (k); similar to that presented in Paper II.

In a way forward, this paper presents a simplified single relationship among these four parameters instead of the three relationships used in Paper II. Here, the support pressure (p_i) is incorporated as numerator in the ratio of shear modulus (G) and vertical stress (σ_v) and stress ratio (k). Relationships for instantaneous and final strain are based on the trend lines having goodness of fit, and are presented as Equation (13) and (14).

$$\varepsilon_{FC} = 4509 \left(\frac{2G(1+p_i)}{\sigma_v\,(1+k)/2} \right)^{-2.09} \tag{13}$$

$$\varepsilon_{IC} = 3065 \left(\frac{2G(1+p_i)}{\sigma_v\,(1+k)/2} \right)^{-2.13} \tag{14}$$

Usefulness of these equations also lies in the fact that long term time dependent tunnel strain as ($\varepsilon_{FC} - \varepsilon_{IC}$) can be estimated. Such time dependent strain (deformation) in tunnel increases considerably as the value of shear modulus or support pressure is reduced or in-situ stresses are increased. However, it is to be noted that the relative goodness of fit of the instantaneous strain compared to the final strain is slightly low, and therefore, some deviation in the instantaneous strain can be expected.

The paper also summarizes component of such time dependent tunnel deformation in total tunnel deformation according to rock mass type. Such values vary according to the parameters as presented in the Equations (13) and (14). However, general trend shows that such time dependent effect is high in schist and schistose mica gneiss; whereas augen mica gneissic rock mass are little affected. Similarly, micaceous phyllite rock mass have high time dependent deformation compared to siliceous phyllite rock mass containing quartzite as intercalation; and graphitic rock mass will have moderate effect of time in tunnel deformation. These results also signify that composition of rock minerals do affect the deformation characteristics of the rock mass. Presence of quartz or silica minerals contributes to lesser deformation while mica rich rock mass experience larger deformation.

4.2.4 Paper IV

Shrestha, P.K. and Panthi, K.K. (2014). Interpretation of deformation characteristics at Kaligandaki Headrace Tunnel using tunnel monitoring records. Submitted to 13th International ISRM Congress 2015, Montreal, Canada.

One of the important tasks in tunnelling is instrumentation and subsequent monitoring of ground movement and support pressures. Two prominent benefit of such monitoring of tunnel deformations are prediction of tunnel closure and back calculation of rock mass properties. Radial deformation of tunnel wall supplemented by deformation in the surrounding rock mass can be a good basis of evaluating rock mass properties through the back calculation process.

This paper evaluates the tunnel deformation records of multiple borehole extensometers (MPBX) installed at three locations and pressure cell records at five locations in four tunnel sections of Kaligandaki headrace tunnel. MPBX records show various degrees of deformation around the tunnel. Similar pattern was also observed in the pressure cell records. The tunnel sections lie in relatively better rock mass compared to the other tunnel sections presented in Paper II and III where tunnel strains exceeded 2%. The rock mass were of average quality having GSI values between 41 and 49, therefore the rock mass was assumed to behave in strain softening manner (Crowder and Bowden, 2004). Unlike elastic brittle and elastic-perfectly plastic behavior of rock mass, the strain softening behavior is relatively a complex task. The post failure behavior where strain softening occurs is difficult to be defined properly (Cai et al., 2007; Alejano et al., 2010). One approach in addressing such issue is use of numerical modelling where plastic strain increments can be determined by back analysis (Itasca, 2009).

2-dimensional plane strain numerical modelling of the tunnel sections with the rock mass as strain softening materials showed high degree of deformation occurred in the tunnel walls compared to the crowns; and plastic regions around the tunnels were butterfly-shaped, similar to the results obtained in Paper I. The analysis also revealed that tunnels in weak and medium strong rock mass in high degree stress anisotropy with vertical stress being major stress will have crowns subjected to tensional cracks whereas compressional failures occur at the walls.

Despite majority of the computed values matching the actual deformation values, few deviations were also observed. One reason of such deviations could be due to inhomogeneity in the rock mass caused by the presence of shear seams, local faults and presence of quartz vein, which is contrary to the assumption made as homogenous and continuous rock mass in the analyses.

4.2.5 Paper V

Shrestha, PK and Panthi, KK (2014). Groundwater effect on faulted rock mass - an evaluation of Modi Khola Pressure Tunnel in the Nepal Himalaya. Rock Mechanics and Rock Engineering, vol. 47(3), pp. 1021-1035.

The significance of this paper lies in the fact that if rock mass is poor, particulate and mixed with gouge material and that there is substantial groundwater effect, large tunnel deformation can be expected even at shallow depths. This paper presents and analyses a severe squeezing case in a tunnel excavated in a faulted rock mass in relatively shallow overburden and under water table. The tunnel was well supported using spilling, shotcrete and closely spaced steel ribs whereas the ground ahead of the tunnel face was improved by grouting. However, the invert was neither supported nor improved by grouting. Analyses show that one of prime reasons of tunnel collapse could be triggering of deformation in the form of invert heave, which ultimately led the wall to move inward and the crown to sink. Had steel strut been used in the invert, a significant reduction in the tunnel deformation would have been possible. However, this would not have stopped the tunnel to deform, particularly at the wall and crown.

Groundwater has a negative effect in the tunnel stability. Presence of effective pore pressure in rock joints causes a reduction in the shear strength of the rock mass (Barla, 2001). In the Modi tunnel, the rock mass was of particulate in nature mixed with fault gouge, presence of water in the rock mass therefore created a flowing condition. Further, numerical analysis with and without ground water showed that relative increment in the tunnel deformation due to groundwater was 4% to 30% depending upon distance from the tunnel face; with average value of 15%. Such effect was high at the spring level than at the crown.

4.3 Summary

The presented papers address issues of plastic deformations in tunnels in various rock mass conditions and stress environments. Moreover, the effects of time on total deformation in the three tunnels and a case of the effect of groundwater in tunnel squeezing are also presented. Paper I summarizes that, instantaneous displacement as computed by the Sulem's approach can be used for evaluation of rock mass parameters and assessment of tunnel stability. Paper II suggested an approach to estimate tunnel strain that also addresses stress anisotropy incorporating stress ratio (k) in a semi-analytical approach. Similarly, Paper III improved the relationship suggested by Paper II. A simplified solution is suggested for estimating instantaneous and final strains. Paper IV shows that inhomogeneity of rock mass can have varying degree of tunnel deformation; whereas Paper V shows how severe deformation can occur in tunnels in faulted rock mass subject to groundwater even if the tunnel is at shallow overburden.

4.4 Limitations

Stability analyses have been performed using 3-dimensional numerical modelling, but the relationships suggested in this study are based on the trendlines of results of 2-dimensional numerical modelling and analytical method. Therefore, some degree of deviation can be expected in estimation of tunnel strain. Accuracy of the results also lies in the reliability of input parameters used in this analysis. Further, the analyses have been done for deformation in the tunnel walls only, which happened to be the largest deformation recorded in most of the tunnel sections. Estimation of strain at tunnel wall only, can be one of the major limitations of the suggested procedure.

5. Conclusions and recommendations

Rock mass quality plays and important role in tunnel stability. Common characteristics of the rock mass in the studied tunnel cases are that the rock mass are schistose, deformed, weak and have low strength, have low degrees of rigidity against deformation and high degrees of strength anisotropy. Tunnels in such rock mass when exposed to high degrees of in-situ stresses are prone to plastic deformation. Such plastic deformations in tunnels can occur at the time of excavation and later. In order to ensure a stable tunnel, understanding the mutual relationship among rock mass property, in-situ stresses, rock support and tunnel deformation is a pre-requisite. This PhD research has addressed these issues.

5.1 Conclusions

On the basis of the studies conducted, following conclusions are drawn:

a. Understanding rock mass response upon tunnel excavation has significant importance when constructing tunnels through squeezing ground. Rock support interaction is always desirable in weak and schistose rocks; and the Convergence Confinement Method is a useful tool for this purpose but has its own limitation.

b. Stress anisotropy has a strong influence on the magnitude of tunnel deformation and, therefore, it should be incorporated in tunnel design.

c. The suggested relationship to estimate tunnel strain incorporating stress ratio together with shear modulus, support pressure and vertical stress can be a basis for an early estimate of tunnel deformation in weak to medium strong and schistose rock mass.

d. Sulem et al. (1987a, b) can be a useful tool in predicting long term tunnel deformation provided that good quality tunnel convergence data are recorded with respect to distance to the tunnel face and time of excavation. However, careful evaluation should be made while computing the deformation variables (m, T, X) and the instantaneous closure ($C_{\infty x}$).

e. The time dependent variables m and T in principle are independent from in-situ stresses and should have similar values for similar type of rock mass. In general,

the values presented in Paper III for different types of rock mass can be a useful reference for the prediction of long term deformation of tunnel walls in similar rock mass conditions. These data can be helpful only when the tunnel has just been excavated and monitoring of convergence has just begun, and no long term data are available yet.

f. Groundwater has an adverse effect in tunnel stability and should be considered in tunnel design. The magnitude of its effect, however, depends on the head of water (water pressure) over the tunnel.

5.2 Recommendations

The Himalayan geology is of complex nature; therefore, the limited studies made here can not represent vivid characteristics of rock mass and all tunnelling problems in that region. There always remains some degree of uncertainty. However, to make good use of the suggested approach, the following recommendations are made.

a. The study conducted is based on limited number of tunnel cases; therefore the suggested relationship must be validated using data from many other well-monitored tunnel projects so as to improve the prediction accuracy.

b. The suggested relationships are suitable for an early estimate of tunnel deformation. An analytical solution or numerical computation that incorporates stress anisotropy and the time effect is recommended to increase accuracy.

References

Aydan Ö., Akagi T., and Kawamoto T. (1993). The squeezing potential of rock around tunnels: theory and prediction. *Rock Mechanics and Rock Engineering,* vol. 2, pp. l37-163.

Alejano, L.R., Rodriguez-Dono, A., Alonso, E., and Fernandez-Manin, G. (2009). Ground reaction curves for tunnels excavated in different quality rock masses showing several types of post-failure behavior. *Tunnelling and Underground Space Technology*, vol. *24*(6), pp. 689-705.

Alejano, L.R., Alonso, E., Rodriguez-Dono, A., and Fernandez-Manin, G. (2010). Application of the convergence-confinement method to tunnels in rock masses exhibiting Hoek–Brown strain-softening behavior. *International Journal of Rock Mechanics and Mining Sciences*, vol. 47(1), pp. 150-160.

Asadollahpour, E., Rahmannejad, R., Asghari, A., and Abdollahipour, A. (2014). Back analysis of closure parameters of Panet equation and Burger's model of Babolak water tunnel conveyance. *International Journal of Rock Mechanics and Mining Sciences*, vol. 68, pp. 159-166.

Barla, G. (1995). Squeezing rocks in tunnels. *ISRM News Journal*, 3/4, pp. 44-49.

Barla, G. (2001): Tunnelling under squeezing conditions. In Tunnelling Mechanics, *Eurosummerschool,* Innsbruck, pp. 169–268.

Barla, G., Bonini, M., and Debernardi, D. (2008). Time dependent deformations in squeezing tunnels. *The 12th international conference of International Association for Computer Methods and Advances in Geomechanics (IACMAG),* Goa, India.

Barton, N., Lien, R., and Lunde, J. (1974). Engineering Classification of Rock Masses for the Design of Tunnel Support. Rock Mechanics, vol. 6, pp 189-236.

Bieniawski, Z.T. (1973): Engineering classification of jointed rock masses. *The Civil Engineer in South Africa*, Dec. pp. 335-343

Bieniawski, Z. T. (1989). Engineering Rock Mass Classification. A complete manual for Engineers and Geologist in Mining, Civil and Petroleum engineering. *John Wiley & Sons, Inc.*, 251p.

Brady, B.H.G., and Brown, E.T. (2006). Rock Mechanics for Underground Mining. *Kulewar Academic Publishers*, Third Edition Reprint. 628p.

Brown, E. T., Bray, J.W., Ladanyi, B., and Hoek, E. (1983). Ground response curves for rock tunnels. *Journal of Geotechnical Engineering,* vol. 109(1), pp. 15-39.

Cai, M., Kaiser, P.K., Tasaka, Y., and Minamic, M. (2007). Determination of residual strength parameters of jointed rock masses using the GSI system. *International Journal of Rock Mechanics and Mining Sciences*, vol. 41(1), pp. 3-19.

Carranza-Torres, C. (2003). Dimensionless graphical representation of the exact elasto-plastic solution of a circular tunnel in a Mohr-Coulomb material subject to uniform far-field stresses. *Rock Mechanics and Rock Engineering*, vol. 36(3), pp. 237-253.

Carranza-Torres, C. (2004). Elasto-plastic solution of tunnel problems using the generalized form of the Hoek-Brown failure criterion. *International Journal of Rock Mechanics and Mining Sciences*, vol. 41(3), pp. 480-481.

Carranza-Torres, C. and Fairhurst, C. (1999). The elasto-plastic response of underground excavations in rock masses that satisfy the Hoek-Brown failure criterion. *International Journal of Rock Mechanics and Mining Sciences,* vol. 36(6), pp. 777-809.

Carranza-Torres, C. and Fairhurst, C. (2000). Application of the convergence-confinement method of tunnel design to rock-masses that satisfy the Hoek-Brown failure criterion. *Tunnelling and Underground Space Technology,* vol. 15(2), pp. 187-213.

Chang, Y. and Stille, H., (1993). Influence of early age properties of shotcrete on tunnel construction sequences. *In Shotcrete for Underground Support VI, American Society of Civil Engineers,* Reston, pp. 110-117.

Chern, J.C., Yu, C.W., and Shiao, F.Y. (1998). Tunnelling in squeezing ground and support estimation. *Proceeding of Regional Symposium on Sedimentary Rock Engineering*, Taipei, pp. 192-202

Civil Construction Consortium (CCC), SA-HH JV. (2002). Construction Report. *Khimti 1 Hydropower Project*, vol. 1, main text.

Crowder, J.J. and Bawden, W.F. (2004). Review of post-peak parameters and behavior of rock masses: current trends and research. *Rocnews, fall. http://www.rockscience.com.*

Debernardi, D. and Barla, G. (2009). New Viscoplastic Model for Design Analysis of Tunnels in Squeezing Conditions. *Rock Mechanics and Rock Engineering*, vol. 42, pp. 259-288.

Deoja, B., Dhital, M., and Wagner, A. (1991). Mountain risk engineering handbook. *International Centre for Integrated Mountain Development (ICIMOD)*, Nepal.

Detournay, E. and Fairhurst, C. (1987). Two-Dimensional Elasto-plastic Analysis of a Long, Cylindrical Cavity under Non-Hydrostatic Loading. *International Journal of Rock Mechanics and Mining Sciences and Geomechanics*, vol. 24(4), pp. 197-211.

Detournay, E. and John, C.M.S. (1988). Design charts for a deep circular tunnel under non-uniform loading. *Rock Mechanics and Rock Engineering*, vol. 21(2), pp. 119-137.

Duncan-Fama, M.E. (1993). Numerical modelling of yield zones in weak rocks. *Comprehensive Rock Engineering*, vol. 2, pp. 49-75.

Fairhurst, C. and Carranza-Torres, C. (2002). Closing the circle. In J. Labuz and J. Bentler (Eds.), *Proceedings of the 50th Annual Geotechnical Engineering Conference*. St. Paul, Minnesota.

Gioda, G. and Cividini, A. (1996). Numerical methods for the analysis of tunnel performance in squeezing rocks. *Rock Mechanics and Rock Engineering*, vol. 29(4), pp. 171-193.

Goel, R.K., Jethwa J.L., and Paithankar, A.G. (1995). Indian experience with Q and RMR systems. *Tunnelling and Underground Space Technology*, vol. 10, pp. 97-109.

Goodman, R. E. (1989). Introduction to Rock Mechanics. *John Wiley and Sons*. 412 p.

Grimstad, E. and Barton, N. (1993). Updating the Q-system for NMT. In *Proceeding of International Symposium on Sprayed Concrete - Modern use of wet mix sprayed concrete for underground support,* pp. 46-66.

Himal Hydro and General Construction Ltd (HH) (2001). Construction Report. *Modi Khola Hydroelectric Project, Nepal*.

Hoek, E. (1998). Tunnel support in weak rock. Keynote address, *Symposium of Sedimentary Rock Engineering*, Taipei, Taiwan.

Hoek, E. and Brown, E.T. (1980). Underground Excavations in Rock. *Institute of Mining and Metallurgy, London*.

Hoek, E. and Brown, E.T. (1997). Practical estimates of rock mass strength. *International Journal of Rock Mechanics and Mining Sciences*, vol. 34(8), pp. 1165-1186.

Hoek, E., Carranza-Torres, C., and Corkum, B. (2002). Hoek-Brown Failure Criterion – 2002 Edition. *Proceedings of North American Rock Mechanics Society Meeting,* Toronto, Canada.

Hoek, E. and Marinos, P. (2000). Predicting Tunnel Squeezing Problems in Weak and Heterogeneous Rockmasses. *Tunnels and Tunnelling International*, vol. 32(11), pp. 34-46 and vol. 32(11), pp. 45-51.

Hoek, E. and Marinos, P.G. (2010). Tunnelling in overstressed rock. Rock Engineering in Difficult Ground Conditions- Soft Rocks and Karst – Vrkljan (ed), *Taylor Francis Group*, London.

Itasca Inc. (2009). FLAC^{3D} User's Manual. http://www.itascacg.com

Jethwa, J.L., Singh, B., and Singh, B. (1984). Estimation of ultimate rock pressure for tunnel linings under squeezing rock conditions – a new approach. Design and Performance of Underground Excavations, *ISRM Symposium, Cambridge, E.T. Brown and J.A. Hudson eds*., pp. 231-238

Kirsch, G. (1898). Die Theorie der Elastizitat und die Bedurinisse der Festigkeitslehre. V.D.J. vol. 42(29).

Kontogianni, V., Psimoulis, P., and Stiros, S. (2006). What is the contribution of time-dependent deformation in tunnel convergence?. *Engineering Geology*, vol. 82, pp. 264-267.

Kovari, K. (1998). Tunnelbau in druckhaftem Gebirge - Tunnelling in squeezing rock. *Tunnel,* vol. 5, pp. 12-31

Lamé, G. (1852). Leçons sur la théorie de lélasticité. Paris: Gauthier-Villars.

Marinos, P. and Hoek, E. (2000). GSI: a geologically friendly tool for rock mass strength estimation. In *Proc. GeoEng2000 Conference, Melbourne*, pp. 1422-1442.

Martin, C.D., Kaiser, P.K., and Christiansson, R. (2003). Stress, instability and design of underground excavations. *International Journal of Rock Mechanics and Mining Sciences*, vol. 40(7), pp. 1027-1047.

Mesri, G., Febres-Cordero, E., Shield, D.R., and Castro, A. (1981). Shear-stress-strain behavior of clays. *Geotechnique,* vol. 31(4), pp. 537-552.

Nepal Electricity Authority (NEA) (2002). Project completion report. Volume I-C, Headrace Tunnel, Volume IV-A, Geology and Geotechnical, Volume V-C Geological Drawings and Exhibits, *Kaligandaki 'A' Hydroelectric Project, Nepal*.

Nepal Electricity Authority (NEA) (2011). Project completion report. Volume 6C, Geology and Geotechnical Report, *Middle Marsyangdi Hydroelectric Project (MMHEP), Nepal*.

Nepal, K.M. (1999). A review of in-situ testing of rock mechanical parameters in hydropower projects of Nepal. *Journal of Nepal Geological Society*, vol. 19, pp. 1-8

Nilsen, B. and Palmström, A. (2000). Engineering Geology and Rock Engineering. Handbook No. 2. *Norwegian Group for Rock Mechanics (NBG)*, 249p.

Nilsen, B. and Thidemann, A. (1993). Rock Engineering. *Norwegian Institute of Technology, Division of Hydraulic Engineering. Hydropower Development Series*, Vol 9. 156p.

Obert, L. (1965). Creep in mine pillars: Report of investigation. Report No. 6703, *U.S. Bureau of Mines*.

Oreste, P.P. (2003a). Analysis of structural interaction in tunnels using the convergence–confinement approach. *Tunnelling and Underground Space Technology*, vol. 18(4), pp. 347-363.

Oreste, P.P. (2003b). A procedure for determining the reaction curve of shotcrete lining considering transient conditions. *Rock Mechanics and rock Engineering*, vol. 36(3), pp. 209-236.

Oreste, P. (2009). The Convergence-Confinement Method: Roles and Limits in Modern Geomechanical Tunnel Design. *American Journal of Applied Sciences*, vol. 6(4), pp. 751-771.

Palmström, A. (1996). Characterizing rock masses by the RMi for use in practical rock engineering: Part 1: The development of the Rock Mass index (RMi). *Tunnelling and Underground Space Technology*, vo. 11(2), pp. 175-188.

Pan, Y.W. and Chen, Y.M. (1990). Plastic zones and characteristics-line families for openings in elasto-plastic rock mass. *Rock Mechanics and Rock Engineering*, vol. 23(4), pp. 275-292.

Pan, Y.W. and Dong, J.J. (1991a). Time-dependent tunnel convergence—I. Formulation of the model. *International Journal of Rock Mechanics and Mining Sciences & Geomechanics*, vol. 28 (6), pp. 469-475.

Pan, Y.W. and Dong, J.J. (1991b). Time-dependent tunnel convergence—II. Advance rate and tunnel-support interaction. *International Journal of Rock Mechanics and Mining Sciences & Geomechanics*, vol. 28 (6), pp. 477-488.

Panet, M. (1979). Time-dependent deformations in underground works. *Proceedings of 4th Conference, ISRM, Montreux.* Vol. 3, pp. 379-290.

Panet, M. (1995). Le calcul des tunnels par la méthod convergence-confinement. *Presses de I'ENPC,* Paris.

Panet, M. (1996). Two Case Histories of Tunnels through Squeezing Rocks. *Rock Mechanics and Rock Engineering*, vol. 39(3), pp. 155-164.

Panet, M. (2001). Recommendations on the convergence confinement method. *Association Francaise des Travaux en Souterrain (AFTES)*, *Paris*, pp. 1-11.

Panthi, K.K. (2006). Analysis of Engineering Geological Uncertainties Analysis Related to Tunnelling in Himalayan Rock Mass Conditions. (Doctoral Thesis at NTNU 2006:41). *Department of Geology and Mineral Resources Engineering, Norwegian University of Science and Technology, Norway*

Panthi, K.K. (2012). Evaluation of rock bursting phenomena in a tunnel in the Himalayas. *Bulletin of Engineering Geology and the Environment*, vol. 71, pp. 761–769

Panthi, K.K and Nilsen, B. (2007). Uncertainty analysis of tunnel squeezing for two tunnel cases from Nepal Himalaya. *International Journal of Rock Mechanics and Mining Sciences*, vol. 44, pp. 67-76.

Paudel, T.R., Dongol, V., and Sharma, R.H. (1998). Construction phase engineering geological study in Modi Khola Hydroelectric Project, Nepal. *Journal of Nepal Geological Society*, vol. 18, pp. 343-355.

Phienwej, N., Thakur, P.K., and Cording, E.J. (2007). Time-Dependent Response of Tunnels Considering Creep Effect. *International Journal of Geo-mechanics*, vol. 7:, pp. 296-306.

Sakurai, S. (1983). Displacement measurements associated with the design of underground openings. *Proceedings of International Symposium on Field Measurements in Geomechanics, Zurich*, vol. 2, pp. 1163-1178.

Salençon, J. (1969). Contraction quasi-statique d'une cavitéa symétrie sphérique ou cylindrique dans un milieu élastoplastique. *Annales des Ponts et Chaussées*, vol. IV, pp. 231–236.

Schubert, W., Button, E.A., Sellner, P.J., and Solak, T. (2003). Analysis of Time Dependent Displacements of Tunnels, *Felsbau*, vol. 21 (5), pp. 96-103.

Sharan, S.K. (2003). Elastic–brittle–plastic analysis of circular openings in Hoek–Brown media. *International Journal of Rock Mechanics and Mining Sciences*, vol. 40(6), pp. 817-824.

Sharan, S.K. (2005). Exact and approximate solutions for displacements around circular openings in elastic–brittle–plastic Hoek–Brown rock. *International Journal of Rock Mechanics and Mining Sciences*, vol. 42(4), pp. 542-549.

Shrestha, G.L. (2005). Stress induced problems in Himalayan tunnels with special reference to squeezing. Doctoral Thesis, *Department of Geology and Mineral Resources Engineering, Norwegian University of Science and Technology, Norway*.

Singh, B., Jethwa J. L., Dube A. K., and Singh B. (1992). Correlation between observed support pressure and rock mass quality. *Tunnelling and Underground Space Technology*, vol. 7, pp. 59-74.

Singh, A. and Mitchell, J.K. (1968). General stress-strain time function for soils. *Journal of Soil Mechanics and Foundation Division*, vol. 97(1), pp. 21-46.

Sulem, J., Panet, M., and Guenot, A. (1987a). Closure Analysis in Deep Tunnels. *International Journal of Rock Mechanics and Mining Sciences and Geomechanics*, vol. 24(3), pp. 145-154.

Sulem, J., Panet, M., and Guenot, A. (1987b). Analytical Solution for Time Dependent Displacements in a Circular Tunnel. *International Journal of Rock Mechanics and Mining Sciences and Geomechanics*, vol. 24(3), pp. 155-164.

Sterpi, D. and Gioda, G. (2009). Visco-plastic Behavior around Advancing Tunnels in Squeezing Rock. *Rock Mechanics and Rock Engineering*, vol. 42, pp. 319-339.

Terzaghi, K. (1946). Rock defects and loads on tunnel supports. *In R.V. Proctor and T. L. White (Eds.), Rock tunneling with steel supports*, pp. 17–99. Commercial Shearing and Stamping Company. Youngstown, OH.

Upreti, B. N. (1999). An overview of the stratigraphy and tectonic of the Nepal Himalaya. *Journal of Asian Earth Sciences*, vol. 17, pp. 577-606.

Vlachopoulos, N. and Diederichs, M.S. (2009). Improved Longitudinal Displacement Profiles for Convergence Confinement Analysis of Deep Tunnels. *Rock Mechanics and Rock Engineering*, vol. 42(2), pp. 131-146.

Vu, T.M., Sulem, J., and Subrin, D. (2013). Anisotropic Closure in Squeezing Rocks: The Example of Saint-Martin-la-Porte Access Gallery. *Rock Mechanics and Rock Engineering,* vol. 46, pp. 231-246.

Wang, S., Yin, X., Tang, H., and Ge, X. (2010). A new approach for analyzing circular tunnel in strain-softening rock masses. *International Journal of Rock Mechanics and Mining Sciences*, vol. 47(1), pp. 170-178.

Part II

Published Papers

Paper I

Title

Analysis of the plastic deformation behavior of schist and schistose mica gneiss at Khimti headrace tunnel, Nepal

Authors:

Shrestha, Pawan Kumar

Panthi, Krishna Kanta

Published on

Bulletin of Engineering Geology and the Environment (2014)

Volume 73(3), pages 759-773

Is not included due to copyright

Paper II

Title

Assessment of the effect of stress anisotropy on tunnel deformation in the Kaligandaki project in the Nepal Himalaya

Authors:

Shrestha, Pawan Kumar

Panthi, Krishna Kanta

Published on

Bulletin of Engineering Geology and the Environment (2014)

Published online 15 July 2014

Is not included due to copyright

Paper III

Title

Predicting plastic deformation in tunnels – an analysis based on tunnel cases from the Nepal Himalaya

Authors:

Shrestha, Pawan Kumar

Panthi, Krishna Kanta

Under review in

Rock Mechanics and Rock Engineering, submitted on 16th September 2014.

(Note: For reading convenience, the paper has been presented in the authors' format)

Is not included due to copyright

Paper IV

Title

Interpretation of deformation characteristics at Kaligandaki Headrace Tunnel using tunnel monitoring record

Authors:

Shrestha, Pawan Kumar

Panthi, Krishna Kanta

Submitted to

13th International ISRM Congress 2015, Montreal, Canada

Is not included due to copyright

Paper V

Title

Groundwater effect on faulted rock mass - an evaluation of Modi Khola Pressure Tunnel in the Nepal Himalaya

Authors:

Shrestha, Pawan Kumar

Panthi, Krishna Kanta

Published on

Rock Mechanics and Rock Engineering (2014)

Volume 47(3): pages 1021-1035.

Is not included due to copyright

Appendix A

List of other publications during the PhD study

Shrestha, P.K. and Panthi, K.K. (2014). *Effectiveness of applied support in tunnels in plastically deformed rock mass – an analysis based on a tunnelling project from the Nepal Himalaya*. Eurock 2014 - Rock Engineering and Rock Mechanics: Structures in and on Rock Masses, Vigo, Spain.

Basnet, C.B.; **Shrestha, P.K.** and Panthi, K.K. (2013). Analysis of Squeezing Phenomenon in the Headrace Tunnel of Chameliya Project, Nepal. Hydro Nepal: Journal of Water, Energy and Environment. Issue no 13.

Shrestha, P.K. and Panthi, K.K. (2012). *Plastic deformation behavior in tunnel in schist and Schistose Mica Gneiss based on a case from Nepal Himalaya*. 13th World Conference of ACUUS: Underground Space Development-Opportunities and Challenges, Singapore.

Shrestha, P.K. and Panthi, K.K. (2011). *Support interaction in plastically deformed rock mass - an analysis of shear zone at Modi Khola Pressure Tunnel, Nepal*. Sixth International Symposium on Sprayed Concrete - Modern Use of Wet Mix Sprayed Concrete for Underground Support, Tromsø, Norway.

Appendix B

FLAC^{3D} Codes Used

(Note: Only representative FLAC^{3D} codes have been presented)

PAPER I
Khimti headrace tunnel Ch 0+607m

```
;-----------------------------------------------------------------------------------------------------------------------
new
title 'KHP Tunnel at Chainage 607m'
; Model Generation
; Tunnel periphery rockmass
gen zone radcyl size 12 7 20 30 rat 1 1 1 1.1 p0 (0,0,0) p1 (50,0,0) p2 (0,14,0) p3 (0,0,50)dim 2 2 2 2
gen zone radtun size 10 7 10 30 rat 1 1 1 1.1 p0 (0,0,0) p1 (0,0,-50) p2 (0,14,0) p3 (50,0,0) p4 (0,14,-50)
        p5 (50,14,0) p6 (50,0,-50) p7 (50,14,-50) dim 2.2 2 2.2 2
gen zone radcyl size 12 10 20 30 rat 1 1 1 1.1 p0 (0,14,0) p1 (50,14,0) p2 (0,24,0) p3 (0,14,50)dim 2 2 2 2
gen zone radtun size 10 10 10 30 rat 1 1 1 1.1 p0 (0,14,0) p1 (0,14,-50) p2 (0,24,0) p3 (50,14,0) p4 (0,24,-50)
        p5 (50,24,0) p6 (50,14,-50) p7 (50,24,-50) dim 2.2 2 2.2 2
gen zone radcyl size 12 13 20 30 rat 1 1 1 1.1 p0 (0,24,0) p1 (50,24,0) p2 (0,50,0) p3 (0,24,50)dim 2 2 2 2
gen zone radtun size 10 13 10 30 rat 1 1 1 1.1 p0 (0,24,0) p1 (0,24,-50) p2 (0,50,0) p3 (50,24,0) p4 (0,50,-50)
        p5 (50,50,0) p6 (50,24,-50) p7 (50,50,-50) dim 2.2 2 2.2 2
group zone rockmass
; Tunnel
gen zon cylinder p0 0 0 0 p1 2 0 0 p2 0 14 0 p3 0 0 2 size 10 7 20
gen zone brick p0 0 0 -2.2 p1 add 2 0 0 p2 add 0 14 0 p3 add 0 0 2.2 size 10 7 10
gen zon cylinder p0 0 14 0 p1 2 14 0 p2 0 24 0 p3 0 14 2 size 10 10 20
gen zone brick p0 0 14 -2.2 p1 add 2 0 0 p2 add 0 10 0 p3 add 0 0 2.2 size 10 10 10
gen zon cylinder p0 0 24 0 p1 2 24 0 p2 0 50 0 p3 0 24 2 size 10 13 20
gen zone brick p0 0 24 -2.2 p1 add 2 0 0 p2 add 0 26 0 p3 add 0 0 2.2 size 10 13 10
group zone Tunnel range group rockmass not
attach face; range z -0.1 0.1
gen zone reflect dip 90 dd 270 origin 0 0 0
group zone rockmass_1 range plane below dip 35 dd 20 ori 0 37 0 group Tunnel not
group zone rockmass_2 range plane above dip 35 dd 20 ori 0 37 0 group Tunnel not
; Boundary Conditions
fix z range z -50.1 -49.9
fix z range z 50.1 49.9
fix x range x -50.1 -49.9
fix x range x 49.9 50.1
fix y range y -0.1 0.1
fix y range y 49.9 50.1
;Gravity
set gravity 0 0 -9.81
; Mechanical Properities
model mech mohr
prop bulk=0.1091e9 shear=0.119e9 coh=0.17e6 fric=30.83 tens=0.0e6 dil 0 density 2730 &
        range plane below dip 35 dd 20 ori 0 37 0
prop bulk=0.095e9 shear=0.104e9 coh=0.16e6 fric=21.21 tens=0.00e6 dil 0 &
        density 2730 range plane above dip 35 dd 20 ori 0 37 0
; Initial Conditions
ini szz -2.65e6 grad 0 0 0.02678e6
ini sxx -0.29e6 grad 0 0 0.002976e6
ini syy -0.29e6 grad 0 0 0.002976e6
ini sxx add -2.72e6 grad 0 0 0
ini syy add -1.27e6 grad 0 0 0
apply szz -1.31e6 range z 49.9 50.1
; History
hist add unbal
hist add gp xdis 2,20,0
hist add gp xdis 5,20,0
```

```
hist add gp zdis 0,20,2
hist add gp zdis 0,20,5
hist add gp xdis 2,20,-1.8
hist add gp xdis 5,20,-1.8
hist add gp xvel 0,20,2
hist add gp zvel 0,20,2
solve elastic ratio 1e-6
ini xdis=0 ydis=0 zdis=0
ini xvel=0 yvel=0 zvel=0
save KHP_model_initial
;-------------------------
;Fishcodes
;-------------------------
;Full Face Excavation
def tunnel_full_excavation
exca_1=exca1
exca_2=exca2
command
model mech mohr null range group Tunnel y @exca_1, @exca_2
solve
end_command
end
;-------------------------
;Shotcrete
def shotcrete_10cm
fed_begin =ed1
fed_end =ed2
command
sel shell id=1 range cyl end1 0,@fed_begin,0 end2 0,@fed_end,0 rad 2
sel shell id=1 range x=1.901,2.001 y=@fed_begin,@fed_end z=-2.2,0
sel shell id=1 range x=-1.901,-2.001 y=@fed_begin,@fed_end z=-2.2,0
;sel del shell range z -1.85 -1.9
sel shell prop iso=(20e9,0.20) thick=0.1
sel node fix x yr zr range x -0.1 0.1
sel node fix y xr zr range y -0.1 0.1
solve
end_command
end
;-------------------------
;Rockbolt
def install_rockbolt_3nos; 3 in crown and wall
y_bolt=ybolt
command
sel cable begin 0,@y_bolt,2.1 end 0,@y_bolt,5.1 nseg 3
sel cable begin 1.48,@y_bolt,1.48 end 3.61,@y_bolt,3.61 nseg 3
sel cable begin -1.48,@y_bolt,1.48 end -3.61,@y_bolt,3.61 nseg 3
endcommand
command
sel cable prop emod 210e9 ytens 1e5 xcarea 3.14e-4 gr_coh 2e5 gr_k 33e6 gr_per 1
endcommand
end
;-------------------------
def install_rockbolt_5nos; 5 in crown and wall
y_bolt=ybolt
command
```

```
sel cable begin 0,@y_bolt,2.1 end 0,@y_bolt,5.1 nseg 3
sel cable begin 1.48,@y_bolt,1.48 end 3.61,@y_bolt,3.61 nseg 3
sel cable begin -1.48,@y_bolt,1.48 end -3.61,@y_bolt,3.61 nseg 3
endcommand
command
sel cable prop emod 210e9 ytens 1e5 xcarea 3.14e-4 gr_coh 2e5 gr_k 33e6 gr_per 1
endcommand
end
;------------------------
def install_rockbolt_6nos
y_bolt=ybolt
command
sel cable begin 0.54,@y_bolt,2.03 end 1.32,@y_bolt,4.93 nseg 3
sel cable begin 1.82,@y_bolt,1.05 end 4.42,@y_bolt,2.55 nseg 3
sel cable begin 2.1,@y_bolt,0.3 end 5.1,@y_bolt,0.3 nseg 3
sel cable begin -0.54,@y_bolt,2.03 end -1.32,@y_bolt,4.93 nseg 3
sel cable begin -1.82,@y_bolt,1.05 end -4.42,@y_bolt,2.55 nseg 3
sel cable begin -2.1,@y_bolt,-0.3 end -5.1,@y_bolt,-0.3 nseg 3
endcommand
command
sel cable prop emod 210e9 ytens 1e5 xcarea 3.14e-4 gr_coh 2e5 gr_k 33e6 gr_per 1
endcommand
end
;------------------------
def install_rockbolt_7nos
y_bolt=ybolt
command
sel cable begin 0,@y_bolt,2.1 end 0,@y_bolt,5.1 nseg 3
sel cable begin 1.35,@y_bolt,1.61 end 3.28,@y_bolt,3.91 nseg 3
sel cable begin 2.07,@y_bolt,0.36 end 5.02,@y_bolt,0.89 nseg 3
sel cable begin 2.1,@y_bolt,-1.0 end 5.1,@y_bolt,-1.0 nseg 3
sel cable begin -1.35,@y_bolt,1.61 end -3.28,@y_bolt,3.91 nseg 3
sel cable begin -2.07,@y_bolt,0.36 end -5.02,@y_bolt,0.89 nseg 3
sel cable begin -2.1,@y_bolt,-1.0 end -5.1,@y_bolt,-1.0 nseg 3
endcommand
command
sel cable prop emod 210e9 ytens 1e5 xcarea 3.14e-4 gr_coh 2e5 gr_k 33e6 gr_per 1
endcommand
end
;------------------------
def install_rockbolt_8nos
y_bolt=ybolt
command
sel cable begin 0.54,@y_bolt,2.03 end 1.32,@y_bolt,4.93 nseg 3
sel cable begin 1.48,@y_bolt,1.48 end 3.61,@y_bolt,3.61 nseg 3
sel cable begin 2.1,@y_bolt,0.0 end 5.1,@y_bolt,0 nseg 3
sel cable begin 2.1,@y_bolt,1.2 end 5.1,@y_bolt,1.2 nseg 3
sel cable begin -0.54,@y_bolt,2.03 end -1.32,@y_bolt,4.93 nseg 3
sel cable begin -1.48,@y_bolt,1.48 end -3.61,@y_bolt,3.61 nseg 3
sel cable begin -2.1,@y_bolt,0.0 end -5.1,@y_bolt,0 nseg 3
sel cable begin -2.1,@y_bolt,1.2 end -5.1,@y_bolt,1.2 nseg 3
endcommand
command
sel cable prop emod 210e9 ytens 1e5 xcarea 3.14e-4 gr_coh 2e5 gr_k 33e6 gr_per 1
endcommand
```

```
end
;------------------------
def install_rockbolt_9nos
y_bolt=ybolt
command
sel cable begin 0,@y_bolt,2.1 end 0,@y_bolt,5.1 nseg 3
sel cable begin 1.05,@y_bolt,1.82 end 2.55,@y_bolt,4.42 nseg 3
sel cable begin 1.82,@y_bolt,1.05 end 4.42,@y_bolt,2.55 nseg 3
sel cable begin 2.1,@y_bolt,-0.0 end 5.1,@y_bolt,-0.0 nseg 3
sel cable begin 2.1,@y_bolt,-1.5 end 5.1,@y_bolt,-1.5 nseg 3
sel cable begin -1.05,@y_bolt,1.82 end -2.55,@y_bolt,4.42 nseg 3
sel cable begin -1.82,@y_bolt,1.05 end -4.42,@y_bolt,2.55 nseg 3
sel cable begin -2.1,@y_bolt,-0.0 end -5.1,@y_bolt,-0.0 nseg 3
sel cable begin -2.1,@y_bolt,-1.5 end -5.1,@y_bolt,-1.5 nseg 3
endcommand
command
sel cable prop emod 210e9 ytens 1e5 xcarea 3.14e-4 gr_coh 2e5 gr_k 33e6 gr_per 1
endcommand
end
;------------------------
;Stage Excavation 587 to 588m
set @exca1 0 @exca2 1
@tunnel_full_excavation
set @ed1 0 @ed2 0.9
@shotcrete_10cm
solve
save Ex_0_1
;Stage Excavation 588 to 590m
set @exca1 1 @exca2 3
@tunnel_full_excavation
set @ed1 0.9 @ed2 2.9
@shotcrete_10cm
sel cable beg -1.93,0.1,0.52 end -4.83,0.1,1.29 nseg 3
sel cable beg -1,0.1,1.73 end -2.5,0.1,4.33 nseg 3
sel cable beg 1,0.1,1.73 end 2.5,0.1,4.33 nseg 3
sel cable beg 1.93,0.1,0.52 end 4.83,0.1,1.29 nseg 3
sel cable prop emod 200e9 ytens 1e5 xcarea 3.14e-4 gr_coh 2e5 gr_k 1e9 gr_per 0.11
solve
save Ex_1_3
;Stage Excavation 590 to 592m
set @exca1 3 @exca2 5
@tunnel_full_excavation
set @ed1 2.9 @ed2 4.9
@shotcrete_10cm
sel cable beg 2,1.75,-0.0 end 5,1.75,-0.0 nseg 3
sel cable beg 1.41,1.75,1.41 end 3.54,1.75,3.54 nseg 3
sel cable beg 0,1.75,2 end 0,1.75,5 nseg 3
sel cable beg -1.41,1.75,1.41 end -3.54,1.75,3.54 nseg 3
sel cable beg -2,1.75,-0.0 end -5,1.75,-0.0 nseg 3
sel cable prop emod 200e9 ytens 1e5 xcarea 3.14e-4 gr_coh 2e5 gr_k 1e9 gr_per 0.11
solve
save Ex_3_5
;Stage Excavation 592 to 594m
set @exca1 5 @exca2 7
@tunnel_full_excavation
```

```
set @ed1 4.9 @ed2 6.9
@shotcrete_10cm
sel cable beg -1.93,3.5,0.52 end -4.83,3.5,1.29 nseg 3
sel cable beg -1,3.5,1.73 end -2.5,3.5,4.33 nseg 3
sel cable beg 1,3.5,1.73 end 2.5,3.5,4.33 nseg 3
sel cable beg 1.93,3.5,0.52 end 4.83,3.5,1.29 nseg 3
sel cable prop emod 200e9 ytens 1e5 xcarea 3.14e-4 gr_coh 2e5 gr_k 1e9 gr_per 0.11
sel cable beg 1.41,5,1.41 end 3.54,5,3.54 nseg 3
sel cable beg 0,5,2 end 0,5,5 nseg 3
sel cable beg -1.41,5,1.41 end -3.54,5,3.54 nseg 3
sel cable prop emod 200e9 ytens 1e5 xcarea 3.14e-4 gr_coh 2e5 gr_k 1e9 gr_per 0.11
solve
save Ex_5_7
;Stage Excavation 594 to 596m
set @exca1 7 @exca2 9
@tunnel_full_excavation
set @ed1 6.9 @ed2 8.9
@shotcrete_10cm
sel cable beg 2,5.5,-1 end 5,5.5,-1 nseg 3
sel cable beg -2,5.5,-1 end -5,5.5,-1 nseg 3
sel cable prop emod 200e9 ytens 1e5 xcarea 3.14e-4 gr_coh 2e5 gr_k 1e9 gr_per 0.11
sel cable beg 1.41,7.5,1.41 end 3.54,7.5,3.54 nseg 3
sel cable beg 0,7.5,2 end 0,7.5,5 nseg 3
sel cable beg -1.41,7.5,1.41 end -3.54,7.5,3.54 nseg 3
sel cable prop emod 200e9 ytens 1e5 xcarea 3.14e-4 gr_coh 2e5 gr_k 1e9 gr_per 0.11
sel cable beg 1.41,8.5,1.41 end 3.54,8.5,3.54 nseg 3
sel cable beg 0,8.5,2 end 0,8.5,5 nseg 3
sel cable beg -1.41,8.5,1.41 end -3.54,8.5,3.54 nseg 3
sel cable prop emod 200e9 ytens 1e5 xcarea 3.14e-4 gr_coh 2e5 gr_k 1e9 gr_per 0.11
solve
;Stage Excavation 596 to 598m
set @exca1 9 @exca2 11
@tunnel_full_excavation
set @ed1 8.9 @ed2 10.9
@shotcrete_10cm
sel cable beg 1.41,10,1.41 end 3.54,10,3.54 nseg 3
sel cable beg 0,10,2 end 0,10,5 nseg 3
sel cable beg -1.41,10,1.41 end -3.54,10,3.54 nseg 3
sel cable beg 2,10,-1.2 end 5,10,-1.2 nseg 3
sel cable prop emod 200e9 ytens 1e5 xcarea 3.14e-4 gr_coh 2e5 gr_k 1e9 gr_per 0.11
solve
;Stage Excavation 598 to 600m
set @exca1 11 @exca2 13
@tunnel_full_excavation
set @ed1 10.9 @ed2 12.9
@shotcrete_10cm
sel cable beg 1.41,12,1.41 end 3.54,12,3.54 nseg 3
sel cable beg 0,12,2 end 0,12,5 nseg 3
sel cable beg -1.41,12,1.41 end -3.54,12,3.54 nseg 3
sel cable beg -2,12,-1.2 end -5,12,-1.2 nseg 3
sel cable prop emod 200e9 ytens 1e5 xcarea 3.14e-4 gr_coh 2e5 gr_k 1e9 gr_per 0.11
solve
;Stage Excavation 600 to 602m
set @exca1 13 @exca2 15
@tunnel_full_excavation
```

```
set @ed1 12.9 @ed2 14.9
@shotcrete_10cm
sel cable beg 1.41,13.5,1.41 end 3.54,13.5,3.54 nseg 3
sel cable beg 0,13.5,2 end 0,13.5,5 nseg 3
sel cable beg -1.41,13.5,1.41 end -3.54,13.5,3.54 nseg 3
sel cable beg -2,13.5,-1.2 end -5,13.5,-1.2 nseg 3
sel cable prop emod 200e9 ytens 1e5 xcarea 3.14e-4 gr_coh 2e5 gr_k 1e9 gr_per 0.11
solve
save Ex_13_15
;Stage Excavation 602 to 604m
set @exca1 15 @exca2 17
@tunnel_full_excavation
set @ed1 14.9 @ed2 16.9
@shotcrete_10cm
sel cable beg 1.41,16.25,1.41 end 3.54,16.25,3.54 nseg 3
sel cable beg 0,16.25,2 end 0,16.25,5 nseg 3
sel cable beg -1.41,16.25,1.41 end -3.54,16.25,3.54 nseg 3
sel cable prop emod 200e9 ytens 1e5 xcarea 3.14e-4 gr_coh 2e5 gr_k 1e9 gr_per 0.11
solve
save Ex_15_17
;Stage Excavation 604 to 606m
set @exca1 17 @exca2 19
@tunnel_full_excavation
set @ed1 16.9 @ed2 18.9
@shotcrete_10cm
sel cable beg 2,17.5,-0.2 end 5,17.5,-0.2 nseg 3
sel cable beg 1.41,17.5,1.41 end 3.54,17.5,3.54 nseg 3
sel cable beg 0,17.5,2 end 0,17.5,5 nseg 3
sel cable beg -1.41,17.5,1.41 end -3.54,17.5,3.54 nseg 3
sel cable beg -2,17.5,-0.2 end -5,17.5,-0.2 nseg 3
sel cable prop emod 200e9 ytens 1e5 xcarea 3.14e-4 gr_coh 2e5 gr_k 1e9 gr_per 0.11
solve
save Ex_17_19
;Stage Excavation 606 to 607m
set @exca1 19 @exca2 20
@tunnel_full_excavation
set @ed1 18.9 @ed2 19.9
@shotcrete_10cm
sel cable beg 2,18.75,-0.2 end 5,18.75,-0.2 nseg 3
sel cable beg 1.41,18.75,1.41 end 3.54,18.75,3.54 nseg 3
sel cable beg 0,18.75,2 end 0,18.75,5 nseg 3
sel cable beg -1.41,18.75,1.41 end -3.54,18.75,3.54 nseg 3
sel cable beg -2,18.75,-0.2 end -5,18.75,-0.2 nseg 3
sel cable prop emod 200e9 ytens 1e5 xcarea 3.14e-4 gr_coh 2e5 gr_k 1e9 gr_per 0.11
solve
save Ex_19_20
;Stage Excavation 607 to 608m
set @exca1 20 @exca2 21
@tunnel_full_excavation
set @ed1 19.9 @ed2 20.9
@shotcrete_10cm
sel cable beg 2,20,-1.7 end 5,20,-1.7 nseg 3
sel cable beg 2,20,-0.2 end 5,20,-0.2 nseg 3
sel cable beg 1.41,20,1.41 end 3.54,20,3.54 nseg 3
sel cable beg 0,20,2 end 0,20,5 nseg 3
```

```
sel cable beg -1.41,20,1.41 end -3.54,20,3.54 nseg 3
sel cable beg -2,20,-0.2 end -5,20,-0.2 nseg 3
sel cable beg -2,20,-1.7 end -5,20,-1.7 nseg 3
sel cable prop emod 200e9 ytens 1e5 xcarea 3.14e-4 gr_coh 2e5 gr_k 1e9 gr_per 0.11
solve
save Ex_20_21
;Stage Excavation 608 to 609m
set @exca1 21 @exca2 22
@tunnel_full_excavation
set @ed1 20.9 @ed2 21.9
@shotcrete_10cm
save Ex_21_22
;Stage Excavation 609 to 610m
set @exca1 22 @exca2 23
@tunnel_full_excavation
set @ed1 21.9 @ed2 22.9
@shotcrete_10cm
sel cable beg -1.93,22,0.52 end -4.83,22,1.29 nseg 3
sel cable beg -1,22,1.73 end -2.5,22,4.33 nseg 3
sel cable beg 1,22,1.73 end 2.5,22,4.33 nseg 3
sel cable beg 1.93,22,0.52 end 4.83,22,1.29 nseg 3
sel cable prop emod 200e9 ytens 1e5 xcarea 3.14e-4 gr_coh 2e5 gr_k 1e9 gr_per 0.11
solve
save Ex_22_23
;Stage Excavation 610 to 612m
set @exca1 23 @exca2 25
@tunnel_full_excavation
set @ed1 22.9 @ed2 24.9
@shotcrete_10cm
sel cable beg 2,25,-1.7 end 5,25,-1.7 nseg 3
sel cable beg 2,25,-0.2 end 5,25,-0.2 nseg 3
sel cable beg 1.41,25,1.41 end 3.54,25,3.54 nseg 3
sel cable beg 0,25,2 end 0,25,5 nseg 3
sel cable beg -1.41,25,1.41 end -3.54,25,3.54 nseg 3
sel cable beg -2,25,-0.2 end -5,25,-0.2 nseg 3
sel cable prop emod 200e9 ytens 1e5 xcarea 3.14e-4 gr_coh 2e5 gr_k 1e9 gr_per 0.11
solve
save Ex_23_25
;Stage Excavation 612 to 614m
set @exca1 25 @exca2 27
@tunnel_full_excavation
set @ed1 24.9 @ed2 26.9
@shotcrete_10cm
sel cable beg 2,26,-1.7 end 5,26,-1.7 nseg 3
sel cable beg 2,26,-0.2 end 5,26,-0.2 nseg 3
sel cable beg 1.41,26,1.41 end 3.54,26,3.54 nseg 3
sel cable beg 0,26,2 end 0,26,5 nseg 3
sel cable beg -1.41,26,1.41 end -3.54,26,3.54 nseg 3
sel cable beg -2,26,-0.2 end -5,26,-0.2 nseg 3
sel cable beg -2,26,-1.2 end -5,26,-1.2 nseg 3
sel cable beg -2,26,-2 end -5,26,-2 nseg 3
sel cable prop emod 200e9 ytens 1e5 xcarea 3.14e-4 gr_coh 2e5 gr_k 1e9 gr_per 0.11
solve
save Ex_25_27
;Stage Excavation 614 to 616m
```

```
set @exca1 27 @exca2 29
@tunnel_full_excavation
set @ed1 26.9 @ed2 28.9
@shotcrete_10cm
sel cable beg 2,27.25,-0.2 end 5,27.25,-0.2 nseg 3
sel cable beg 1.41,27.25,1.41 end 3.54,27.25,3.54 nseg 3
sel cable beg 0,27.25,2 end 0,27.25,5 nseg 3
sel cable beg -1.41,27.25,1.41 end -3.54,27.25,3.54 nseg 3
sel cable beg -2,27.25,-0.2 end -5,27.25,-0.2 nseg 3
sel cable beg -2,27.25,-1.7 end -5,27.25,-1.7 nseg 3
sel cable prop emod 200e9 ytens 1e5 xcarea 3.14e-4 gr_coh 2e5 gr_k 1e9 gr_per 0.11
solve
save Ex_27_29
;Stage Excavation 616 to 618m
set @exca1 29 @exca2 31
@tunnel_full_excavation
set @ed1 28.9 @ed2 30.9
@shotcrete_10cm
sel cable beg 2,28.5,-0.2 end 5,28.5,-0.2 nseg 3
sel cable beg 1.41,28.5,1.41 end 3.54,28.5,3.54 nseg 3
sel cable beg 0,28.5,2 end 0,28.5,5 nseg 3
sel cable beg -1.41,28.5,1.41 end -3.54,28.5,3.54 nseg 3
sel cable beg -2,28.5,-0.2 end -5,28.5,-0.2 nseg 3
sel cable beg -2,28.5,-1.7 end -5,28.5,-1.7 nseg 3
sel cable prop emod 200e9 ytens 1e5 xcarea 3.14e-4 gr_coh 2e5 gr_k 1e9 gr_per 0.11
sel cable beg 2,30,-0.6 end 5,30,-0.6 nseg 3
sel cable beg 2,30,-0.6 end 5,30,-0.6 nseg 3
sel cable prop emod 200e9 ytens 1e5 xcarea 3.14e-4 gr_coh 2e5 gr_k 1e9 gr_per 0.11
solve
save Ex_29_31
;Stage Excavation 618 to 620m
set @exca1 31 @exca2 33
@tunnel_full_excavation
set @ed1 30.9 @ed2 32.9
@shotcrete_10cm
sel cable beg 2,31,-1.7 end 5,31,-1.7 nseg 3
sel cable beg 2,31,-0.2 end 5,31,-0.2 nseg 3
sel cable beg 1.41,31,1.41 end 3.54,31,3.54 nseg 3
sel cable beg 0,31,2 end 0,31,5 nseg 3
sel cable beg -1.41,31,1.41 end -3.54,31,3.54 nseg 3
sel cable beg -2,31,-0.2 end -5,31,-0.2 nseg 3
sel cable prop emod 200e9 ytens 1e5 xcarea 3.14e-4 gr_coh 2e5 gr_k 1e9 gr_per 0.11
sel cable beg 2,32,-0.2 end 5,32,-0.2 nseg 3
sel cable beg 1.41,32,1.41 end 3.54,32,3.54 nseg 3
sel cable beg 0,32,2 end 0,32,5 nseg 3
sel cable beg -1.41,32,1.41 end -3.54,32,3.54 nseg 3
sel cable beg -2,32,-0.2 end -5,32,-0.2 nseg 3
sel cable prop emod 200e9 ytens 1e5 xcarea 3.14e-4 gr_coh 2e5 gr_k 1e9 gr_per 0.11
solve
save Ex_31_33
;Stage Excavation 620 to 622m
set @exca1 33 @exca2 35
@tunnel_full_excavation
set @ed1 32.9 @ed2 34.9
@shotcrete_10cm
```

```
sel cable beg 2,33.5,-0.5 end 5,33.5,-0.5 nseg 3
sel cable beg 1.41,33.5,1.41 end 3.54,33.5,3.54 nseg 3
sel cable beg 0,33.5,2 end 0,33.5,5 nseg 3
sel cable beg -1.41,33.5,1.41 end -3.54,33.5,3.54 nseg 3
sel cable beg -2,33.5,-0.2 end -5,33.5,-0.2 nseg 3
sel cable beg -2,33.5,-1.7 end -5,33.5,-1.7 nseg 3
sel cable prop emod 200e9 ytens 1e5 xcarea 3.14e-4 gr_coh 2e5 gr_k 1e9 gr_per 0.11
solve
save Ex_33_35
;Stage Excavation 622 to 624m
set @exca1 35 @exca2 37
@tunnel_full_excavation
set @ed1 34.9 @ed2 36.9
@shotcrete_10cm
sel cable beg -2,35,-0.5 end -5,35,-0.5 nseg 3
sel cable beg -1.93,35,0.52 end -4.83,35,1.29 nseg 3
sel cable beg -1,35,1.73 end -2.5,35,4.33 nseg 3
sel cable beg 1,35,1.73 end 2.5,35,4.33 nseg 3
sel cable beg 1.93,35,0.52 end 4.83,35,1.29 nseg 3
sel cable beg 2,35,-0.5 end 5,35,-0.5 nseg 3
sel cable prop emod 200e9 ytens 1e5 xcarea 3.14e-4 gr_coh 2e5 gr_k 1e9 gr_per 0.11
sel cable beg 2,36.5,-1 end 5,36.5,-1 nseg 3
sel cable beg 2,36.5,0 end 5,36.5,0 nseg 3
sel cable beg 1.41,36.5,1.41 end 3.54,36.5,3.54 nseg 3
sel cable beg 0,36.5,2 end 0,36.5,5 nseg 3
sel cable beg -1.41,36.5,1.41 end -3.54,36.5,3.54 nseg 3
sel cable beg -2,36.5,0 end -5,36.5,0 nseg 3
sel cable beg -2,36.5,-1 end -5,36.5,-1 nseg 3
sel cable prop emod 200e9 ytens 1e5 xcarea 3.14e-4 gr_coh 2e5 gr_k 1e9 gr_per 0.11
solve
save Excn_35_37
return
;-----------------------------------------------------------------------------------------------------------------------------------------------
```

PAPER II
Kaligandaki Headrace Tunnel Ch 0+739m

```
;-----------------------------------------------------------------------------------------------------------------------------
new
title 'KGA Tunnel Ch 0+739m'
; generate model
gen zon radcyl p0 0 0 0 p1 27 0 0 p2 0 0.2 0 p3 0 0 25 dim 4.15 4.15 4.15 4.15 size 5 1 14 30 rat 1 1 1 1.1
gen zon radtun p0 0 0 0 p1 0 0 -25 p2 0 0.2 0 p3 27 0 0 dim 4.15 4.15 4.15 4.15 size 7 1 8 30 rat 1 1 1 1.1
gen zon bric p0 0 0 25 p1 add 27 0 0 p2 add 0 0.2 0 p3 add 0 0 20 size 7 1 3 rat 1 1 1.5
gen zon bric p0 27 0 25 p1 add 18 0 0 p2 add 0 0.2 0 p3 add 0 0 20 size 4 1 3 rat 1 1 1.5
gen zon bric p0 27 0 0 p1 add 18 0 0 p2 add 0 0.2 0 p3 add 0 0 25 size 4 1 7 rat 1 1 1
gen zon bric p0 27 0 -25 p1 add 18 0 0 p2 add 0 0.2 0 p3 add 0 0 25 size 4 1 7 rat 1 1 1
gen zon bric p0 0 0 -45 p1 add 27 0 0 p2 add 0 0.2 0 p3 add 0 0 20 size 8 1 3 rat 1 1 0.75
gen zon bric p0 27 0 -45 p1 add 18 0 0 p2 add 0 0.2 0 p3 add 0 0 20 size 4 1 3 rat 1 1 0.75
group zone rockmass
gen zon cylinder p0 0 0 0 p1 4.15 0 0 p2 0 0.2 0 p3 0 0 4.15 size 8 1 14
gen zone brick p0 0 0 -4.15 p1 add 4.15 0 0 p2 add 0 0.2 0 p3 add 0 0 4.15 p4 add 4.15 0.2 0 p5 add 0 0.2 4.15 &
        p6 add 4.15 0 4.15 p7 add 4.15 0.2 4.15 size 8 1 7
group zone Tunnel range group rockmass not
attach face range z -0.1 0.1
gen zone reflect dip 90 dd 270 origin 0 0 0
;Material Propery
model mech hoekbrown
prop bulk 127.86e6 shear 139.49e6 hbs 2.33e-5 hbmb 0.1551 hbsigci 18.68e6 hba 0.544 hbs3cv 0
prop density 2750
;Boundary Condition
fix z range z -45.01 -44.99
fix z range z 44.99 45.01
fix x range x -45.01 -44.99
fix x range x 44.99 45.01
fix y
;Initial stress
set gravity 0 0 -9.81
ini szz -6.53e6 grad 0 0 0.026978e6
ini sxx -2.49e6 grad 0 0 0.002998e6
ini syy -3.15e6 grad 0 0 0.002998e6
apply sxx -2.49e6 grad 0 0 0.002998e6 range x 44.9 45.1
apply sxx -2.49e6 grad 0 0 0.002998e6 range x -44.9 -45.1
apply syy -3.15e6 grad 0 0 0.002998e6 range y -0.1 0.1
apply syy -3.15e6 grad 0 0 0.002998e6 range y 0.1 0.3
apply szz -5.31e6 range z 44.9 45.1
apply szz -7.74e6 range z -44.9 -45.1
;History
hist add unbal
hist add gp zdisp 0 0 4.15
hist add gp xdisp 4.15 0 0
hist add gp xdisp 4.15 0 -3.11
solve
ini xdis 0 ydis 0 zdis 0
ini xvel 0 yvel 0 zvel 0
save Initial_739m
; SP 0.1 MPa
model mech hoekbrown null range group Tunnel
;Internal support pressure
apply nstress -0.1e6 range cylinder end1 0 0 0 end2 0 0.2 0 radius 4.15 z 0 4.15
```

```
apply sxx -0.1e6 range z 0 -4.15 x 4.15 4.15
apply sxx -0.1e6 range z 0 -4.15 x -4.15 -4.15
solve
save 739m_SP_0.1
; SP 0.2 MPa
rest Initial_739m
model mech hoekbrown null range group Tunnel
;Internal support pressure
apply nstress -0.2e6 range cylinder end1 0 0 0 end2 0 0.2 0 radius 4.15 z 0 4.15
apply sxx -0.2e6 range z 0 -4.15 x 4.15 4.15
apply sxx -0.2e6 range z 0 -4.15 x -4.15 -4.15
solve
save 739m_ SP_0.2
; SP 0.3 MPa
rest Initial_739m
model mech hoekbrown null range group Tunnel
;Internal support pressure
apply nstress -0.3e6 range cylinder end1 0 0 0 end2 0 0.2 0 radius 4.15 z 0 4.15
apply sxx -0.3e6 range z 0 -4.15 x 4.15 4.15
apply sxx -0.3e6 range z 0 -4.15 x -4.15 -4.15
solve
save 739m_SP_0.3
; SP 0.4 MPa
rest Initial_739m
model mech hoekbrown null range group Tunnel
;Internal support pressure
apply nstress -0.4e6 range cylinder end1 0 0 0 end2 0 0.2 0 radius 4.15 z 0 4.15
apply sxx -0.4e6 range z 0 -4.15 x 4.15 4.15
apply sxx -0.4e6 range z 0 -4.15 x -4.15 -4.15
solve
save 739m_ SP_0.4
; SP 0.5 MPa
rest Initial_739m
model mech hoekbrown null range group Tunnel
;Internal support pressure
apply nstress -0.5e6 range cylinder end1 0 0 0 end2 0 0.2 0 radius 4.15 z 0 4.15
apply sxx -0.5e6 range z 0 -4.15 x 4.15 4.15
apply sxx -0.5e6 range z 0 -4.15 x -4.15 -4.15
solve
save 739m _SP_0.5
; SP 0.6 MPa
rest Initial_739m
model mech hoekbrown null range group Tunnel
;Internal support pressure
apply nstress -0.6e6 range cylinder end1 0 0 0 end2 0 0.2 0 radius 4.15 z 0 4.15
apply sxx -0.6e6 range z 0 -4.15 x 4.15 4.15
apply sxx -0.6e6 range z 0 -4.15 x -4.15 -4.15
solve
save 739m _SP_0.6
; SP 0.7 MPa
rest Initial_739m
model mech hoekbrown null range group Tunnel
;Internal support pressure
apply nstress -0.7e6 range cylinder end1 0 0 0 end2 0 0.2 0 radius 4.15 z 0 4.15
```

```
apply sxx -0.7e6 range z 0 -4.15 x 4.15 4.15
apply sxx -0.7e6 range z 0 -4.15 x -4.15 -4.15
solve
save 739m _SP_0.7
; SP 0.8 MPa
rest Initial_739m
model mech hoekbrown null range group Tunnel
;Internal support pressure
apply nstress -0.8e6 range cylinder end1 0 0 0 end2 0 0.2 0 radius 4.15 z 0 4.15
apply sxx -0.8e6 range z 0 -4.15 x 4.15 4.15
apply sxx -0.8e6 range z 0 -4.15 x -4.15 -4.15
solve
save 739m _SP_0.8
; SP 0.9 MPa
rest Initial_739m
model mech hoekbrown null range group Tunnel
;Internal support pressure
apply nstress -0.9e6 range cylinder end1 0 0 0 end2 0 0.2 0 radius 4.15 z 0 4.15
apply sxx -0.9e6 range z 0 -4.15 x 4.15 4.15
apply sxx -0.9e6 range z 0 -4.15 x -4.15 -4.15
solve
save 739m_SP_0.9
; SP 1 MPa
rest Initial_739m
model mech hoekbrown null range group Tunnel
;Internal support pressure
apply nstress -1e6 range cylinder end1 0 0 0 end2 0 0.2 0 radius 4.15 z 0 4.15
apply sxx -1e6 range z 0 -4.15 x 4.15 4.15
apply sxx -1e6 range z 0 -4.15 x -4.15 -4.15
solve
save 739m _SP_1
; SP 1.1 MPa
rest Initial_739m
model mech hoekbrown null range group Tunnel
;Internal support pressure
apply nstress -1.1e6 range cylinder end1 0 0 0 end2 0 0.2 0 radius 4.15 z 0 4.15
apply sxx -1.1e6 range z 0 -4.15 x 4.15 4.15
apply sxx -1.1e6 range z 0 -4.15 x -4.15 -4.15
solve
save 739m_SP_1.1
; SP 1.2 MPa
rest Initial_739m
model mech hoekbrown null range group Tunnel
;Internal support pressure
apply nstress -1.2e6 range cylinder end1 0 0 0 end2 0 0.2 0 radius 4.15 z 0 4.15
apply sxx -1.2e6 range z 0 -4.15 x 4.15 4.15
apply sxx -1.2e6 range z 0 -4.15 x -4.15 -4.15
solve
save 739m_SP_1.2
; SP 1.3 MPa
rest Initial_739m
model mech hoekbrown null range group Tunnel
;Internal support pressure
apply nstress -1.3e6 range cylinder end1 0 0 0 end2 0 0.2 0 radius 4.15 z 0 4.15
```

```
apply sxx -1.3e6 range z 0 -4.15 x 4.15 4.15
apply sxx -1.3e6 range z 0 -4.15 x -4.15 -4.15
solve
save 739m_SP_1.3
; SP 1.4 MPa
rest Initial_739m
model mech hoekbrown null range group Tunnel
;Internal support pressure
apply nstress -1.4e6 range cylinder end1 0 0 0 end2 0 0.2 0 radius 4.15 z 0 4.15
apply sxx -1.4e6 range z 0 -4.15 x 4.15 4.15
apply sxx -1.4e6 range z 0 -4.15 x -4.15 -4.15
solve
save 739m_SP_1.4
; SP 1.6 MPa
rest Initial_739m
model mech hoekbrown null range group Tunnel
;Internal support pressure
apply nstress -1.6e6 range cylinder end1 0 0 0 end2 0 0.2 0 radius 4.15 z 0 4.15
apply sxx -1.6e6 range z 0 -4.15 x 4.15 4.15
apply sxx -1.6e6 range z 0 -4.15 x -4.15 -4.15
solve
save 739m_SP_1.6
; SP 1.8 MPa
rest Initial_739m
model mech hoekbrown null range group Tunnel
;Internal support pressure
apply nstress -1.8e6 range cylinder end1 0 0 0 end2 0 0.2 0 radius 4.15 z 0 4.15
apply sxx -1.8e6 range z 0 -4.15 x 4.15 4.15
apply sxx -1.8e6 range z 0 -4.15 x -4.15 -4.15
solve
save 739m_SP_1.8
; SP 2 MPa
rest Initial_739m
model mech hoekbrown null range group Tunnel
;Internal support pressure
apply nstress -2e6 range cylinder end1 0 0 0 end2 0 0.2 0 radius 4.15 z 0 4.15
apply sxx -2e6 range z 0 -4.15 x 4.15 4.15
apply sxx -2e6 range z 0 -4.15 x -4.15 -4.15
solve
save 739m_SP_2
; SP 2.4 MPa
rest Initial_739m
model mech hoekbrown null range group Tunnel
;Internal support pressure
apply nstress -2.4e6 range cylinder end1 0 0 0 end2 0 0.2 0 radius 4.15 z 0 4.15
apply sxx -2.4e6 range z 0 -4.15 x 4.15 4.15
apply sxx -2.4e6 range z 0 -4.15 x -4.15 -4.15
solve
save 739m_SP_2.4
return
;-----------------------------------------------------------------------------------------------------------------------------------------------
```

PAPER IV
Kaligandaki Headrace Tunnel Ch 1+609m

```
;-----------------------------------------------------------------------------------------------------------------------------
new
title 'KGA Tunnel Ch 1+609m'
; generate model
gen zon radcyl p0 0 0 0 p1 27 0 0 p2 0 0.2 0 p3 0 0 25 dim 4.15 4.15 4.15 4.15 size 5 1 14 30 rat 1 1 1 1.05
gen zon radtun p0 0 0 0 p1 0 0 -25 p2 0 0.2 0 p3 27 0 0 dim 4.025 4.15 4.025 4.15 size 7 1 8 30 rat 1 1 1 1.05
gen zon brick p0 3.1125 0 -4.025 p1 add 1.0375 0 0 p2 add 0 0.2 0 p3 add 0.8675 0 2.875 p4 add 1.0375 0.2 0 &
        p5 add 0.8675 0.2 2.875 p6 add 1.0375 0 2.875 p7 add 1.0375 0.2 2.875 size 2 1 5 rat 1 1 1
gen zon brick p0 3.98 0 -1.15 p1 add 0.17 0 0 p2 add 0 0.2 0 p3 add 0.13 0 0.575 p4 add 0.17 0.2 0 &
        p5 add 0.13 0.2 0.575 p6 add 0.17 0 0.575 p7 add 0.17 0.2 0.575 size 2 1 1 rat 1 1 1
gen zon wedge p0 4.11 0 -0.575 p1 add 0.04 0 0 p2 add 0 0.2 0 p3 add 0.04 0 0.575 size 2 1 1 rat 1 1 1
gen zon bric p0 0 0 25 p1 add 27 0 0 p2 add 0 0.2 0 p3 add 0 0 20 size 7 1 3 rat 1 1 1.5
gen zon bric p0 27 0 25 p1 add 18 0 0 p2 add 0 0.2 0 p3 add 0 0 20 size 4 1 3 rat 1 1 1.5
gen zon bric p0 27 0 0 p1 add 18 0 0 p2 add 0 0.2 0 p3 add 0 0 25 size 4 1 7 rat 1 1 1
gen zon bric p0 27 0 -25 p1 add 18 0 0 p2 add 0 0.2 0 p3 add 0 0 25 size 4 1 7 rat 1 1 1
gen zon bric p0 0 0 -45 p1 add 27 0 0 p2 add 0 0.2 0 p3 add 0 0 20 size 8 1 3 rat 1 1 0.75
gen zon bric p0 27 0 -45 p1 add 18 0 0 p2 add 0 0.2 0 p3 add 0 0 20 size 4 1 3 rat 1 1 0.75
group zone rockmass
gen zon cylinder p0 0 0 0 p1 4.15 0 0 p2 0 0.2 0 p3 0 0 4.15 size 6 1 14
gen zone brick p0 0 0 -1.15 p1 add 3.98 0 0 p2 add 0 0.2 0 p3 add 0 0 0.575 p4 add 3.98 0.2 0 p5 add 0 0.2 0.575 &
        p6 add 4.11 0 0.575 p7 add 4.11 0.2 0.575 size 6 1 1
gen zone brick p0 0 0 -0.575 p1 add 4.11 0 0 p2 add 0 0.2 0 p3 add 0 0 0.575 p4 add 4.11 0.2 0 p5 add 0 0.2 0.575 &
        p6 add 4.15 0 0.575 p7 add 4.15 0.2 0.575 size 6 1 1
gen zone brick p0 0 0 -4.025 p1 add 3.1125 0 0 p2 add 0 0.2 0 p3 add 0 0 2.875 p4 add 3.1125 0.2 0 &
        p5 add 0 0.2 2.875 p6 add 3.98 0 2.875 p7 add 3.98 0.2 2.875 size 6 1 5
group zone Tunnel range group rockmass not
attach face range z -0.1 0.1
gen zone reflect  dip 90 dd 270 origin 0 0 0
;Material Propery
model mech strainsoft
prop bulk 1285e6 shear 1402e6 coh 1.04e6 fric 27.35 ten 6.23e4 dil 6.84 ftab 1 ctab 2 ttab 3
table 1 0 27.35 0.015 25.72 0.015 25.72
table 2 0 1.04e6 0.015 0.94e6 0.015 0.94e6
table 3 0 6.23e4 0.015 4.6e4 0.015 4.6e4
prop density 2750
;Boundary Condition
fix z range z -45.01 -44.99
fix z range z 44.99 45.01
fix x range x -45.01 -44.99
fix x range x 44.99 45.01
fix y
;Initial Stress
set gravity 0 0 -9.81
ini szz -13.49e6 grad 0 0 0.026978e6
ini sxx -3.26e6 grad 0 0 0.002998e6
ini syy -3.93e6 grad 0 0 0.002998e6
;History
hist add unbal
hist add gp zdisp 0 0 4.15
hist add gp xdisp -3.93 0 -1.4
hist add gp xdisp 3.93 0 -1.4
solve
ini xdis 0 ydis 0 zdis 0
ini xvel 0 yvel 0 zvel 0
save Initial_Ch_1609m
; no support pressure
model mech strainsoft null range group Tunnel
solve
save no_support_pressure
;apply Internal support pressure
rest Initial_Ch_1609m
```

```
model mech strainsoft null range group Tunnel
apply nstress -0.58e6 range cylinder end1 0 0 0 end2 0 0.2 0 radius 4.15 z 1.5 3.5 x 2 4
apply nstress -0.05e6 range cylinder end1 0 0 0 end2 0 0.2 0 radius 4.15 z 1.5 3.15 x -2 -4
apply nstress -0.12e6 range cylinder end1 0 0 0 end2 0 0.2 0 radius 4.15 z 3.5 4.15
apply nstress -0.05e6 range cylinder end1 0 0 0 end2 0 0.2 0 radius 4.15 z 0 1.5 x 4 4.15
apply nstress -0.05e6 range cylinder end1 0 0 0 end2 0 0.2 0 radius 4.15 z 0 1.5 x -4 -4.15
apply sxx -0.05e6 range z 0 -0.575 x 4.11 4.15
apply sxx -0.05e6 range z 0 -0.575 x -4.11 -4.15
apply sxx -0.05e6 range z -0.575 -1.15 x 3.98 4.11
apply sxx -0.05e6 range z -0.575 -1.15 x -3.98 -4.11
apply sxx -0.05e6 range z -4.025 -1.15 x 3.1125 3.98;plane dip 73.21 dd 270 origin 3.98 0 -1.15
apply sxx -0.05e6 range z -4.025 -1.15 x -3.1125 -3.98;plane dip 73.21 dd 270 origin 3.98 0 -1.15
solve
save Ch_1609m_SP_actual_x30
return
;-----------------------------------------------------------------------------------------------------------------------------------------------
```

Paper V
Groundwater effect – Modi tunnel

```
;-----------------------------------------------------------------------------------------------------------------------------------------
new
config fluid

; Model generation

gen zon cylinder p0 0 0 0 p1 2.34 0 0 p2 0 16 0 p3 0 0 2.34 size 3 4 10
gen zon cylinder p0 0 16 0 p1 add 2.34 0 0 p2 add 0 40 0 p3 add 0 0 2.34 size 3 20 10
gen zon cylinder p0 0 56 0 p1 add 2.34 0 0 p2 add 0 20 0 p3 add 0 0 2.34 size 3 5 10
group zone tunnel_arch
gen zone brick p0 0 0 -2.34 p1 add 2.34 0 0 p2 add 0 16 0 p3 add 0 0 2.34 size 3 4 5
gen zone brick p0 0 16 -2.34 p1 add 2.34 0 0 p2 add 0 40 0 p3 add 0 0 2.34 size 3 20 5
gen zone brick p0 0 56 -2.34 p1 add 2.34 0 0 p2 add 0 20 0 p3 add 0 0 2.34 size 3 5 5
group zone tunnel_bench range group tunnel_arch not
gen zon cshell p0 0 16 0 p1 add 6.24 0 0 p2 add 0 40 0 p3 add 0 0 6.24 dim 2.34 2.34 2.34 2.34 size 5 20 10
gen zon cshell p0 0 56 0 p1 add 6.24 0 0 p2 add 0 20 0 p3 add 0 0 6.24 dim 2.34 2.34 2.34 2.34 size 5 5 10
group zone arch_grouted_rockmass range group tunnel_arch not group tunnel_bench not
gen zon brick p0 2.34 16 -2.34 p1 add 3.9 0 0 p2 add 0 40 0 p3 add 0 0 2.34 size 5 20 5
gen zon brick p0 2.34 56 -2.34 p1 add 3.9 0 0 p2 add 0 20 0 p3 add 0 0 2.34 size 5 5 5
group zone wall_grouted_rockmass range group tunnel_arch not group tunnel_bench not group
arch_grouted_rockmass not
gen zon cshell p0 0 0 0 p1 6.24 0 0 p2 0 16 0 p3 0 0 6.24 dim 2.34 2.34 2.34 2.34 size 5 4 10
gen zon brick p0 2.34 0 -2.34 p1 add 3.9 0 0 p2 add 0 16 0 p3 add 0 0 2.34 size 5 4 5
gen zon radcyl p0 0 0 0 p1 25 0 0 p2 0 16 0 p3 0 0 25 dim 6.24 6.24 6.24 6.24 size 5 4 10 12 rat 1 1 1 1
gen zon radcyl p0 0 16 0 p1 25 16 0 p2 0 56 0 p3 0 16 25 dim 6.24 6.24 6.24 6.24 size 5 20 10 12 rat 1 1 1 1
gen zon radcyl p0 0 56 0 p1 25 56 0 p2 0 76 0 p3 0 56 25 dim 6.24 6.24 6.24 6.24 size 5 5 10 12 rat 1 1 1 1
gen zone radtun p0 0 0 0 p1 0 0 -25 p2 0 16 0 p3 25 0 0 dim 2.34 6.24 2.34 6.24 size 5 4 8 12 rat 1 1 1 1
gen zone radtun p0 0 16 0 p1 0 16 -25 p2 0 56 0 p3 25 16 0 dim 2.34 6.24 2.34 6.24 size 5 20 8 12 rat 1 1 1 1
gen zone radtun p0 0 56 0 p1 0 56 -25 p2 0 76 0 p3 25 56 0 dim 2.34 6.24 2.34 6.24 size 5 5 8 12 rat 1 1 1 1
gen zon brick p0 0 0 25 p1 add 40 0 0 p2 add 0 16 0 p3 add 0 0 20 size 8 4 5
gen zon brick p0 0 16 25 p1 add 40 0 0 p2 add 0 40 0 p3 add 0 0 20 size 8 20 5
gen zon brick p0 0 56 25 p1 add 40 0 0 p2 add 0 20 0 p3 add 0 0 20 size 8 5 5
gen zon brick p0 0 0 -45 p1 add 25 0 0 p2 add 0 16 0 p3 add 0 0 20 size 8 4 3
gen zon brick p0 0 16 -45 p1 add 25 0 0 p2 add 0 40 0 p3 add 0 0 20 size 8 20 3
gen zon brick p0 0 56 -45 p1 add 25 0 0 p2 add 0 20 0 p3 add 0 0 20 size 8 5 3
gen zon brick p0 25 0 -45 p1 add 15 0 0 p2 add 0 16 0 p3 add 0 0 20 size 3 4 3
gen zon brick p0 25 16 -45 p1 add 15 0 0 p2 add 0 40 0 p3 add 0 0 20 size 3 20 3
gen zon brick p0 25 56 -45 p1 add 15 0 0 p2 add 0 20 0 p3 add 0 0 20 size 3 5 3
gen zon bric p0 25 0 -25 p1 add 15 0 0 p2 add 0 16 0 p3 add 0 0 50 size 3 4 10 rat 1 1 1
gen zon bric p0 25 16 -25 p1 add 15 0 0 p2 add 0 40 0 p3 add 0 0 50 size 3 20 10 rat 1 1 1
gen zon bric p0 25 56 -25 p1 add 15 0 0 p2 add 0 20 0 p3 add 0 0 50 size 3 5 10 rat 1 1 1

gen zone reflect dip 90 dd 270 origin (0,0,0)

gen zon bric p0 -70 0 45 p1 add 30 0 0 p2 add 0 16 0 p3 add 0 0 35 size 6 4 4 rat 1 1 1
gen zon bric p0 -70 16 45 p1 add 30 0 0 p2 add 0 40 0 p3 add 0 0 35 size 6 20 4 rat 1 1 1
gen zon bric p0 -70 56 45 p1 add 30 0 0 p2 add 0 20 0 p3 add 0 0 35 size 6 5 4 rat 1 1 1
gen zon bric p0 -70 0 80 p1 add 30 0 0 p2 add 0 16 0 p3 add 0 0 45 size 6 4 4 rat 1 1 1
gen zon bric p0 -70 16 80 p1 add 30 0 0 p2 add 0 40 0 p3 add 0 0 45 size 6 20 4 rat 1 1 1
gen zon bric p0 -70 56 80 p1 add 30 0 0 p2 add 0 20 0 p3 add 0 0 45 size 6 5 4 rat 1 1 1
gen zon bric p0 -70 0 25 p1 add 30 0 0 p2 add 0 16 0 p3 add 0 0 20 size 6 4 5 rat 1 1 1
gen zon bric p0 -70 16 25 p1 add 30 0 0 p2 add 0 40 0 p3 add 0 0 20 size 6 20 5 rat 1 1 1
gen zon bric p0 -70 56 25 p1 add 30 0 0 p2 add 0 20 0 p3 add 0 0 20 size 6 5 5 rat 1 1 1
gen zon bric p0 -70 0 -25 p1 add 30 0 0 p2 add 0 16 0 p3 add 0 0 50 size 6 4 10 rat 1 1 1
gen zon bric p0 -70 16 -25 p1 add 30 0 0 p2 add 0 40 0 p3 add 0 0 50 size 6 20 10 rat 1 1 1
gen zon bric p0 -70 56 -25 p1 add 30 0 0 p2 add 0 20 0 p3 add 0 0 50 size 6 5 10 rat 1 1 1
gen zon bric p0 -70 0 -45 p1 add 30 0 0 p2 add 0 16 0 p3 add 0 0 20 size 6 4 3 rat 1 1 1
gen zon bric p0 -70 16 -45 p1 add 30 0 0 p2 add 0 40 0 p3 add 0 0 20 size 6 20 3 rat 1 1 1
gen zon bric p0 -70 56 -45 p1 add 30 0 0 p2 add 0 20 0 p3 add 0 0 20 size 6 5 3 rat 1 1 1
gen zon uwedge p0 -40 0 80 p1 add 40 0 0 p2 add 0 16 0 p3 add 0 0 45 size 8 4 4
gen zon uwedge p0 -40 16 80 p1 add 40 0 0 p2 add 0 40 0 p3 add 0 0 45 size 8 20 4
```

```
gen zon uwedge p0 -40 56 80 p1 add 40 0 0 p2 add 0 20 0 p3 add 0 0 45 size 8 5 4
gen zon bric p0 -40 0 45 p1 add 40 0 0 p2 add 0 16 0 p3 add 0 0 35 size 8 4 4 rat 1 1 1
gen zon bric p0 -40 16 45 p1 add 40 0 0 p2 add 0 40 0 p3 add 0 0 35 size 8 20 4 rat 1 1 1
gen zon bric p0 -40 56 45 p1 add 40 0 0 p2 add 0 20 0 p3 add 0 0 35 size 8 5 4 rat 1 1 1
gen zon uwedge p0 0 0 45 p1 add 40 0 0 p2 add 0 16 0 p3 add 0 0 35 size 8 4 4
gen zon uwedge p0 0 16 45 p1 add 40 0 0 p2 add 0 40 0 p3 add 0 0 35 size 8 20 4
gen zon uwedge p0 0 56 45 p1 add 40 0 0 p2 add 0 20 0 p3 add 0 0 35 size 8 5 4
gen zon bric p0 40 0 -45 p1 add 49 0 0 p2 add 0 16 0 p3 add 0 0 20 size 10 4 3 rat 1 1 1
gen zon bric p0 40 16 -45 p1 add 49 0 0 p2 add 0 40 0 p3 add 0 0 20 size 10 20 3 rat 1 1 1
gen zon bric p0 40 56 -45 p1 add 49 0 0 p2 add 0 20 0 p3 add 0 0 20 size 10 5 3 rat 1 1 1
gen zon bric p0 40 0 -25 p1 add 49 0 0 p2 add 0 16 0 p3 add 0 0 50 size 10 4 10 rat 1 1 1
gen zon bric p0 40 16 -25 p1 add 49 0 0 p2 add 0 40 0 p3 add 0 0 50 size 10 20 10 rat 1 1 1
gen zon bric p0 40 56 -25 p1 add 49 0 0 p2 add 0 20 0 p3 add 0 0 50 size 10 5 10 rat 1 1 1
gen zon uwedge p0 40 0 25 p1 add 49 0 0 p2 add 0 16 0 p3 add 0 0 20 size 10 4 5
gen zon uwedge p0 40 16 25 p1 add 49 0 0 p2 add 0 40 0 p3 add 0 0 20 size 10 20 5
gen zon uwedge p0 40 56 25 p1 add 49 0 0 p2 add 0 20 0 p3 add 0 0 20 size 10 5 5

attach face

group zone phyllitic_quartzite range plane below dip -32.35 dd 116 ori 0 -30 0 group tunnel_arch not group &
        tunnel_bench not group arch_grouted_rockmass not group wall_grouted_rockmass not
group zone phyllitic_schist range plane above dip -32.35 dd 116 ori 0 -30 0 plane below dip -32.35 dd 116 &
        ori 0 14 0 group tunnel_arch not group tunnel_bench not group arch_grouted_rockmass not  &
        group wall_grouted_rockmass not
group zone fault range plane above dip -32.35 dd 116 ori 0 14 0 plane below dip -32.35 dd 116 ori 0 79 0 &
        group tunnel_arch not group tunnel_bench not group arch_grouted_rockmass not  &
        group wall_grouted_rockmass not
group zone quartzite range plane above dip -32.35 dd 116 ori 0 79 0 group tunnel_arch not &
        group tunnel_bench not group arch_grouted_rockmass not  group wall_grouted_rockmass not
group zone conglomerate range plane above dip -10 dd 90 ori 0 37.5 25 group tunnel_arch not &
        group tunnel_bench not group arch_grouted_rockmass not group wall_grouted_rockmass not

;Mechanical properities

model mech mohr
pro density 2680 bulk 0.939e9 she 0.794e9  fric 49 coh 0.36e6 ten 0.014e6 dil 15 &
        range plane below dip -32.35 dd 116 ori 0 -30 0
pro density 2730 bulk 136e6 she 148e6 fric 27 coh 0.12e6 ten 0.002e6 dil 8 &
        range plane above dip -32.35 dd 116 ori 0 -30 0
pro density 2660 bulk 4.91e6 she 3.68e6  fric 17 coh 0.058e6 ten 0 dil 0 &
        range plane above dip -32.35 dd 116 ori 0 14 0
pro density 2660 bulk 2.37e9 she 1.78e9  fric 57 coh 0.57e6 ten 0.031e6 dil 18 &
        range plane above dip -32.35 dd 116 ori 0 79 0
pro density 2600 bulk 1.52e9 she 1.14e9 fric 47 coh 0.754e6 ten 0.026e6 dil 15 &
        range plane above dip -10 dd 90 ori 0 37.5 25

;Assign fluid model

model fluid fl_iso
prop por 0.01 perm 10e-07 range plane below dip -32.35 dd 116 ori 0 14 0
prop por 0.25 perm 10e-05 range plane above dip -32.35 dd 116 ori 0 14 0
prop por 0.01 perm 10e-06 range plane above dip -32.35 dd 116 ori 0 79 0
ini fdens 1000
ini ftens 0
ini fmod 2e9
ini sat 0 range plane above dip 3.6 dd 90 ori 0 38 21.6
ini sat 1 range plane below dip 3.6 dd 90 ori 0 38 21.6

;Initial pore pressure distribution

ini pp 0.207e6 grad -0.06292e4 0 -0.981e4 range x 0 89 z -45 15
fix pp range x 88.9 89.1
ini pp 0.207e6 grad -0.06285e4 0 -0.981e4 range x 0 -70 Z -45 25
```

```
fix pp range x -70.1 -69.9

;Initial Conditions

set gravity 0 0 -9.81
ini szz -3.25e6 grad 0 0 0.026e6 range x -70 -40
ini szz -2.08e6 grad 0.02925e6 0 0.026e6 range x 0 -40
ini szz -2.08e6 grad 0.02275e6 0 0.026e6 range x 0 40
ini szz -1.64e6 grad 0.0106e6 0 0.026e6 range x 40 89
ini sxx -0.8125e6 grad 0 0 0.0065e6 range x -70 -40
ini sxx -0.52e6 grad 0.0073e6 0 0.0065e6 range x 0 -40
ini sxx -0.52e6 grad 0.00568e6 0 0.0065e6 range x 0 40
ini sxx -0.41e6 grad 0.00265e6 0 0.0065e6 range x 40 89
ini syy -0.8125e6 grad 0 0 0.0065e6 range x -70 -40
ini syy -0.52e6 grad 0.0073e6 0 0.0065e6 range x 0 -40
ini syy -0.52e6 grad 0.00568e6 0 0.0065e6 range x 0 40
ini syy -0.41e6 grad 0.00265e6 0 0.0065e6 range x 40 89
ini sxx add -0.81e6 grad 0 0 0 range z -45 25
ini syy add -3.92e6 grad 0 0 0 range z -45 25


;Boundary Conditions

fix x range x -70.1 -69.9
fix x range x 88.9 89.1
fix y range y -0.1 0.1
fix y range y 75.9 76.1
fix x range z -45.1 -44.9
fix y range z -45.1 -44.9
fix z range z -45.1 -44.9-

set mech on
set fluid off

hist add unbal
hist add gp xdis -2.34,25,0
hist add gp xdis -2.34,25,-1.6
hist add gp xdis -2.34,25,-2.2
hist add gp zdis 0,25,2.34
hist add gp xdis -2.34,35,0
hist add gp xdis -2.34,35,-1.6
hist add gp xdis -2.34,35,-2.2
hist add gp zdis 0,35,2.34
hist add gp xdis -2.35,40
hist add gp xdis -2.35,40
hist add gp xdis -2.35,40,-2.2 ; 16
hist add gp zdis 0,40,2.35 ;17
hist add gp xdis -2.34,45,0 ; 18
hist add gp xdis -2.34,45,-1.6 ; 19
hist add gp xdis -2.34,45,-2.2 ; 20
hist add gp zdis 0,45,2.34 ;21
hist fltime

solve elastic

save modi_initial

ini xdis=0 ydis=0 zdis=0
ini xvel=0 yvel=0 zvel=0
save modi_initial_no_disp

;Fish codes
;Arch Excavation
```

```
def tunnel_arch_excavation
exca_1=exca1
exca_2=exca2
command
model mech mohr null range group tunnel_arch y @exca_1, @exca_2
model fluid fl_null range group tunnel_arch y @exca_1, @exca_2
apply pp 0 range group tunnel_arch y @exca_1, @exca_2
ini fmod 2e9
set fluid on mech off
step 5000
set fluid off mech on
ini fmod 0
solve
end_command
end

;Bench Excavation

def tunnel_bench_excavation
exca_3=exca3
exca_4=exca4
command
model mech mohr null range group tunnel_bench y @exca_3, @exca_4
model fluid fl_null range group tunnel_bench y @exca_3, @exca_4
apply pp 0 range group tunnel_bench y @exca_3, @exca_4
ini fmod 2e9
set fluid on mech off
step 5000
set fluid off mech on
ini fmod 0
solve
end_command
end

;Full Face Excavation

def tunnel_full_excavation
exca_5=exca5
exca_6=exca6
command
model mech mohr null range group tunnel_arch y @exca_5, @exca_6
model mech mohr null range group tunnel_bench y @exca_5, @exca_6
model fluid fl_null range group tunnel_arch y @exca_5, @exca_6
model fluid fl_null range group tunnel_bench y @exca_5, @exca_6
apply pp 0 range group tunnel_arch y @exca_5, @exca_6
apply pp 0 range group tunnel_bench y @exca_5, @exca_6
ini fmod 2e9
set fluid on mech off
step 5000
set fluid off mech on
ini fmod 0
solve
end_command
end

;Arch shotcrete

def shotcrete_arch
ed_begin =ed1
ed_end =ed2
command
sel shell id=1 range cyl end1 0,@ed_begin,0 end2 0,@ed_end,0 rad 2.34
```

```
sel shell prop iso=(10e9,0.20) thick=0.1
sel node fix x yr zr range x -0.1 0.1
sel node fix y xr zr range y -0.1 0.1
sel delete shell range x=-2.34,2.34 y=@ed_begin,@ed_end z=-2.34,0.01
end_command
end

;Wall shotcrete

def shotcrete_wall
wled_begin =ed3
wled_end =ed4
command
sel shell id=1 range x=2.24,2.34 y=@wled_begin,@wled_end z=-2.34,0.01
sel shell id=1 range x=-2.2401,-2.3401 y=@wled_begin,@wled_end z=-2.34,0.01
sel shell prop iso=(10e9,0.20) thick=0.1
sel node fix x yr zr range x -0.1 0.1
sel node fix y xr zr range y -0.1 0.1
end_command
end

;Full perimeter shotcrete

def shotcrete_full
fed_begin =ed5
fed_end =ed6
command
sel shell id=1 range cyl end1 0,@fed_begin,0 end2 0,@fed_end,0 rad 2.34
sel shell id=1 range x=2.24,2.34 y=@fed_begin,@fed_end z=-2.34,0
sel shell id=1 range x=-2.2401,-2.3401 y=@fed_begin,@fed_end z=-2.34,0
sel shell prop iso=(10e9,0.20) thick=0.1
sel node fix x yr zr range x -0.1 0.1
sel node fix y xr zr range y -0.1 0.1
end_command
end

;75mm thick fullperimeter shotcrete

def shotcrete_full_75
sfed_begin =ed7
sfed_end =ed8
command
sel shell id=1 range cyl end1 0,@sfed_begin,0 end2 0,@sfed_end,0 rad 2.34
sel shell id=1 range x=2.24,2.34 y=@sfed_begin,@sfed_end z=-2.34,0
sel shell id=1 range x=-2.2401,-2.3401 y=@sfed_begin,@sfed_end z=-2.34,0
sel shell prop iso=(10e9,0.20) thick=0.075
sel node fix x yr zr range x -0.1 0.1
sel node fix y xr zr range y -0.1 0.1
end_command
end

;Steel Rib

def steel_rib_arch
 y_beam=ybeam
 loop kk (0,17)
  x_1=2.34*cos(kk*10*pi/180)
  x_2=2.34*cos((kk+1)*10*pi/180)

 z_1=2.34*sin(kk*10*pi/180)
 z_2=2.34*sin((kk+1)*10*pi/180)
command
sel beam id=3  begin=(@x_1,@y_beam,@z_1) end=(@x_2,@y_beam,@z_2) nseg=3
```

```
end_command
end_loop
command
sel beam id 3 prop e 210e9 nu 0.25 xcarea 0.0034 xciy 1.45e-5 xciz 4.39e-6 xcj 1.88e-5
sel node fix y; xr zr ; free to move in x and z direction
end_command
end

def steel_rib_wall
y_beamw=ybeamw
x_1w_right=2.34
x_2w_right=2.34
x_1w_left=-2.34
x_2w_left=-2.34
z_1w=0
z_2w=-2.35
command
sel beam id=3  begin=(@x_1w_right,@y_beamw,@z_1w) end=(@x_2w_right,@y_beamw,@z_2w) nseg=3
sel beam id=3  begin=(@x_1w_left,@y_beamw,@z_1w) end=(@x_2w_left,@y_beamw,@z_2w) nseg=3
end_command
command
sel beam id 3 prop e 210e9 nu 0.25 xcarea 0.0034 xciy 1.45e-5 xciz 4.39e-6 xcj 1.88e-5
sel node fix y
end_command
end

;Staged excavation

model mech mohr null range group tunnel_arch y 0, 2
model mech mohr null range group tunnel_bench y 0, 2
model fluid fl_null range group tunnel_arch y 0, 2
model fluid fl_null range group tunnel_bench y 0, 2
apply pp 0 range group tunnel_arch y 0, 2
apply pp 0 range group tunnel_bench y 0, 2
ini fmod 2e9
set fluid on mech off
step 50000
set fluid off mech on
ini fmod 0
solve
save after_50000_steps
set @ed7 0 @ed8 1.9
@shotcrete_full_75
set @ybeam 0.1
@steel_rib_arch
set @ybeamw 0.1
@steel_rib_wall
set @ybeam 1
@steel_rib_arch
set @ybeamw 1
@steel_rib_wall
set @ybeam 2
@steel_rib_arch
set @ybeamw 2
@steel_rib_wall
solve
ini xdis=0 ydis=0 zdis=0
ini xvel=0 yvel=0 zvel=0
set @exca5 2 @exca6 4
@tunnel_full_excavation
set @ed7 1.9 @ed8 3.9
@shotcrete_full_75
set @ybeam 3
```

```
@steel_rib_arch
set @ybeamw 3
@steel_rib_wall
set @ybeam 4
@steel_rib_arch
set @ybeamw 4
@steel_rib_wall
solve
set @exca5 4 @exca6 6
@tunnel_full_excavation
set @ed7 3.9 @ed8 5.9
@shotcrete_full_75
set @ybeam 5
@steel_rib_arch
set @ybeamw 5
@steel_rib_wall
set @ybeam 6
@steel_rib_arch
set @ybeamw 6
@steel_rib_wall
solve
t @exca5 6 @exca6 8
@tunnel_full_excavation
set @ed7 5.9 @ed8 7.9
@shotcrete_full_75
set @ybeam 7
@steel_rib_arch
set @ybeamw 7
@steel_rib_wall
set @ybeam 8
@steel_rib_arch
set @ybeamw 8
@steel_rib_wall
solve
set @exca5 8 @exca6 10
@tunnel_full_excavation
set @ed7 7.9 @ed8 9.9
@shotcrete_full_75
set @ybeam 9
@steel_rib_arch
set @ybeamw 9
@steel_rib_wall
set @ybeam 10
@steel_rib_arch
set @ybeamw 10
@steel_rib_wall
solve
set @exca5 10 @exca6 11
@tunnel_full_excavation
set @ed7 9.9 @ed8 10.9
@shotcrete_full_75
set @ybeam 11
@steel_rib_arch
set @ybeamw 11
@steel_rib_wall
solve
set @exca5 11 @exca6 12
@tunnel_full_excavation
set @ed7 10.9 @ed8 11.9
@shotcrete_full_75
set @ybeam 12
@steel_rib_arch
set @ybeamw 12
```

```
@steel_rib_wall
solve
set @exca5 12 @exca6 13
@tunnel_full_excavation
set @ed7 11.9 @ed8 12.9
@shotcrete_full_75
set @ybeam 13
@steel_rib_arch
set @ybeamw 13
@steel_rib_wall
solve
set @exca5 13 @exca6 14
@tunnel_full_excavation
set @ed7 12.9 @ed8 13.9
@shotcrete_full_75
set @ybeam 14
@steel_rib_arch
set @ybeamw 14
@steel_rib_wall
solve
set @exca5 14 @exca6 15
@tunnel_full_excavation
set @ed7 13.9 @ed8 14.9
@shotcrete_full_75
set @ybeam 15
@steel_rib_arch
set @ybeamw 15
@steel_rib_wall
solve
save E15m
model mech mohr range group arch_grouted_rockmass y 15 19
prop bulk 29.36e6 shea 22.02e6 den 2660 fric 28 coh 0.12e6 dil 9 ten 0.0004e6 &
        range group arch_grouted_rockmass y 15 19
model mech mohr range group tunnel_arch y 15 19
prop bulk 29.36e6 shea 22.02e6 den 2660 fric 28 coh 0.12e6 dil 9 ten 0.0004e6 range group tunnel_arch y 15 19
solve
set @exca5 15 @exca6 16
@tunnel_full_excavation
set @ed7 14.9 @ed8 15.9
@shotcrete_full_75
set @ybeam 16
@steel_rib_arch
set @ybeamw 16
@steel_rib_wall
solve
set @exca1 16 @exca2 17
@tunnel_arch_excavation
set @ed1 15.9 @ed2 16.9
@shotcrete_arch
set @ybeam 16.3
@steel_rib_arch
set @ybeam 16.6
@steel_rib_arch
set @ybeam 16.9
@steel_rib_arch
solve
set @exca1 17 @exca2 18
@tunnel_arch_excavation
set @ed1 16.9 @ed2 17.9
@shotcrete_arch
set @ybeam 17.2
@steel_rib_arch
set @ybeam 17.5
```

```
@steel_rib_arch
set @ybeam 17.8
@steel_rib_arch
solve
save E18m
model mech mohr range group arch_grouted_rockmass y 19 23
prop bulk 29.36e6 shea 22.02e6 den 2660 fric 28 coh 0.12e6 dil 9 ten 0.0004e6 &
        range group arch_grouted_rockmass y 19 23
model mech mohr range group tunnel_arch y 19 23
prop bulk 29.36e6 shea 22.02e6 den 2660 fric 28 coh 0.12e6 dil 9 ten 0.0004e6 range group tunnel_arch y 19 23
solve

;heading

set @exca1 18 @exca2 19
@tunnel_arch_excavation
set @ed1 17.9 @ed2 18.9
@shotcrete_arch
;steel rib arch
set @ybeam 18.1
@steel_rib_arch
set @ybeam 18.4
@steel_rib_arch
set @ybeam 18.7
@steel_rib_arch
set @ybeam 19
@steel_rib_arch
solve
set @exca1 19 @exca2 20
@tunnel_arch_excavation
set @ed1 18.9 @ed2 19.9
@shotcrete_arch
;steel rib arch
set @ybeam 19.3
@steel_rib_arch
set @ybeam 19.6
@steel_rib_arch
set @ybeam 19.9
@steel_rib_arch
solve
set @exca1 20 @exca2 21
@tunnel_arch_excavation
set @ed1 19.9 @ed2 20.9
@shotcrete_arch
;steel rib arch
set @ybeam 20.2
@steel_rib_arch
set @ybeam 20.5
@steel_rib_arch
set @ybeam 20.8
@steel_rib_arch
solve
set @exca1 21 @exca2 22
@tunnel_arch_excavation
set @ed1 20.9 @ed2 21.9
@shotcrete_arch
;steel rib arch
set @ybeam 21.1
@steel_rib_arch
set @ybeam 21.4
@steel_rib_arch
set @ybeam 21.7
@steel_rib_arch
```

```
set @ybeam 22
@steel_rib_arch
solve
save E18_22_heading
model mech mohr range group wall_grouted_rockmass y 15 19
prop bulk 29.36e6 shea 22.02e6 den 2660 fric 28 coh 0.12e6 dil 9 ten 0.0004e6 &
        range group wall_grouted_rockmass y 15 19
model mech mohr range group arch_grouted_rockmass y 23 27
prop bulk 29.36e6 shea 22.02e6 den 2660 fric 28 coh 0.12e6 dil 9 ten 0.0004e6 &
        range group arch_grouted_rockmass y 23 27
model mech mohr range group tunnel_arch y 23 27
prop bulk 29.36e6 shea 22.02e6 den 2660 fric 28 coh 0.12e6 dil 9 ten 0.0004e6 range group tunnel_arch y 23 27
solve

;bench excavation

set @exca3 16 @exca4 18
@tunnel_bench_excavation
set @ed3 15.9 @ed4 17.9
@shotcrete_wall
;steel rib wall
set @ybeamw 16.3
@steel_rib_wall
set @ybeamw 16.6
@steel_rib_wall
set @ybeamw 16.9
@steel_rib_wall
set @ybeamw 17.2
@steel_rib_wall
set @ybeamw 17.5
@steel_rib_wall
set @ybeamw 17.8
@steel_rib_wall
solve

;heading excavation

set @exca1 22 @exca2 23
@tunnel_arch_excavation
set @ed1 21.9 @ed2 22.9
@shotcrete_arch
;steel rib arch
set @ybeam 22.5
@steel_rib_arch
set @ybeam 23
@steel_rib_arch
solve
save E23m
set @exca1 23 @exca2 24
@tunnel_arch_excavation
set @ed1 22.9 @ed2 23.9
@shotcrete_arch
;steel rib arch
set @ybeam 23.5
@steel_rib_arch
set @ybeam 24
@steel_rib_arch
solve
model mech mohr range group wall_grouted_rockmass y 19 23
prop bulk 29.36e6 shea 22.02e6 den 2660 fric 28 coh 0.12e6 dil 9 ten 0.0004e6 &
        group wall_grouted_rockmass y 19 23
;bench excavation
set @exca3 18 @exca4 20
```

```
@tunnel_bench_excavation
set @ed3 17.9 @ed4 19.9
@shotcrete_wall
;steel rib wall
set @ybeamw 18.1
@steel_rib_wall
set @ybeamw 18.4
@steel_rib_wall
set @ybeamw 18.7
@steel_rib_wall
set @ybeamw 19
@steel_rib_wall
set @ybeamw 19.3
@steel_rib_wall
set @ybeamw 19.6
@steel_rib_wall
set @ybeamw 19.9
@steel_rib_wall
solve

;heading excavation

set @exca1 24 @exca2 25
@tunnel_arch_excavation
set @ed1 23.9 @ed2 24.9
@shotcrete_arch
;steel rib arch
set @ybeam 24.5
@steel_rib_arch
set @ybeam 25
@steel_rib_arch
save E25m
solve
set @exca1 25 @exca2 26
@tunnel_arch_excavation
set @ed1 24.9 @ed2 25.9
@shotcrete_arch
;steel rib arch
set @ybeam 25.5
@steel_rib_arch
set @ybeam 26
@steel_rib_arch
solve
save E26m
model mech mohr range group arch_grouted_rockmass y 27 31
prop bulk 29.36e6 shea 22.02e6 den 2660 fric 28 coh 0.12e6 dil 9 ten 0.0004e6 &
        range group arch_grouted_rockmass y 27 31
model mech mohr range group tunnel_arch y 27 31
prop bulk 29.36e6 shea 22.02e6 den 2660 fric 28 coh 0.12e6 dil 9 ten 0.0004e6 &
        range group tunnel_arch y 27 31
solve

;bench excavation

set @exca3 20 @exca4 22
@tunnel_bench_excavation
set @ed3 19.9 @ed4 21.9
@shotcrete_wall
;steel rib wall
set @ybeamw 20.2
@steel_rib_wall
set @ybeamw 20.5
@steel_rib_wall
```

```
set @ybeamw 20.8
@steel_rib_wall
set @ybeamw 21.1
@steel_rib_wall
set @ybeamw 21.4
@steel_rib_wall
set @ybeamw 21.7
@steel_rib_wall
set @ybeamw 22
@steel_rib_wall
solve
save 20_22_bench

;heading excavation

set @exca1 26 @exca2 27
@tunnel_arch_excavation
set @ed1 25.9 @ed2 26.9
@shotcrete_arch
;steel rib arch
set @ybeam 26.5
@steel_rib_arch
set @ybeam 27
@steel_rib_arch
solve
save 26_27_arch
set @exca1 27 @exca2 28
@tunnel_arch_excavation
set @ed1 26.9 @ed2 27.9
@shotcrete_arch
;steel rib arch
set @ybeam 27.5
@steel_rib_arch
set @ybeam 28
@steel_rib_arch
solve
save 27_28_arch
model mech mohr range group wall_grouted_rockmass y 23 27
prop bulk 29.36e6 shea 22.02e6 den 2660 fric 28 coh 0.12e6 dil 9 ten 0.0004e6 &
        range group wall_grouted_rockmass y 23 27

;bench excavation

set @exca3 22 @exca4 24
@tunnel_bench_excavation
set @ed3 21.9 @ed4 23.9
@shotcrete_wall
;steel rib wall
set @ybeamw 22.5
@steel_rib_wall
set @ybeamw 23
@steel_rib_wall
set @ybeamw 23.5
@steel_rib_wall
set @ybeamw 24
@steel_rib_wall
solve
save 22_24_bench

;heading excavation

set @exca1 28 @exca2 29
@tunnel_arch_excavation
```

```
set @ed1 27.9 @ed2 28.9
@shotcrete_arch
;steel rib arch
set @ybeam 28.5
@steel_rib_arch
set @ybeam 29
@steel_rib_arch
solve
save 28_29_arch

set @exca1 29 @exca2 30
@tunnel_arch_excavation
set @ed1 28.9 @ed2 29.9
@shotcrete_arch
;steel rib arch
set @ybeam 29.5
@steel_rib_arch
set @ybeam 30
@steel_rib_arch
solve
save E30m
model mech mohr range group arch_grouted_rockmass y 31 35
prop bulk 29.36e6 shea 22.02e6 den 2660 fric 28 coh 0.12e6 dil 9 ten 0.0004e6 &
        range group arch_grouted_rockmass y 31 35
model mech mohr range group tunnel_arch y 31 35
prop bulk 29.36e6 shea 22.02e6 den 2660 fric 28 coh 0.12e6 dil 9 ten 0.0004e6 &
        range group tunnel_arch y 31 35
solve

;bench excavation

set @exca3 24 @exca4 26
@tunnel_bench_excavation
set @ed3 23.9 @ed4 25.9
@shotcrete_wall
;steel rib wall
set @ybeamw 24.5
@steel_rib_wall
set @ybeamw 25
@steel_rib_wall
set @ybeamw 25.5
@steel_rib_wall
set @ybeamw 26
@steel_rib_wall
solve
save 24_26_bench

;heading excavation

set @exca1 30 @exca2 31
@tunnel_arch_excavation
set @ed1 29.9 @ed2 30.9
@shotcrete_arch
;steel rib arch
set @ybeam 30.5
@steel_rib_arch
set @ybeam 31
@steel_rib_arch
solve

set @exca1 31 @exca2 32
@tunnel_arch_excavation
set @ed1 30.9 @ed2 31.9
```

```
@shotcrete_arch
;steel rib arch
set @ybeam 31.5
@steel_rib_arch
set @ybeam 32
@steel_rib_arch
solve
save 31_32_arch_excavation
model mech mohr range group wall_grouted_rockmass y 27 31
prop bulk 29.36e6 shea 22.02e6 den 2660 fric 28 coh 0.12e6 dil 9 ten 0.0004e6 &
        range group wall_grouted_rockmass y 27 31
;benching

set @exca3 26 @exca4 28
@tunnel_bench_excavation

set @ed3 25.9 @ed4 27.9
@shotcrete_wall
;steel rib wall
set @ybeamw 26.5
@steel_rib_wall
set @ybeamw 27
@steel_rib_wall
set @ybeamw 27.5
@steel_rib_wall
set @ybeamw 28
@steel_rib_wall
solve
save 26_28_bench

;heading excavation

set @exca1 32 @exca2 33
@tunnel_arch_excavation
set @ed1 31.9 @ed2 32.9
@shotcrete_arch
;steel rib arch
set @ybeam 32.5
@steel_rib_arch
set @ybeam 33
@steel_rib_arch
solve
save 32_33_arch

set @exca1 33 @exca2 34
@tunnel_arch_excavation
set @ed1 32.9 @ed2 33.9
@shotcrete_arch
;steel rib arch
set @ybeam 33.5
@steel_rib_arch
set @ybeam 34
@steel_rib_arch
solve
save E34m
model mech mohr range group arch_grouted_rockmass y 35 39
prop bulk 29.36e6 shea 22.02e6 den 2660 fric 28 coh 0.12e6 dil 9 ten 0.0004e6 range group &
        arch_grouted_rockmass y 35 39
model mech mohr range group tunnel_arch y 35 39
prop bulk 29.36e6 shea 22.02e6 den 2660 fric 28 coh 0.12e6 dil 9 ten 0.0004e6 &
        range group tunnel_arch y 35 39
solve
```

```
;bench

set @exca3 28 @exca4 30
@tunnel_bench_excavation
set @ed3 27.9 @ed4 29.9
@shotcrete_wall
;steel rib wall
set @ybeamw 28.5
@steel_rib_wall
set @ybeamw 29
@steel_rib_wall
set @ybeamw 29.5
@steel_rib_wall
set @ybeamw 30
@steel_rib_wall
solve
save 28_30_bench

;heading excavation

set @exca1 34 @exca2 35
@tunnel_arch_excavation
set @ed1 33.9 @ed2 34.9
@shotcrete_arch
;steel rib arch
set @ybeam 34.5
@steel_rib_arch
set @ybeam 35
@steel_rib_arch
solve
save 34_35_arch
set @exca1 35 @exca2 36
@tunnel_arch_excavation
set @ed1 34.9 @ed2 35.9
@shotcrete_arch
;steel rib arch
set @ybeam 35.5
@steel_rib_arch
set @ybeam 36
@steel_rib_arch
solve
save 35_36_arch
model mech mohr range group wall_grouted_rockmass y 31 35
prop bulk 29.36e6 shea 22.02e6 den 2660 fric 28 coh 0.12e6 dil 9 ten 0.0004e6 &
        range group wall_grouted_rockmass y 31 35
;bench

set @exca3 30 @exca4 32
@tunnel_bench_excavation
set @ed3 29.9 @ed4 31.9
@shotcrete_wall
;steel rib wall
set @ybeamw 30.5
@steel_rib_wall
set @ybeamw 31
@steel_rib_wall
set @ybeamw 31.5
@steel_rib_wall
set @ybeamw 32
@steel_rib_wall
solve
save 30_32_bench
```

```
;heading excavation

set @exca1 36 @exca2 37
@tunnel_arch_excavation
set @ed1 35.9 @ed2 36.9
@shotcrete_arch
;steel rib arch
set @ybeam 36.5
@steel_rib_arch
set @ybeam 37
@steel_rib_arch
solve
save 36_37_arch
set @exca1 37 @exca2 38
@tunnel_arch_excavation
set @ed1 36.9 @ed2 37.9
@shotcrete_arch
;steel rib arch
set @ybeam 37.5
@steel_rib_arch
set @ybeam 38
@steel_rib_arch
solve
save E38m
model mech mohr range group arch_grouted_rockmass y 39 43
prop bulk 29.36e6 shea 22.02e6 den 2660 fric 28 coh 0.12e6 dil 9 ten 0.0004e6 &
        range group arch_grouted_rockmass y 39 43
model mech mohr range group tunnel_arch y 39 43
prop bulk 29.36e6 shea 22.02e6 den 2660 fric 28 coh 0.12e6 dil 9 ten 0.0004e6 range group tunnel_arch y 39 43
solve

;bench

set @exca3 32 @exca4 34
@tunnel_bench_excavation
set @ed3 31.9 @ed4 33.9
@shotcrete_wall
;steel rib wall
set @ybeamw 32.5
@steel_rib_wall
set @ybeamw 33
@steel_rib_wall
set @ybeamw 33.5
@steel_rib_wall
set @ybeamw 34
@steel_rib_wall
solve
save 32_34_bench

;heading excavation

set @exca1 38 @exca2 39
@tunnel_arch_excavation
set @ed1 37.9 @ed2 38.9
@shotcrete_arch
;steel rib arch
set @ybeam 38.5
@steel_rib_arch
set @ybeam 39
@steel_rib_arch
solve
save 38_39_arch
set @exca1 39 @exca2 40
```

```
@tunnel_arch_excavation
set @ed1 38.9 @ed2 39.9
@shotcrete_arch
;steel rib arch
set @ybeam 39.5
@steel_rib_arch
set @ybeam 40
@steel_rib_arch
solve
save 39_40_arch
model mech mohr range group wall_grouted_rockmass y 35 39
prop bulk 29.36e6 shea 22.02e6 den 2660 fric 28 coh 0.12e6 dil 9 ten 0.0004e6 &
        range group wall_grouted_rockmass y 35 39
;bench

set @exca3 34 @exca4 36
@tunnel_bench_excavation
set @ed3 33.9 @ed4 35.9
@shotcrete_wall
;steel rib wall
set @ybeamw 34.5
@steel_rib_wall
set @ybeamw 35
@steel_rib_wall
set @ybeamw 35.5
@steel_rib_wall
set @ybeamw 36
@steel_rib_wall
solve
save 34_36_bench

;heading excavation

set @exca1 40 @exca2 41
@tunnel_arch_excavation
set @ed1 39.9 @ed2 40.9
@shotcrete_arch
;steel rib arch
set @ybeam 40.5
@steel_rib_arch
set @ybeam 41
@steel_rib_arch
solve
save 40_41_arch
set @exca1 41 @exca2 42
@tunnel_arch_excavation
set @ed1 40.9 @ed2 41.9
@shotcrete_arch
;steel rib arch
set @ybeam 41.5
@steel_rib_arch
set @ybeam 42
@steel_rib_arch
solve
save E42m
model mech mohr range group arch_grouted_rockmass y 43 47
prop bulk 29.36e6 shea 22.02e6 den 2660 fric 28 coh 0.12e6 dil 9 ten 0.0004e6 &
        range group arch_grouted_rockmass y 43 47
model mech mohr range group tunnel_arch y 43 47
prop bulk 29.36e6 shea 22.02e6 den 2660 fric 28 coh 0.12e6 dil 9 ten 0.0004e6 &
        range group tunnel_arch y 43 47
solve
```

```
;bench

set @exca3 36 @exca4 38
@tunnel_bench_excavation
set @ed3 35.9 @ed4 37.9
@shotcrete_wall
;steel rib wall
set @ybeamw 36.5
@steel_rib_wall
set @ybeamw 37
@steel_rib_wall
set @ybeamw 37.5
@steel_rib_wall
set @ybeamw 38
@steel_rib_wall
solve
save 36_38_bench

;heading excavation

set @exca1 42 @exca2 43
@tunnel_arch_excavation
set @ed1 41.9 @ed2 42.9
@shotcrete_arch
;steel rib arch
set @ybeam 42.5
@steel_rib_arch
set @ybeam 43
@steel_rib_arch
solve
save 42_43_arch
set @exca1 43 @exca2 44
@tunnel_arch_excavation
set @ed1 42.9 @ed2 43.9
@shotcrete_arch
;steel rib arch
set @ybeam 43.5
@steel_rib_arch
set @ybeam 44
@steel_rib_arch
solve
save 43_44_arch
model mech mohr range group wall_grouted_rockmass y 39 43
prop bulk 29.36e6 shea 22.02e6 den 2660 fric 28 coh 0.12e6 dil 9 ten 0.0004e6 &
        range group wall_grouted_rockmass y 39 43
;bench

set @exca3 38 @exca4 40
@tunnel_bench_excavation
set @ed3 37.9 @ed4 39.9
@shotcrete_wall
;steel rib wall
set @ybeamw 38.5
@steel_rib_wall
set @ybeamw 39
@steel_rib_wall
set @ybeamw 39.5
@steel_rib_wall
set @ybeamw 40
@steel_rib_wall
solve
save 38_40_bench
```

```
;heading excavation

set @exca1 44 @exca2 45
@tunnel_arch_excavation
set @ed1 43.9 @ed2 44.9
@shotcrete_arch
;steel rib arch
set @ybeam 44.5
@steel_rib_arch
set @ybeam 45
@steel_rib_arch
solve
save 44_45_arch

set @exca1 45 @exca2 46
@tunnel_arch_excavation
set @ed1 44.9 @ed2 45.9
@shotcrete_arch
;steel rib arch
set @ybeam 45.5
@steel_rib_arch
set @ybeam 46
@steel_rib_arch
solve
save E42_46

model mech mohr range group arch_grouted_rockmass y 47 51
prop bulk 29.36e6 shea 22.02e6 den 2660 fric 28 coh 0.12e6 dil 9 ten 0.0004e6 &
        range group arch_grouted_rockmass y 47 51
model mech mohr range group tunnel_arch y 47 51
prop bulk 29.36e6 shea 22.02e6 den 2660 fric 28 coh 0.12e6 dil 9 ten 0.0004e6 &
        range group tunnel_arch y 47 51
solve

;bench

set @exca3 40 @exca4 42
@tunnel_bench_excavation
set @ed3 39.9 @ed4 41.9
@shotcrete_wall
;steel rib wall
set @ybeamw 40.5
@steel_rib_wall
set @ybeamw 41
@steel_rib_wall
set @ybeamw 41.5
@steel_rib_wall
set @ybeamw 42
@steel_rib_wall
solve
save 40_42_bench

;heading excavation

set @exca1 46 @exca2 47
@tunnel_arch_excavation
set @ed1 45.9 @ed2 46.9
@shotcrete_arch
;steel rib arch
set @ybeam 46.5
@steel_rib_arch
set @ybeam 47
@steel_rib_arch
```

```
solve
save 46_47_arch

set @exca1 47 @exca2 48
@tunnel_arch_excavation
set @ed1 46.9 @ed2 47.9
@shotcrete_arch
;steel rib arch
set @ybeam 47.5
@steel_rib_arch
set @ybeam 48
@steel_rib_arch
solve
save 47_48_arch
model mech mohr range group wall_grouted_rockmass y 43 47
prop bulk 29.36e6 shea 22.02e6 den 2660 fric 28 coh 0.12e6 dil 9 ten 0.0004e6 &
        range group wall_grouted_rockmass y 43 47
;bench

set @exca3 42 @exca4 44
@tunnel_bench_excavation
set @ed3 41.9 @ed4 43.9
@shotcrete_wall
;steel rib wall
set @ybeamw 42.5
@steel_rib_wall
set @ybeamw 43
@steel_rib_wall
set @ybeamw 43.5
@steel_rib_wall
set @ybeamw 44
@steel_rib_wall
solve
save 42_44_bench

;heading excavation

set @exca1 48 @exca2 49
@tunnel_arch_excavation
set @ed1 47.9 @ed2 48.9
@shotcrete_arch
;steel rib arch
set @ybeam 48.5
@steel_rib_arch
set @ybeam 49
@steel_rib_arch
solve
save 48_49_arch
set @exca1 49 @exca2 50
@tunnel_arch_excavation
set @ed1 48.9 @ed2 49.9
@shotcrete_arch
;steel rib arch
set @ybeam 49.5
@steel_rib_arch
set @ybeam 50
@steel_rib_arch
solve
save E50m
model mech mohr range group arch_grouted_rockmass y 51 55
prop bulk 29.36e6 shea 22.02e6 den 2660 fric 28 coh 0.12e6 dil 9 ten 0.0004e6 &
        range group arch_grouted_rockmass y 51 55
```

```
model mech mohr range group tunnel_arch y 51 55
prop bulk 29.36e6 shea 22.02e6 den 2660 fric 28 coh 0.12e6 dil 9 ten 0.0004e6 &
        range group tunnel_arch y 51 55
solve

;bench

set @exca3 44 @exca4 46
@tunnel_bench_excavation
set @ed3 43.9 @ed4 45.9
@shotcrete_wall
;steel rib wall
set @ybeamw 44.5
@steel_rib_wall
set @ybeamw 45
@steel_rib_wall
set @ybeamw 45.5
@steel_rib_wall
set @ybeamw 46
@steel_rib_wall
solve
save 44_46_bench

;heading excavation

set @exca1 50 @exca2 51
@tunnel_arch_excavation
set @ed1 49.9 @ed2 50.9
@shotcrete_arch
;steel rib arch
set @ybeam 50.5
@steel_rib_arch
set @ybeam 51
@steel_rib_arch
solve
save 50_51_arch
set @exca1 51 @exca2 52
@tunnel_arch_excavation
set @ed1 50.9 @ed2 51.9
@shotcrete_arch
;steel rib arch
set @ybeam 51.5
@steel_rib_arch
set @ybeam 52
@steel_rib_arch
solve
save 51_52_arch
model mech mohr range group wall_grouted_rockmass y 47 51
prop bulk 29.36e6 shea 22.02e6 den 2660 fric 28 coh 0.12e6 dil 9 ten 0.0004e6 &
        range group wall_grouted_rockmass y 47 51

;bench

set @exca3 46 @exca4 48
@tunnel_bench_excavation
set @ed3 45.9 @ed4 47.9
@shotcrete_wall
;steel rib wall
set @ybeamw 46.5
@steel_rib_wall
set @ybeamw 47
@steel_rib_wall
set @ybeamw 47.5
```

```
@steel_rib_wall
set @ybeamw 48
@steel_rib_wall
solve
save 46_48_bench

;heading excavation

set @exca1 52 @exca2 53
@tunnel_arch_excavation
set @ed1 51.9 @ed2 52.9
@shotcrete_arch
;steel rib arch
set @ybeam 52.5
@steel_rib_arch
set @ybeam 53
@steel_rib_arch
solve
save 52_53_arch

set @exca1 53 @exca2 54
@tunnel_arch_excavation
set @ed1 52.9 @ed2 53.9
@shotcrete_arch
;steel rib arch
set @ybeam 53.5
@steel_rib_arch
set @ybeam 54
@steel_rib_arch
solve
save E50_54_arch
model mech mohr range group arch_grouted_rockmass y 54 59
prop bulk 29.36e6 shea 22.02e6 den 2660 fric 28 coh 0.12e6 dil 9 ten 0.0004e6 &
        range group arch_grouted_rockmass y 54 59
model mech mohr range group tunnel_arch y 54 59
prop bulk 29.36e6 shea 22.02e6 den 2660 fric 28 coh 0.12e6 dil 9 ten 0.0004e6 &
        range group tunnel_arch y 54 59
solve

;bench

set @exca3 48 @exca4 50
@tunnel_bench_excavation
set @ed3 47.9 @ed4 49.9
@shotcrete_wall
;steel rib wall
set @ybeamw 48.5
@steel_rib_wall
set @ybeamw 49
@steel_rib_wall
set @ybeamw 49.5
@steel_rib_wall
set @ybeamw 50
@steel_rib_wall
solve
save 48_50_bench
;heading
set @exca1 54 @exca2 55
@tunnel_arch_excavation

set @ed1 53.9 @ed2 54.9
@shotcrete_arch
;steel rib arch
```

```
set @ybeam 54.5
@steel_rib_arch
set @ybeam 55
@steel_rib_arch
solve
save E54_55_arch
set @exca1 55 @exca2 56
@tunnel_arch_excavation
set @ed1 54.9 @ed2 55.9
@shotcrete_arch
;steel rib arch
set @ybeam 55.5
@steel_rib_arch
set @ybeam 56
@steel_rib_arch
solve
save E55_56_arch
model mech mohr range group wall_grouted_rockmass y 50 54
prop bulk 29.36e6 shea 22.02e6 den 2660 fric 28 coh 0.12e6 dil 9 ten 0.0004e6 range &
        group wall_grouted_rockmass y 50 54

;bench
set @exca3 50 @exca4 52
@tunnel_bench_excavation
set @ed3 49.9 @ed4 51.9
@shotcrete_wall
;steel rib wall
set @ybeamw 50.5
@steel_rib_wall
set @ybeamw 51
@steel_rib_wall
set @ybeamw 51.5
@steel_rib_wall
set @ybeamw 52
@steel_rib_wall
solve
save 50_52_bench
;heading
set @exca1 56 @exca2 57
@tunnel_arch_excavation
set @ed1 55.9 @ed2 56.9
@shotcrete_arch
;steel rib arch
set @ybeam 56.5
@steel_rib_arch
set @ybeam 57
@steel_rib_arch
solve
save E56_57_arch
set @exca1 57 @exca2 58
@tunnel_arch_excavation
set @ed1 56.9 @ed2 57.9
@shotcrete_arch
;steel rib arch
set @ybeam 57.5
@steel_rib_arch
set @ybeam 58
@steel_rib_arch
solve
save E57_58_arch
return
;-----------------------------------------------------------------------------------------------------------------------------------------
```